

Enzyme supported crystallization of chiral amino acids

Inaugural-Dissertation

zur Erlangung des Doktorgrades der
Mathematisch-Naturwissenschaftlichen Fakultät der
Heinrich-Heine-Universität Düsseldorf

vorgelegt von

Kerstin Würges

aus Frankfurt a. M.

Köln, März 2011

aus dem Institut für Bio- und Geowissenschaften, IBG-1: Biotechnologie,
des Forschungszentrums Jülich

Gedruckt mit der Genehmigung der
Mathematisch-Naturwissenschaftlichen Fakultät der
Heinrich-Heine-Universität Düsseldorf

Referent: Apl. Prof. Dr. Martina Pohl
Koreferent: Prof. Dr. Karl-Erich Jaeger

Tag der mündlichen Prüfung: 04.05.2011

„Der Wille öffnet die Türen zum Erfolg“

(Louis Pasteur, 1822-1895)

To my family and Björn

ABSTRACT

Chiral molecules are versatile building blocks for the synthesis of pharmaceuticals and fine chemicals. α -amino acids (natural and non-natural ones) represent one major group among these chiral molecules having, with the exception of glycine, at least one chiral center. Besides fermentative production methods, amino acids are also synthesized chemically as racemates. Thus, for chiral applications, the enantiomers have to be separated. To overcome yield limitations of simple enantioseparation processes, which are generally limited to 50 %, the aim of this thesis was the development of new processes for the efficient production and separation of chiral amino acids by the combination of enzymatic racemization/isomerization and crystallization. To achieve this goal, two different approaches have been investigated starting from either racemic or enantiopure substrates:

- 1) *Enzyme-assisted preferential crystallization* combines the crystallization of a single enantiomer from a racemic solution with enzymatic racemization of the remaining enantiomer. This concept is only applicable to the relatively small group of conglomerate forming racemates. Asparagine was identified as a suitable model substrate for preferential crystallization and enzymatic racemization using the purified amino acid racemase AArac2440 from *Pseudomonas putida* KT2440. A process for the dynamic resolution of L-asparagine from a supersaturated racemic solution was developed in a 20 mL scale, and the product *ee* could be increased significantly by enzymatic racemization of the remaining D-asparagine during crystallization. This process is a modification of a classical dynamic kinetic resolution, where product separation occurs *via* enantioselective crystallization instead of asymmetric transformation.
- 2) The second approach focuses on the *production of chiral allo-threonine from threonine by enzymatic isomerization and crystallization*. Both enantiomers of the valuable *allo*-threonine have been produced with good yields from low-priced threonine using purified amino acid racemase AArac12996 from *Pseudomonas putida* NBRC12996. Product separation was performed by simple crystallization from the reaction solution, which was possible due to the lower solubility limit of *allo*-threonine compared to threonine.

The presented approaches are samples of new promising methods for the production and separation of chiral amino acids. Further investigations on improved catalysts may expand the general application scope of these methods to even more versatile substance groups.

KURZFASSUNG

Chirale Moleküle finden u. A. Anwendung als vielseitig einsetzbare Intermediate in der Synthese von pharmazeutisch wirksamen Substanzen und Feinchemikalien. Natürliche wie auch unnatürliche α -Aminosäuren, die mit Ausnahme von Glycin mindestens ein asymmetrisches C-Atom besitzen, stellen dabei eine wichtige Gruppe dieser chiralen Bausteine dar. Aminosäuren können sowohl fermentativ als auch mittels chemischer Synthese in Form von Racematen hergestellt werden. Für die Anwendung als chirale Intermediate muss somit gegebenenfalls eine Enantiomertrennung erfolgen. Um die Ausbeute über die bei einfachen Trennverfahren üblichen 50 % zu steigern, sollten im Rahmen dieser Doktorarbeit neue und effiziente Prozesse zur Produktion und Abtrennung chiraler Aminosäuren entwickelt werden. Dies erfolgte durch die Kombination einer enzymatischen Racemisierung bzw. Isomerisierung mit einer Kristallisation zur Produktabtrennung. Ausgehend von entweder racemischen oder chiralen Aminosäuren wurden zwei verschiedene Prozessansätze untersucht:

- 1) Die *Enzymunterstützte bevorzugte Kristallisation* vereint die Kristallisation eines einzelnen Enantiomers aus einer racemischen Lösung mit der enzymatischen Racemisierung des verbleibenden Enantiomers. Die bevorzugte Kristallisation kann nur für eine relativ kleine Gruppe der sogenannten konglomeratbildenden Racemate angewendet werden, zu der auch die proteinogene Aminosäure Asparagin zählt. Sie stellt zudem ein geeignetes Substrat der Aminosäureracemase AArac2440 aus *Pseudomonas putida* dar. Ein Modellprozess zur dynamischen Abtrennung von L-Asparagin aus einer übersättigten racemischen Lösung wurde im 20 mL Maßstab entwickelt. Durch die enzymatische Racemisierung des verbleibenden D-Asparagins während der bevorzugten Kristallisation, konnte ein deutlicher Anstieg des Enantiomerenüberschusses in den Produktkristallen erzielt werden. Dieser Prozess kann als eine neue Variante der klassischen dynamisch kinetischen Racematspaltung angesehen werden, bei der die Produktabtrennung durch bevorzugte Kristallisation anstelle einer asymmetrischen Transformation erfolgt.
- 2) Der zweite untersuchte Prozess umfasst die *Produktion von chiraalem allo-Threonin aus Threonin durch enzymatische Isomerisierung und Kristallisation*. Beide Enantiomere des hochpreisigen *allo*-Threonins konnten mit guten Reinheiten und Ausbeuten aus dem preiswerten Ausgangsmaterial Threonin hergestellt werden. Die Isomerisierung von D- und L-Threonin zu L- bzw. D-*allo*-Threonin erfolgte dabei mit Hilfe der reinen Aminosäureracemase AArac12996 aus *Pseudomonas putida* NBRC12996. Durch einfache Kristallisation des weniger löslichen *allo*-Threonins aus der Reaktionslösung konnte eine effiziente Produktabtrennung erreicht werden.

Die hier präsentierten Prozesse zur Herstellung enantiomerenreiner Aminosäuren sind Beispiele für neue vielversprechende Methoden zur Produktion und Abtrennung chiraler Aminosäuren. Durch die Entwicklung verbesserter Biokatalysatoren mit erweiterten Substratspektren, könnte die Anwendungsbreite dieser neuen Methoden auf weitere interessante chirale Stoffgruppen erweitert werden.

LIST OF PUBLICATIONS

1. **Würges, K.**, Petruševska, K., Serçi, S., Wilhelm, S., Wandrey, C., Seidel-Morgenstern, A., Elsner, M. P., Lütz, S., Enzyme-assisted physicochemical enantioseparation processes - part I: Production and characterization of a recombinant amino acid racemase. *Journal of Molecular Catalysis B: Enzymatic* (2009) 58: 10-16.
2. Petruševska-Seebach, K., **Würges, K.**, Seidel-Morgenstern, A., Lütz, S., Elsner, M. P., Enzyme-assisted physicochemical enantioseparation processes - Part II: Solid-liquid equilibria, preferential crystallization, chromatography and racemization reaction. *Chemical Engineering Science* (2009) 64: 2473-2482.
3. **Würges, K.**, Petruševska-Seebach, K., Elsner, M. P., Lütz, S., Enzyme-assisted physicochemical enantioseparation processes - part III: Overcoming yield limitations by dynamic kinetic resolution of asparagine via preferential crystallization and enzymatic racemization. *Biotechnology and Bioengineering* (2009) 104: 1235-1239.
4. **Würges, K.**, Mackfeld, U., Pohl, M., Wiechert, W., Kubitzki, T. An efficient route to both enantiomers of *allo*-threonine by simultaneous amino acid catalyzed isomerization of threonine and crystallization. *Advanced Synthesis & Catalysis* (2011) DOI: 10.1002/adsc.201100051.

LIST OF POSTER PRESENTATIONS

1. **Würges, K.**, Lütz, S., Pohl, M., Wiechert, W., Kubitzki, T., Dynamic kinetic resolution by preferential crystallization and enzymatic racemization, *28 DEHEMA-Jahrestagung der Biotechnologen* (2010) Aachen (Germany)
2. **Würges, K.**, Lütz, S., Pohl, M., Wiechert, W., Kubitzki, T., Characterization of amino acid racemases as a tool to access enantiomerically pure amino acids by preferential crystallization, *5th International Congress on Biocatalysis* (2010) Hamburg (Germany)
3. **Würges, K.**, Petruševska-Seebach, K., Elsner, M. P., Lütz, S., Enzyme-assisted preferential crystallization: Yield improvement of L-asparagine by enzymatic *in situ* racemization, *9th International Symposium on Biocatalysis* (2009) Bern (Switzerland)
4. Petruševska-Seebach, K., **Würges, K.**, Seidel-Morgenstern, A., Lütz, S., Elsner, M. P., Productivity Enhancement of enantioseparation in combination with enzymatic reaction, *2nd European Process Intensification Conference* (2009) Venice (Italy)
5. **Würges, K.**, Petruševska, K., Elsner, M. P., Lütz, S., Wandrey, C., Seidel-Morgenstern, A., Preferential crystallization of L-amino acids from racemic solutions: Overcoming yield limitations by enzymatic racemization in a continuous reactor system, *European BioPerspectives* (2008) Hannover (Germany)
6. **Würges, K.**, Petruševska, K., Elsner, M. P., Lütz, S., Wandrey, C., Seidel-Morgenstern, A., Enzyme supported preferential crystallization of enantiopure amino acids, *15th International Workshop on Industrial Crystallization* (2008) Magdeburg (Germany)
7. Petruševska, K., Elsner, M. P., **Würges, K.**, Lütz, S., Wandrey, C., Seidel-Morgenstern, A., Enantioseparation processes involving racemization step, *20th International Symposium on Chirality* (2008) Geneva (Switzerland)
8. Petruševska, K., Elsner, M. P., **Würges, K.**, Lütz, S., Wandrey, C., Seidel-Morgenstern, A., Productivity enhancement of amino acids by crystallization and racemization, *19th Polish Conference of Chemical and Process Engineering* (2007) Rzeszów (Poland)

ACKNOWLEDGEMENT

First of all I like to express my gratitude to those people who made this PhD project possible. Very special thanks to

Prof. Dr. em. Christian Wandrey and Prof. Dr. Wolfgang Wiechert for the opportunity to work on this project and the excellent working conditions at the institute, for the continuous interest in my work as well as the helpful suggestions and discussions.

Apl. Prof. Dr. Martina Pohl for help and motivation whenever this work was facing difficulties and for her extraordinary commitment to her group members.

Prof. Dr. Karl-Erich Jaeger for his engagement at the beginning of this work in helping me to qualify for a doctoral thesis at the Faculty of Mathematics and Natural Sciences of the Heinrich-Heine University Düsseldorf and for his kindness to evaluate this work as a coreferee.

I also like to thank Dr. Stephan Lütz and Dr. Tina Kubitzki for supervision of the every-day work, the helpful discussions and always good suggestions.

Many thanks also to Dr. Martin Elsner, Katerina Petruševska-Seebach and Prof. Dr. Andreas Seidel-Morgenstern from the Max Planck Institute Magdeburg for their cooperation in this project and the opportunity to learn about preferential crystallization during my visits in Magdeburg.

During the last three years many people of the group of *Biocatalysis and Biosensors* (former group of *Technical Biocatalysis*) supported me and my work, which I also like to thank here:

Ursula Mackfeld for her continuous help with technical problems in the laboratory, her always good ideas and of course for her tireless and outstanding work.

Doris Hahn for her help in cloning “bullheaded” genes and transforming “reluctant” cells.

Stefanie Jacob for her good and dedicated work throughout her Diploma Thesis and the long evenings she spent at the institute watching crystals grow.

Saskia Schuback and Sebastian Grefen for helping in the laboratory whenever it was needed.

Carina Schmöhl for her interest in my work and her engagement in learning something new.

Furthermore I like to thank Dr. Susanne Wilhelm and Dr. Stefanie Serci from the Institute of Molecular Enzyme Technology of the Heinrich-Heine University Düsseldorf for guiding and helping me during the beginning of my biomolecular lab experiences, for giving me the opportunity to work in their laboratories and for good cooperation.

Thanks also to Dr. Jan van Ooyen for the supply of *E. coli* XL1-blue for rational protein design experiments and his always good advices concerning cloning and transformation.

Very special thanks to my “roommates” and colleagues of offices 124 and 305 who made work at the institute so much easier by their permanent support, always encouraging words and mostly helpful discussions.

At this point I also like to express my sincere gratitude to all the rest of my colleagues of the *Biocatalysis and Biosensors* group as well as of the former group of *Technical Biocatalysis* for their generous help in technical and theoretical questions and for the excellent working atmosphere every day.

I also like to thank Marianne Hess for her precious work in organizing and managing the institute and for her helpfulness in every situation. Work became so much easier by that.

And finally I like to thank my family and Björn for their constant support, encouragement and love during the last years, for giving me the self-confidence I needed and for making me what I am.

TABLE OF CONTENTS

1	INTRODUCTION	2
1.1	Biocatalysis	2
1.1.1	Biocatalysis – an ancient art.....	2
1.1.2	Biocatalysis in industry	3
1.1.3	Advantages and challenges of biocatalysis	4
1.2	Chirality in industry	7
1.2.1	Chiral compounds in chemical and pharmaceutical industry.....	7
1.2.2	Nomenclature of chiral centers	7
1.2.3	Asymmetric biocatalysis in industry	8
1.3	Chiral resolution methods.....	9
1.3.1	Enzyme catalyzed resolution of racemates	9
1.3.2	Preferential crystallization.....	10
1.3.3	Enzyme-assisted preferential crystallization.....	12
1.4	α-amino acids.....	12
1.4.1	Production methods of amino acids	13
1.4.2	Industrial applications of amino acids.....	14
1.4.3	Asparagine.....	15
1.4.4	Threonine and its stereoisomers	16
1.5	Enzymes and their classification	18
1.6	Racemases.....	19
1.6.1	Overview	19
1.6.2	Structure, function and catalytic mechanism of PLP-dependent amino acid racemases	20
1.6.3	Applications of amino acid racemases	22

2	AIM OF THE THESIS	24
3	PUBLICATIONS	26
I	Enzyme-assisted physicochemical enantioseparation processes - Part I: Production and characterization of a recombinant amino acid racemase	26
II	Enzyme-assisted physicochemical enantioseparation processes - Part II: Solid- liquid equilibria, preferential crystallization, chromatography and racemization reaction	34
III	Enzyme-assisted physicochemical enantioseparation processes - Part III: Overcoming yield limitations by dynamic kinetic resolution of asparagine via preferential crystallization and enzymatic racemization	45
IV	An efficient route to both enantiomers of <i>allo</i>-threonine by simultaneous amino acid catalyzed isomerization of threonine and crystallization	51
	Corrections.....	60
4	DISCUSSION	62
4.1	Amino acid racemases AArac2440 and AArac12996	63
4.1.1	Overexpression and secretion.....	63
4.1.2	Purification from cell extract and medium.....	64
4.1.3	Enzyme characterization	67
4.1.4	Structural homologies	71
4.1.5	Rational protein design of AArac2440.....	72
4.2	Crystallization of amino acids	73
4.2.1	Conglomerates vs. racemic compounds	73
4.2.2	Preferential crystallization of asparagine	74
4.2.3	Crystallization of <i>allo</i> -threonine from diastereomeric solutions.....	76
4.3	Enzyme-assisted preferential crystallization of asparagine.....	77
4.3.1	Reactor setups	78
4.3.2	Process performance	80
4.3.3	Benefits and limits.....	82
4.4	Production of chiral <i>allo</i>-threonine	83
4.4.1	Identification of threonine isomers	83

4.4.2	Process modes	85
4.4.3	Benefits and limits of the new <i>allo</i> -threonine process	89
4.4.4	Added value by threonine isomerization.....	90
5	CONCLUSIONS.....	93
6	REFERENCES	95
	APPENDIX.....	XIII

ABBREVIATIONS AND SYMBOLS

Abbreviations

AA	amino acid
AArac12996	amino acid racemase from <i>P. putida</i> strain NBRC12996
AArac2440	amino acid racemase from <i>P. putida</i> strain KT2440
AIDS	acquired immune deficiency syndrome
Ala	alanine
<i>allo</i> -Thr	<i>allo</i> -threonine
<i>aq</i>	in solution
Arg	arginine
Asn	asparagine
Asp	aspartate
CIP	Cahn-Ingold-Prelog
CL	lyophilisate of crude cell extract
CLIB	Cluster industrielle Biotechnologie
Cm	chloramphenicol
DAP	diaminopimelic acid
DEAE	diethylaminoethyl
DKR	dynamic kinetic resolution
DNA	deoxyribonucleic acid
dNTP	deoxynucleoside triphosphate
EC	enzyme commission
FDA	US Food and Drug administration
GABA	γ -aminobutyric acid
GlcNAc	N-acetylglucosamine
Glu	glutamate
HMM	Hidden Markov Model
HPLC	high-performance liquid chromatography
IPTG	isopropyl β -D-1-thiogalactopyranoside
KPi	potassium phosphate buffer
LB	lysogeny broth (<i>Luria-Bertani medium</i>)
Met	methionine

MurNAc	N-acetylmuramic acid
NADH	nicotinamide adenine dinucleotide, reduced form
NADPH	nicotinamide adenine dinucleotide phosphate, reduced form
n.d.	not determined
NMR	nuclear magnetic resonance
NN	neural networks
P	product
PCR	polymerase chain reaction
pdb	protein data bank
PL	lyophilisate of purified cell extract
S	substrate
SDS-PAGE	sodium dodecyl sulfate polyacrylamide gel electrophoresis
Thr	threonine

Symbols

α	solubility ratio	-
a	ratio between D- and L-isomers of Thr	-
b	ratio between Thr and <i>allo</i> -Thr	-
$c_{\text{cryst/sat}}$	crystallization/saturation concentration at $T_{\text{cryst/sat}}$	g/L
c_{prot}	protein concentration	mg/mL
de	diastereomeric excess	%
ee	enantiomeric excess	%
$k_{\text{cryst/rac}}$	crystallization/racemization constant	s^{-1}
K_m	Michaelis-Menten constant	mM
$m_{\text{seed/feed/product}}$	mass of seed crystals/feed/product	mg
rpm	rounds per minute	min^{-1}
STY	space time yield	$\text{g}/(\text{L}\cdot\text{d})$
$t_{1/2}$	half life	d
T	temperature	$^{\circ}\text{C}$
$T_{\text{cryst/sat}}$	crystallization/saturation temperature	$^{\circ}\text{C}$
U	units of enzyme activity	$\mu\text{mol}/\text{min}$
V	volume	mL
V_{max}	maximum enzyme activity	U/mg
vol.%	volume percentage	%

CHAPTER 1

INTRODUCTION

1 Introduction

1.1 Biocatalysis

1.1.1 Biocatalysis – an ancient art

Humans have used biocatalysts already since about 6000 to 8000 years, when the old Egyptians utilized microorganisms such as yeast to brew beer and to bake bread. Processes like the fermentation of milk for cheese or yoghurt preparation or the production of vinegar by microbial oxidation followed. However, it took millenniums until the biological principles had been explored. It was only in 1833 when the French chemists Anselme Payen (1795-1871) and Jean-François Persoz (1805-1868) isolated a starch hydrolyzing amylase complex from malt, which they called diastase (Payen *et al.*, 1833). The scientific basis for biocatalytic reactions occurring during fermentation processes was first described in the middle of the 19th century by Louis Pasteur (1822-1895), who demonstrated the existence of microorganisms and their effect on fermentation in the so called “germ theory” (Walsh, 1913). At the same time Pasteur established the fundamentals of stereochemistry by the resolution of racemic tartaric acid (Pasteur, 1897) and identified the ability of microorganisms to degrade single enantiomers from racemates while the other one remains unmodified (Turner, 1998). However, it was not before the year 1877 when the German physiologist Wilhelm Kühne (1837-1900) used the term *enzyme* for the first time to describe non-living substances that were able to catalyze chemical reactions (Kühne, 1877). Another pioneer in enzyme catalysis was the German chemist Emil Fischer (1852-1919) who elucidated essential aspects of enzyme catalysis and showed that, besides whole cells, also enzymes are able to distinguish between chiral molecules (Fischer, 1894). Although the nature of enzymes was not clear at this point, they were already known to satisfy three criteria required for being a catalyst (Yuryev *et al.*, 2010):

1. The catalytic agent is not altered during the reaction.
2. Small amounts of catalytic agent are adequate for the conversion of large amounts of substrate.
3. The catalytic agent does not affect the final reaction equilibrium.

A few years later, Eduard Buchner (1860-1917) showed that a cell-free extract of yeast cells was sufficient for the fermentation of sugar. He identified the soluble active ingredient as a protein and called it *zymase* (Buchner, 1897). Buchner thereby proved that enzyme catalysis was a chemical process not necessarily linked to living cells, and thus paved the way for modern biocatalytic processes. In 1926 Sumner was able to crystallize urease and thereby finally proofed that enzymes indeed were proteins (Sumner *et al.*, 1950).

1.1.2 Biocatalysis in industry

Nowadays, biocatalysis is an important tool for the chemical industry. In highly selective reactions it enables the synthesis of complex compounds. The success story of industrial applications of enzymes began in 1874, when Christian Hansen started the first company for the production of standardized enzyme preparations, namely rennet for cheese making (Buchholz *et al.*, 2000). From thereon biocatalytic processes gained more and more influence for industrial food processing such as in chill-proofing of beer, the addition of malt extract (13500 t in 1922), or in dough making (Tauber, 1949).

The discovery of the chemical structure and composition of DNA and RNA by Watson and Crick in 1953 and its meaning for protein expression initiated a new era of biotechnology (Watson *et al.*, 1953). Due to the development of recombinant gene technologies enzymes became easily accessible on a large scale for commercial applications. The obvious advantages of biocatalysts over classical chemical catalysts, such as chemo-, regio- and enantioselectivity, mild reaction conditions, environmental friendliness, and high catalytic efficiencies, led to about 150 implemented biocatalytic processes in industry from the 1970's until today (Woodley, 2008). For example, microorganisms are used for the production of bulk chemicals (*e.g.* methanol, ethanol, acryl amid), organic acids (*e.g.* citric acid, maleic acid, gluconic acid), polysaccharides (*e.g.* xanthan), vitamins (*e.g.* vitamins B and C, biotin), and amino acids (*e.g.* L-glutamate, L-threonine). Most of these products are applied in the food and feed industry as well as in the pharmaceutical or chemical industry. Besides, enzymes are used as additives in detergents and foods or for diagnostic purposes. Biocatalysis is particularly valuable for the production of fine chemicals, since the enzymes' high regio- and enantioselectivity offers new routes to enantiopure complex molecules, which in many cases are hard to synthesize chemically. Despite their natural environment, enzymes can also be applied in non-conventional media such as organic solvents or ionic liquids which paves the way for synthetic routes with new substrates and/or products or altered selectivity (Würges *et al.*, 2005).

About 50 % of all industrial biotransformations are performed as batch processes in which approximately 1-10 % of the process costs can be attributed to the biocatalyst (Straathof *et al.*, 2002). Although many enzymes have substrate and product scopes that are much broader than the natural ones, in many cases the creation of robust and suitable biocatalysts by evolutionary methods has been advantageous. Thus, the process does not have to be adapted to the catalyst anymore, but the catalyst is developed for a commercially optimal process. In addition, the combination of chemo- and biocatalysis provides new opportunities for chiral syntheses. An example for the improvement of an industrial process by biocatalysis is the synthesis of cortisone. The chemical approach by Merck included 31 reaction steps and about 615 kg of deoxycholic acid were required for the synthesis of 1 kg cortisone (220 \$/g). By enzymatic hydroxylation of progesterone to 11 α -hydroxyprogesterone by *Rhizopus arrhizus*,

the synthesis was simplified leading to a vast reduction of the production costs (6 \$/g) (Yuryev *et al.*, 2010). Figure 1 gives an overview about the world market of biotechnological processes and their share among chemical products in the year 2001 and the sales that were expected in 2010 (Festel *et al.*, 2004).

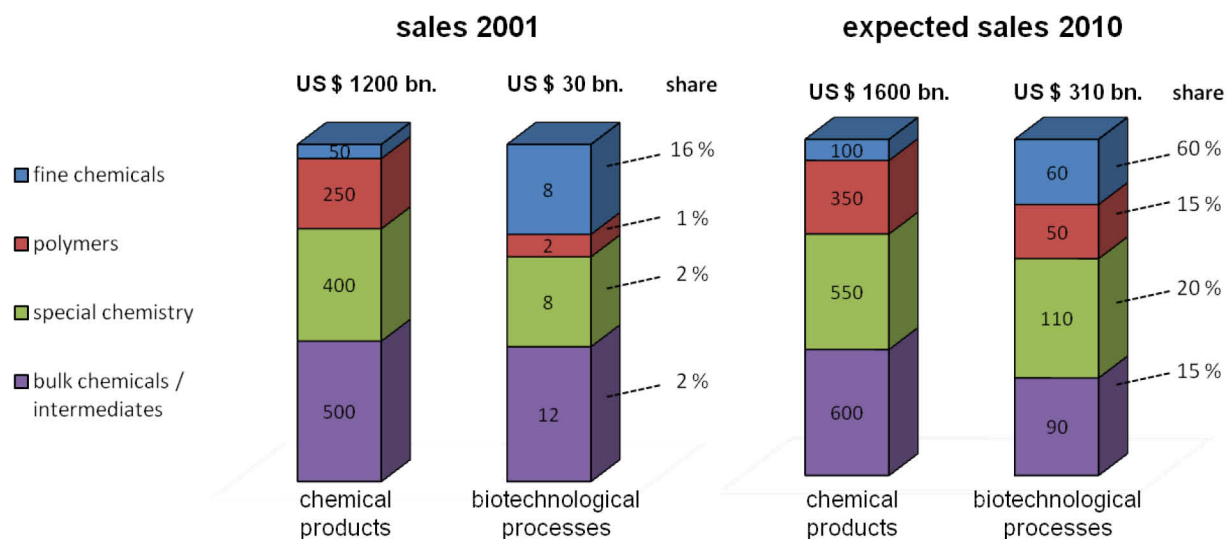


Figure 1: Sales of chemical products in the years 2001 and 2010 (expected) with share of biotechnological processes (Festel *et al.*, 2004).

Ran *et al.* shortly reviewed recent applications of biocatalysis for chemical syntheses at industrial scale (Ran *et al.*, 2008). Nevertheless, the number and diversity of biocatalytic applications are modest probably due to limitations such as enzyme availability, substrate scope and operational stability. However, due to breakthroughs in the fields of genomics, evolutionary methods and rational protein design, many new industrial applications are expected (Schoemaker *et al.*, 2003).

1.1.3 Advantages and challenges of biocatalysis

Compared to classical chemical synthesis biocatalysis provides many **advantages**:

1. *Selectivity*: Enzymes are able to catalyze reactions with very high chemo-, regio- and enantioselectivity. This ability makes them particularly interesting for the production of fine chemicals and pharmaceutical intermediates, which are often, if at all, only accessible by chemical multi-step reactions. Using molecular biological methods, such as directed evolution and rational protein design, or reaction engineering, these properties can be adjusted according to the desired application.

2. *Mild reaction conditions*: Enzymes have the ability to reduce the activation energy for the catalyzed reaction and thus enable reactions under comparatively mild conditions. Usually temperatures between 15 °C and 80 °C, pH-values between pH 3 and pH 8 and atmospheric pressure are applied for enzymatic reactions. Thereby, not only undesired side reactions like product isomerization or rearrangement can be reduced (Patel, 2006), but also additional protection and deprotection reactions can be avoided (Schmid *et al.*, 2001).
3. *Efficient catalysis*: Enzymes operate catalytically rather than stoichiometrically and thus are able to increase turnover numbers up to 10^8 - 10^{12} times (Frey *et al.*, 2006). High product yields and purities are a result of extraordinary selectivity.
4. *Catalytic promiscuity*: Enzymes offer an enormous range of different catalytic reactions. Depending on their source organism, they are adapted to the whole area of possible environmental properties occurring in the different ecological niches on earth. Although many enzymes only use very specific substrates in their physiological environment, the possible substrate scope is usually much broader than the natural one (Schoemaker *et al.*, 2003). This allows the production of chemicals that do not occur in the natural organism's metabolism. An example is the synthesis of propane-1,3-diol from glucose by recombinant *E. coli* (Sturmer *et al.*, 2006).
5. *Environmental friendliness*: Due to their nature, enzymes usually operate in aqueous solutions and buffers and without the need of organic solvents, thus producing less toxic waste compared to chemical processes. Enzyme catalyzed reactions are rarely endo- or exothermic, thereby reducing the energy that is required for heating or cooling during the process. In contrast to classical chemical syntheses, where heavy metals are often used as catalysts, enzymes are completely bio-degradable. In addition, biocatalytic reactions normally use $(C_6)_n$ -sources from renewable resources such as glucose, which makes them nearly CO₂-neutral.

However, due to limitations mainly caused by poor enzyme availability, stability and a narrow reaction scope, biocatalysis also has to face **challenges**:

1. *Downstream processing*: Product purification is the final and often cost intensive step of biocatalytic processes. Due to natural evolution, enzymes usually operate under comparatively low substrate and product concentrations (in contrast to chemical reactions) far from those required in industrial processes. This hampers downstream processing since large amounts of water have to be removed. Alternative methods involve multi-phase reaction media for *in situ* product removal, such as liquid-liquid extraction, which is usually done by organic solvents.
2. *Cofactor regeneration*: One major limitation of numerous reactions is the necessary regeneration of reduced cofactors (NADH, NADPH) during redoxreactions. The enzyme-coupled approach uses a coenzyme for cofactor regeneration either *in vivo*

during whole cell biotransformations, or by the addition of the coenzyme (*e.g.* formate dehydrogenase). The substrate-coupled approach uses only one enzyme and an auxiliary cosubstrate, which is oxidized for cofactor regeneration (*e.g.* oxidation of 2-propanol to acetone). Another method for cofactor regeneration is the electrochemical approach. Here electrons are supplied by an electrode and transferred *via* mediators (*e.g.* rhodium complexes) to the reduced cofactors (Goldberg *et al.*, 2007).

3. *Long development times*: New developments in biocatalysis tend to take several months from lab to production scale, which is much too long for many companies that have to fulfill customers' needs usually in a much shorter time. Hence, these time-consuming developments led to a loss of investors in the biotechnological sector (Hoffritz, 2007). A close cooperation between industry and academic research with the aim of further catalyst and process development is a powerful tool to overcome this bottleneck. Clusters of biotech- and pharmaceutical companies as well as academic facilities like CLIB 2021 are pointing in the right direction (CLIB2021, 2007).

Both, advantages and challenges are summarized in Figure 2.

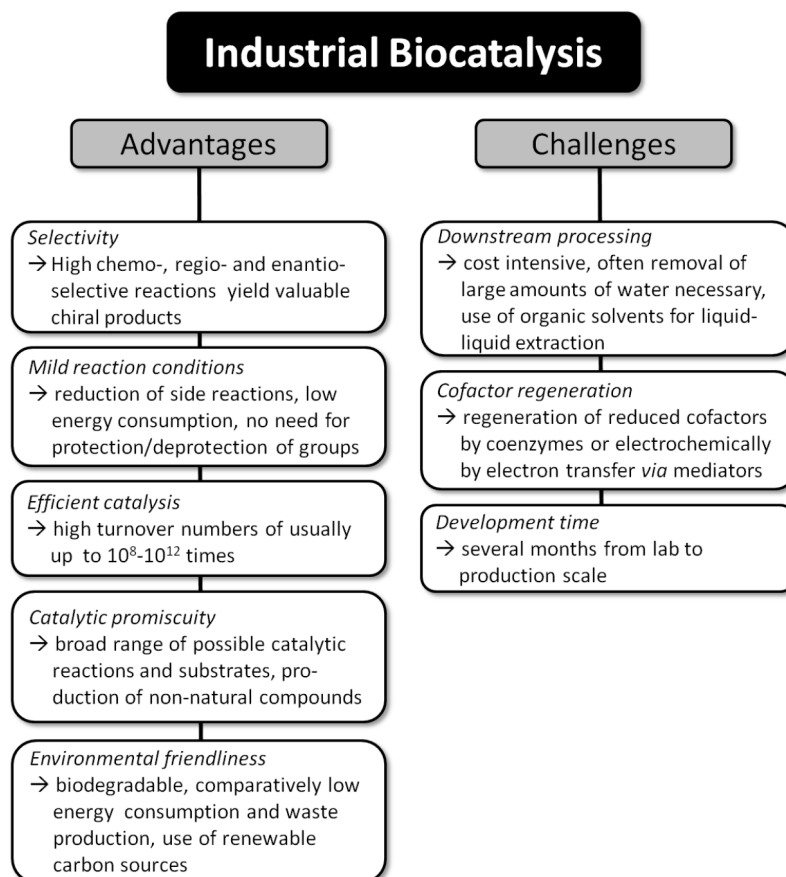


Figure 2: Advantages and challenges of industrial biocatalysis.

However, the general challenge that industrial biocatalysis still has to face, is to change the mind-set of organic chemists for the use of enzymes in chemo-enzymatic syntheses. Since classical chemical methods have been used for decades, biocatalysis is often only objected as the last opportunity if everything else had failed (Thayer, 2006).

1.2 Chirality in industry

1.2.1 Chiral compounds in chemical and pharmaceutical industry

Chirality is a key factor for the safety and efficacy of many drugs. Due to the chiral nature of living organisms (Breslow *et al.*, 2009; Lee *et al.*, 2010) chiral compounds can have dramatically different biological activities and toxicities. In more than 40 % of enantiomerically pure products, chirality originates from a chiral precursor. Thus, the production of single enantiomers as building blocks for the pharmaceutical and chemical industry has become increasingly important. In general, there are two different approaches for the *de novo* synthesis of enantiomerically pure compounds. Either an achiral starting material is converted to a chiral non-racemic product or a racemic mixture is resolved to yield an enantiomerically pure compound. In addition, single enantiomers can be resolved from racemates for example by crystallization (production of (*S*)-naproxen) or chromatography (separation of D,L-*tert*-leucine) (Bommarius *et al.*, 1998).

Of course, single enantiomers can also be produced by chemical or chemo-enzymatic synthesis, but biocatalysis often offers advantages over classical chemical synthesis methods, as enzyme catalyzed reactions usually are highly selective (Patel, 2008). Not only driven by the strict policies of the *Food and Drug Administration* (FDA) for the development of new stereoisomeric drugs (FDA, 1992), the share of chiral pharmaceuticals has increased significantly during the last decade from ca. 25 % in 1999 to ca. 54 % in 2007 (Schulze *et al.*, 1999; Ran *et al.*, 2008).

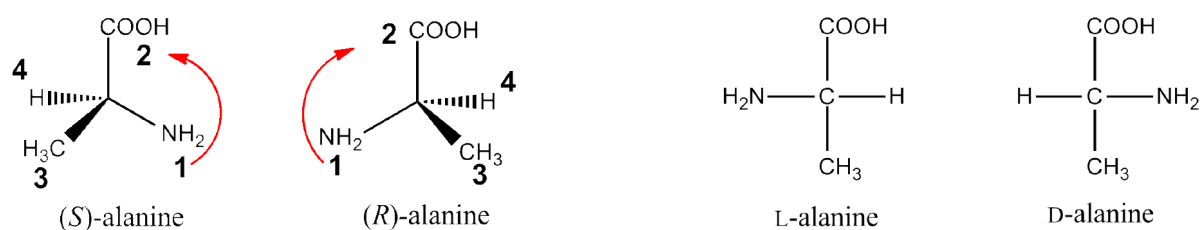
Considering the market for chiral intermediates, which was expected to reach at least US \$ 30 billion by the year 2010 with annual growth rates of more than 10 % (Archer *et al.*, 2009), it is obvious that also production methods involving biocatalytic steps gain importance in this field. Therefore, already in the year 2008 the share of biocatalysis for the production of chiral intermediates was estimated to 20 % (Patel, 2008).

1.2.2 Nomenclature of chiral centers

The most common way to describe the absolute configuration of a chiral center of organic molecules is the Cahn-Ingold-Prelog (CIP) convention. The groups that are attached to a chiral center are ranked by their priority starting with the highest one. The molecule is then

oriented in space, so that the substituent with the lowest priority points away from the observer. The sense of rotation of a curve passing through the substituents with priorities 1, 2 and 3 distinguishes the stereoisomers into *R* (rectus, Latin for right) or *S* (sinister, Latin for left, Scheme 1 left).

Another nomenclature is the DL-system (devised by Emil Fischer in 1891) which relies on the chemical correlation of the configuration of the chiral center to D-glyceraldehyde. All bonds are depicted as horizontal or vertical lines. The carbon chain is depicted vertically with the C₁-atom at the top. Depending on the direction of the substituent with the highest priority at the chiral C-atom, the isomer is either named D (dextro, Greek for right) or L (levo, Greek for left) (Scheme 1, right). The DL-nomenclature is unrelated to the rotation direction of polarized light which is indicated by (+) or (−) and is only used for carbohydrates and amino acids, where the DL-nomenclature has been applied traditionally (Stryer, 2007).



Scheme 1: Enantiomers of alanine. **Left:** Cahn-Ingold-Prelog nomenclature. **Right:** DL-nomenclature, represented in the Fischer-projection.

1.2.3 Asymmetric biocatalysis in industry

Despite the great achievements of chemists with respect to creating chiral molecules, the recognition and creation of chiral centers is an intrinsic property of life. Enzymes offer opportunities for resolving existing chiral centers (*e.g.* kinetic resolution with hydrolases; (Schulze *et al.*, 1999)) or, even more interesting, to create new chiral centers *via* asymmetric reactions such as the reduction of carbonyl compounds using dehydrogenases or *via* carbonylation by lyases (Woodley, 2008). In addition, biocatalysis often provides a direct one-step approach to a desired intermediate without any protection/deprotection steps, which are often required using chemical syntheses. Thereby, biocatalysis leads to a drastic reduction of process steps and the associated E-factor (Environmental factor: E-factor = total waste [kg] / product [kg]; (Sheldon, 1994)). Companies which involve biocatalysis for the synthesis of chiral intermediates are for example Evonic, BASF, Avecia, Lonza, DSM, Daicel, Kaneka, Dow-Pharma, Codexis, Merck, Schering-Plough, GlaxoSmithKline and Pfizer. Progress in cultivation technology, molecular cloning, site-directed mutagenesis and directed evolution of biocatalysts have gained access to a variety of enzymes as tools for asymmetric biocatalysis, which is already considered an excellent competitive technology for chemical syntheses. Numerous examples for chemo-enzymatic syntheses of various biologically active

compounds or precursors thereof can be found in literature. A good survey is given by Patel (Patel, 2008).

Besides *de novo* syntheses of chiral compounds, the development of methods for the preparation of optically pure compounds from racemates by deracemization or dynamic kinetic resolution is one of the present challenges in asymmetric synthesis.

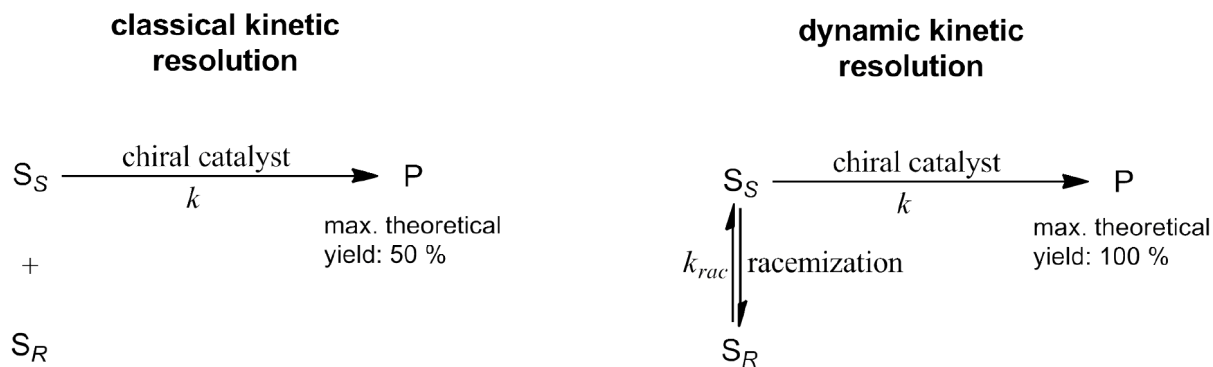
1.3 Chiral resolution methods

Besides the advances in asymmetric syntheses, the optical resolution of racemates is still the most important approach for industrial synthesis of enantiopure compounds (Ebbbers *et al.*, 1997). Since enantiomers have identical chemical and physical properties (apart from the optical rotation of linearly polarized light) separation can be quite elaborate. Possible methods include *preferential crystallization of one enantiomer* (Lorenz *et al.*, 2006; Lorenz *et al.*, 2007), *resolution by formation of diastereomers, asymmetric transformations* (Fogassy *et al.*, 2006), and *separation by chromatography based on chiral interactions* (Francotte, 2001). In the following paragraphs enzyme catalyzed resolution of racemates, as well as the preferential crystallization of single enantiomers from racemic solutions will be explained in more detail.

1.3.1 Enzyme catalyzed resolution of racemates

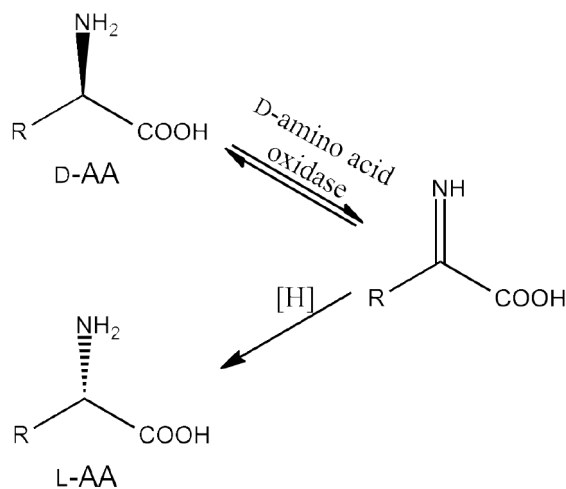
Enzyme catalyzed resolution of racemates may be achieved *via* two different approaches: (dynamic) kinetic resolution and deracemization.

Classical kinetic resolution, the conversion of one enantiomer of a racemate to a product, is hampered by a maximum theoretical yield of 50 %. A more elegant and efficient way is the so-called dynamic kinetic resolution (DKR), where an *in situ* racemization step of the non-converted enantiomer is implemented into the process (Bäckvall, 2008). As a consequence, the enantiopure product is obtained in theoretically 100 % yield (Scheme 2). Racemization can be obtained either by thermal treatment, chemically (acids, bases) or enzymatically using racemases.



Scheme 2: Comparison of classical kinetic resolution and dynamic kinetic resolution processes. S_S and S_R : substrate enantiomers; P: product; k : catalytic rate constant; k_{rac} : racemization constant.

Another related approach for the complete transformation of a racemate into one single enantiomer is the so-called deracemization. In this case two enantiomers are interconverted by a stereoinversion process so that a racemate is transformed to a non-racemic mixture. Deracemization reactions usually involve redox processes *via* the corresponding imine (Scheme 3), as shown for the interconversion of α -amino acids by an enantioselective amino acid oxidase and a chemical reducing agent (Enright *et al.*, 2003).



Scheme 3: Deracemization of racemic α -amino acid by combination of an enantioselective amino acid oxidase with a non-selective reduction.

Good reviews about DKR and deracemization processes can be found in literature (Stecher *et al.*, 1997; May *et al.*, 2002; Turner, 2004).

1.3.2 Preferential crystallization

Preferential crystallization (PC) is an interesting method for the optical resolution of racemic solutions which is applicable to conglomerate forming systems. In contrast to racemic

compounds, which consist of equimolar amounts of two enantiomers embedded in a regular pattern within the crystal, a conglomerate is a mixture of two crystalline enantiomers that are, in principle, mechanically separable. A third type of crystalline racemates are the so-called solid solutions (Jacques *et al.*, 1994).

Due to the attempt of a system to reach its thermodynamic equilibrium, the direct crystallization of enantiopure crystals from a conglomerate forming system is an attractive procedure. The principle of this kinetically controlled crystallization is shown in Figure 3. The driving force for PC is provided by supersaturation of the racemic solution. This can be achieved most easily by cooling the solution from its saturation temperature T_{sat} to its crystallization temperature T_{cryst} , at which it is supersaturated but still within the metastable zone (region in which no spontaneous crystallization is likely to occur). Within this zone the solution will return to its thermodynamic equilibrium with delay. There the liquid phase is racemic and the solid phase consists of a mixture of crystals of both enantiomers. By seeding the supersaturated solution with enantiopure crystals, a homochiral surface area for crystal growth is offered. Therefore, the liquid phase composition does not shift directly from the starting composition (A) to the equilibrium composition (C), but follows a trajectory from (A) over (B) to (C). As long as the trajectory does not alter its linear direction, it is possible to collect enantiopure crystals. Detailed treatises of this process can be found in literature (Jacques *et al.*, 1994; Rodrigo *et al.*, 2004; Lorenz *et al.*, 2006). Conglomerate forming systems are rare and can be estimated to about 10 % of all racemates (Collet, 1999).

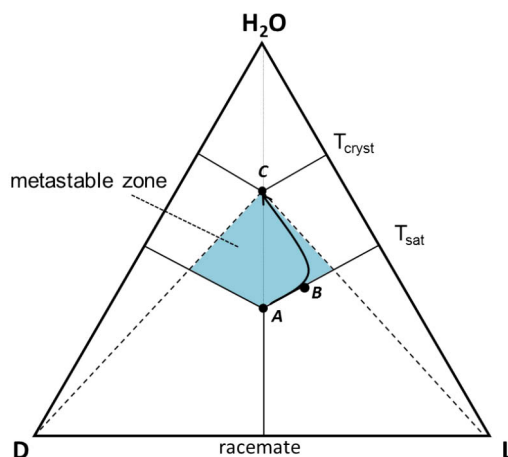
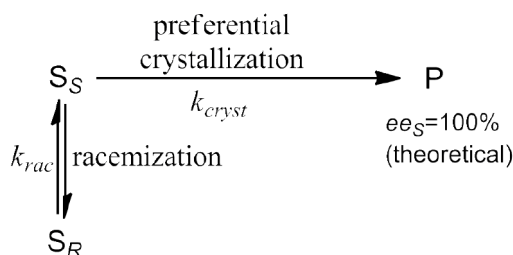


Figure 3: Principle of preferential crystallization (PC) of D-enantiomer for conglomerate forming systems in a ternary phase diagram. By cooling the solution from the saturation temperature (T_{sat}) to the crystallization temperature (T_{cryst}) the system becomes supersaturated. PC is initiated by seeding with enantiopure crystals. The arrow represents the shift of the solution composition during PC.

1.3.3 Enzyme-assisted preferential crystallization

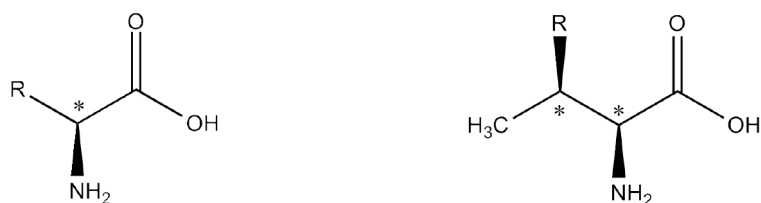
By combination of PC with enzymatic *in situ* racemization in solution, the formation of an enantiomeric excess, and thus crystallization of the counter-enantiomer, can be avoided. In contrast to DKR, where resolution is achieved by chiral biotransformation to an easy separable product (Scheme 2, right), the desired enantiomer is separated by crystallization. The enzyme catalyzes the auxiliary racemization reaction.



Scheme 4: Enzyme-assisted preferential crystallization. S_S and S_R : substrate enantiomers; P: crystalline product; k_{cryst} : crystallization constant; k_{rac} : racemization constant.

1.4 α -amino acids

α -amino acids (AA) are indispensable building blocks of life (Leuchtenberger *et al.*, 2005) and therefore are of great importance for biologically active compounds such as proteins, natural antibiotics, nucleotides or neurotransmitter (*e.g.* GABA). AA consist of an amino group ($-\text{NH}_2$), a carboxyl group ($-\text{COOH}$), a hydrogen ($-\text{H}$), and a characteristic rest (residue), which determines the chemical properties of each AA (Scheme 5). These groups can be bound to the central chiral C-atom (*) in two different sterical conformations leading to L- and D-isomers of each AA. Natural proteins are built up of the 20 proteinogenic L-AA (encoded by the universal genetic code) and thus giving them their chiral properties (Stryer, 2007). Most proteinogenic AA bear only one chiral center. Exceptions are threonine and isoleucine which possess two chiral centers at α - and β -position. Structural motifs thereof are found in many biological molecules making AA particularly interesting for synthetic applications.



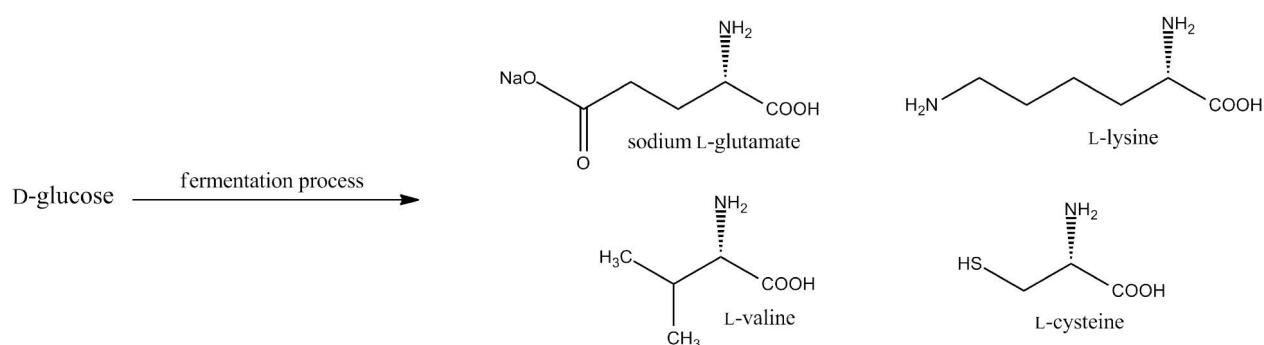
Scheme 5: Structures of chiral α -amino acids consisting of amino group, carboxyl group, hydrogen, and characteristic rest substituted to chiral C-atom. Left: one chiral center. Right: two chiral centers (threonine R: OH, isoleucine R: CH_2CH_3).

There are fourteen L-AA which can be essential for human and/or animal nutrition (Bercovici *et al.*, 1995). Although significantly less frequent, there are also several D-AA occurring in nature. D-alanine, D-glutamate and D-2-aminoadipic acid (non-proteinogenic), for example, are found in the cell walls of microorganisms or in certain secondary metabolites. Moreover, D-serine functions as a signaling molecule in mammalian brains and D-aspartate is a mediator in endocrine systems (Yoshimura *et al.*, 2003). In a variety of organisms such as yeasts, archaea, plants, insects and other eucaryots further D-amino acids have been found. These D-AA are only a few among hundreds of structurally varied proteinogenic AA found in peptides of cell walls and capsules of numerous bacteria and fungi as well as in various natural antibiotics (Soloshonok *et al.*, 2009). Due to their versatile occurrence in living organisms, natural and non-natural AA represent one group of key molecules for life sciences.

1.4.1 Production methods of amino acids

The production of AA is a multibillion dollar business, including the 20 proteinogenic ones and a variety of other naturally and non-naturally occurring AA. There are four major production methods for AA: *extraction from protein hydrolysates*, *chemical synthesis*, *fermentation*, and *biocatalysis*. Mainly the last two biotechnological processes have contributed to the rapid development of the AA market since the 1980s (Leuchtenberger *et al.*, 2005).

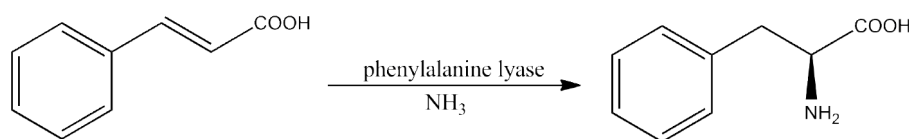
Fermentation of AA is the method of choice for large-scale productions of L-AA. Microorganisms which convert nutrients to various components using their natural or designed metabolic pathways for production of the desired AA are used. Raw materials, such as glucose or corn syrup, are used as a carbon source (Scheme 6). Today there are highly efficient industrial fermentation processes for several AA. For example L-glutamate is produced as a flavor enhancer in a scale of 1.2 million tons/year mainly by Ajinomoto Group, and about 600000 tons/year of L-lysine are produced by Evonik using *Corynebacterium glutamicum*. An efficient fermentation process for L-cysteine (4500 tons/year) has been developed recently by Wacker AG (Gröger *et al.*, 2009).



Scheme 6: Selected amino acids produced *via* fermentation.

Further examples for the fermentative production of AA are L-threonine (40000 tons/year), L-phenylalanine (13000 tons/year) and L-valine (1000 tons/year) (Eggeling *et al.*, 2006).

While natural AA are mainly produced by fermentation, non-natural ones and derivatives thereof can be produced by a broad range of versatile biocatalytic technologies, which are mainly based on enzymatic approaches using hydrolases, oxidoreductases and lyases for enzymatic resolution, DKR or asymmetric synthesis. An example for the enzyme catalyzed production of an L-AA is the addition of ammonia to cinnamic acid using lyases yielding the synthetic sweetener L-phenylalanine (Scheme 7). Several DKR processes for the biocatalytic production of natural and non-natural L-AA have been established by Evonik, such as the resolution of chemically synthesized racemic N-acetyl-AA using a stereospecific L-acylase from *Aspergillus oryzae*, which hydrolyzes only the L-enantiomer. The free L-AA is then separated by crystallization while the remaining N-acetyl-D-AA is recycled by thermal racemization (May *et al.*, 2002). A detailed review about biocatalytic production methods of AA using different enzymatic approaches was published by Gröger and Dietz (Gröger *et al.*, 2009).



Scheme 7: Enzyme catalyzed production of L-phenylalanine by the addition of ammonia to cinnamic acid using phenylalanine lyase.

1.4.2 Industrial applications of amino acids

Due to their functionality and special features arising from chirality, AA are widely applied in the pharmaceutical, agrochemical and food industry. L-glutamate for example is used as a flavor enhancer or glycine as sweetener by the food industry. The pharmaceutical industry requires in particular essential AA for infusions or dietary foods. In addition, there is a huge market for AA (mainly methionine and lysine) as feed additives for pig and poultry nutrition. For synthetic applications, natural as well as synthetic AA have been used as a chiral pool for the preparation of numerous biologically and pharmacologically active compounds. Examples are Valaciclovir, a reverse-transcriptase inhibitor used against herpes simplex, which is based on L-valine (Drauz, 1997) and carbapenem antibiotics incorporating chiral *allo*-threonine derivatives. New peptide drugs, synthesized from AA building blocks, are increasingly developed. Besides, tailor-made AA have gained increasing importance for the preparation of new synthetic enzymes, hormones and immunestimulants. Furthermore, sterically modified AA have found fundamental applications in the rational *de novo* design of peptides and peptidomimetics with enhanced metabolic stability and altered physiological functions (Soloshonok *et al.*, 2009).

In particular, D-AA are becoming increasingly important building blocks for the production of pharmaceuticals and fine chemicals and as chiral auxiliaries in organic syntheses. Applications of D-AA for example include their use as key components in β -lactam antibiotics (e.g. D-phenylglycine), fertility drugs and anticoagulants (Patel, 2008). Presently there are more than 20 D-AA produced at pilot- or technical scale, being not only frequently more potent than the corresponding L-AA, but also often more stable *in vivo* against enzyme degradation (Bommarius *et al.*, 1998; Straathof *et al.*, 2002).

The total market for proteinogenic AA in the year 2004 was estimated to approximately US \$ 4.5 billion. The biggest contribution was made by feed AA (56 %), followed by AA used in the food sector (32 %). The remaining AA are required in the pharmaceutical and cosmetics industry mainly for chiral syntheses of active ingredients (Figure 4). According to a study by the *Business Communication Company*, the AA market for synthetic applications alone was expected to reach US \$ 1 billion in the year 2009 with an annual growth rate of 7 %. While biotechnological and pharmaceutical applications account for about half of the total, they are rising fastest with an average annual growth rate of 9.8 % (Brown, 2005).

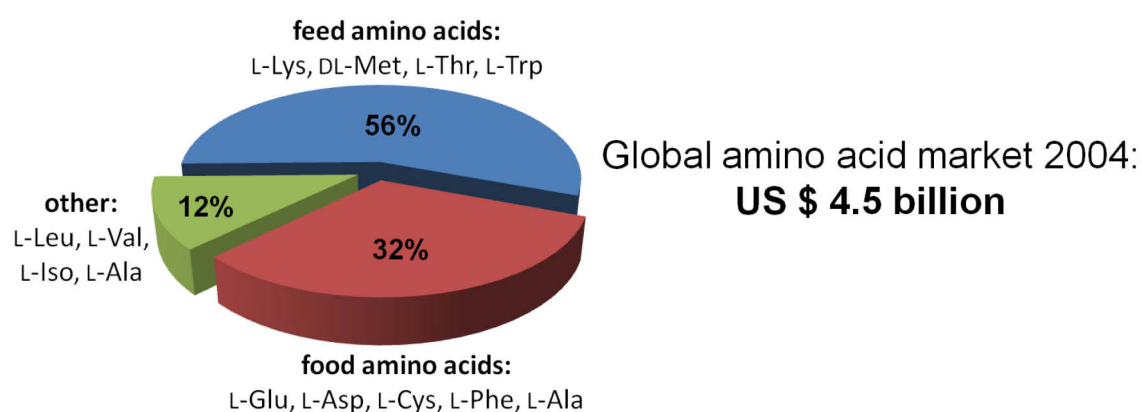
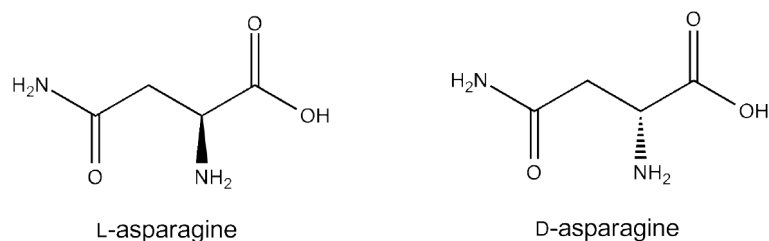


Figure 4: Global amino acid market in the year 2004. Overall volume: US \$ 4.5 billion.

Considering the ubiquitous presence of AA, it is apparent that important markets for them have developed within the pharmaceutical-, food- and feed industry including the products listed above.

1.4.3 Asparagine

Asparagine (Asn) is a non-essential hydrophilic proteinogenic α -amino acid which is involved in the metabolic control of cell functions in nerve and brain tissue. Asn has a carboxyamido side chain (Scheme 8). The biosynthesis of Asn starts from oxalacetate and proceeds *via* aspartate (Asp), which is subsequently amidated using glutamate as an amine donor (Stryer, 2007).

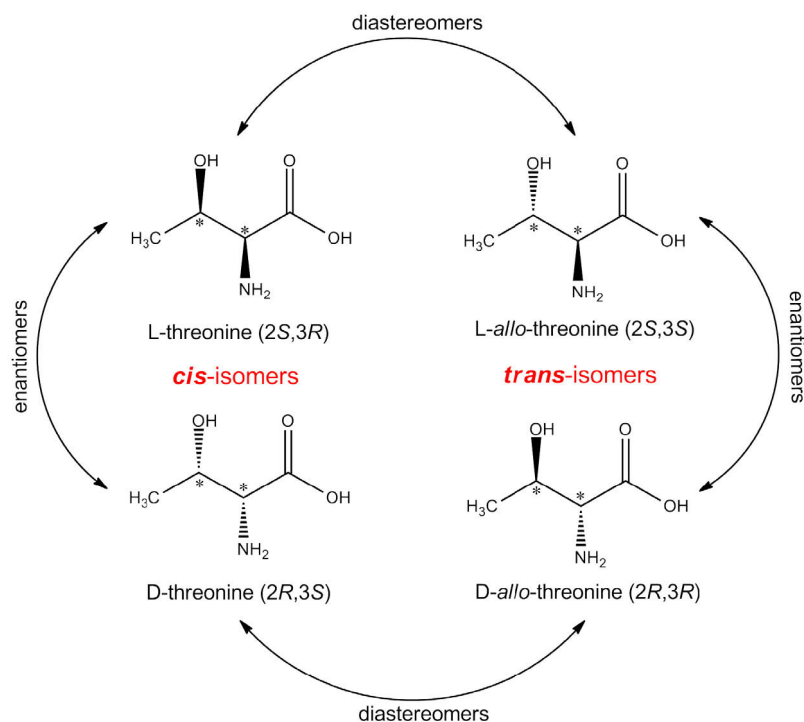


Scheme 8: Enantiomers of asparagine.

Asn is not an essential AA for humans and higher animals and thus is not used as food or feed additive. However, due to its crystallization properties it was chosen as a model substrate for enzyme-assisted preferential crystallization. Besides threonine it is the only proteinogenic AA acid that forms conglomerates as solid racemate (chapter 1.3.2). L-Asn can be produced at small scale by extraction from protein hydrolysates or by enzymatic amidation of Asp using asparagine synthetase.

1.4.4 Threonine and its stereoisomers

Threonine (Thr) is a polar β -hydroxy- α -amino acid. Like isoleucine it is one of the two proteinogenic AA with two chiral centers and thus exists in four distinct stereoisomeric forms (Scheme 9). Both *cis*-isomers as well as both *trans*-isomers are mirror-images (enantiomers) of each other. The *trans*-isomers of Thr are called *allo*-threonine (*allo*-Thr) and differ from Thr by the stereoconformation of the α -amino and the β -hydroxy groups, which are pointing into opposite directions. Thr and *allo*-Thr are called diastereomers.



Scheme 9: Stereoisomers of threonine.

L-Thr is an essential AA and is produced mainly by fermentation with optimized strains of *Escherichia coli* and *Serratia marcescens* (Leuchtenberger *et al.*, 2005). The enzymes for the synthesis of L-Thr (*e.g.* threonine synthase) are overexpressed so that L-Thr can be produced in high concentrations up to 100 g/L (Ikeda *et al.*, 2003). Down-stream processing is performed after biomass separation and pH adjustment by concentration and crystallization (Hermann, 2003). Main producers are Ajinomoto, ADM and Evonik with annual production rates of about 40000 tons (Eggeling *et al.*, 2006).

The vast bulk of L-Thr is used as feed additive as it is the limiting AA in growing pigs and poultry. However, enantiomerically pure β -substituted α -amino acids, including the stereoisomers of Thr, are valuable building blocks for the synthesis of peptidomimetics and enzyme inhibitors. The incorporation of a β -substituent into an α -amino acid generally leads to restricted conformational flexibility in peptides, offering the prospect for the development of high affinity ligands for receptors (Enright *et al.*, 2003). Hence, each isomer is a useful intermediate for the synthesis of chiral compounds such as antibiotics (Kataoka *et al.*, 1998).

allo-Thr is a constituent of many biologically active peptides since its functionalized β -carbon is involved in many biomolecular recognition processes. Examples for bioactive compounds having Thr-residues are phytotoxic syringopeptins, the antiviral agent viscosin (Burke *et al.*, 1989), the antibiotic cyclodepsipeptide complex CDPC 3510 isolated from *Fusarium* (Flippin *et al.*, 1989), or the glycopeptidolipid antigens from mycobacteria responsible for pulmonary and disseminated infectious diseases particular in AIDS patients. The incorporation of D-*allo*-Thr instead of L-Thr in the backbone of peptides and proteins increases resistance towards proteolysis. By conserving the natural (*R*)-stereochemistry at the β -carbon while inverting the α -configuration, enzymatic attacks can be inhibited. Moreover, peptide analogues with *allo*-Thr may have an enzyme-inhibitory effect, since the β -hydroxy group acts as recognition site in many enzymatic processes. An extensive list of bioactive compounds with *allo*-Thr residues is given by Wipf and Miller (Wipf *et al.*, 1993).

In plants and microorganisms, Thr is synthesized from Asp *via* α -aspartyl-semialdehyde and homoserine which undergoes *O*-phosphorylation. The resulting *O*-phospho-homoserine is then hydrolyzed with relocation of the OH-group (Chassagnole *et al.*, 2001).

In spite of its biological relevance, the use of *allo*-Thr for large-scale syntheses is hampered by high costs of multi-step production processes and careful purification steps (see Discussion).

1.5 Enzymes and their classification

Enzymes are proteins that catalyze chemical reactions by decreasing the activation energy and thus increasing the reaction rate. In general they do not alter the reaction equilibrium itself but increase the speed at which it is reached. This is achieved by stabilizing the transition state of the reactants from which they decay into one or more products. The activity of enzymes is given in Units (U) and is defined as the amount of enzyme that catalyzes the conversion of one μmol of substrate per minute at standard conditions.

According to the *Nomenclature Committee of the International Union of Biochemistry and Molecular Biology* (NC-IUBMB) enzymes are divided into six main classes due to their reaction specificity (Table 1). Each class is divided into further subclasses and groups assigning a defined EC number (enzyme commission number) to every single enzyme. This enzyme code consists of the letters EC followed by 4 numbers separated by dots. The first number defines the enzyme class, whereas the following numbers sub-classify the enzyme according to its natural type of reaction, the substrate and the coenzyme (if required).

Table 1: Classification of enzymes according to NC-IUBMB.

Enzyme class	Catalyzed reaction	Major subclasses
1. Oxidoreductases	redox reactions (transfer of electrons)	dehydrogenases, oxidases, reductases, peroxidases, catalases, oxygenases, hydroxylases
2. Transferases	transfer of functional groups	transketolases, transaminases, kinases
3. Hydrolases	hydrolysis reactions	proteases, lipases, esterases, glycosidases, peptidases, amidases, amylases
4. Lyases	addition of groups to double bonds or formation of double bonds by non-hydrolytic cleavage	decarboxylases, aldolases, (de-) hydratases, synthases
5. Isomerases	transfer of groups within molecule for structural or geometrical rearrangement	racemases, epimerases, mutases
6. Ligases	ligation of two substrates by condensation reactions coupled to ATP cleavage (formation of C-C, C-S, C-N, C-O bonds)	carboxylases, synthetases

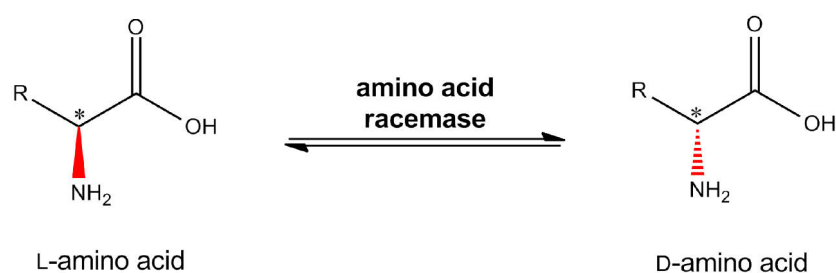
1.6 Racemases

1.6.1 Overview

Racemization is defined as the irreversible formation of a racemate from a pure enantiomer and is associated with the loss of optical activity (Ebbers *et al.*, 1997). Therefore, it can be described as an energetic ‘downhill’ reaction due to an increase of entropy and is thus often considered as an undesired side reaction rather than a useful biotransformation (Eliel *et al.*, 2001).

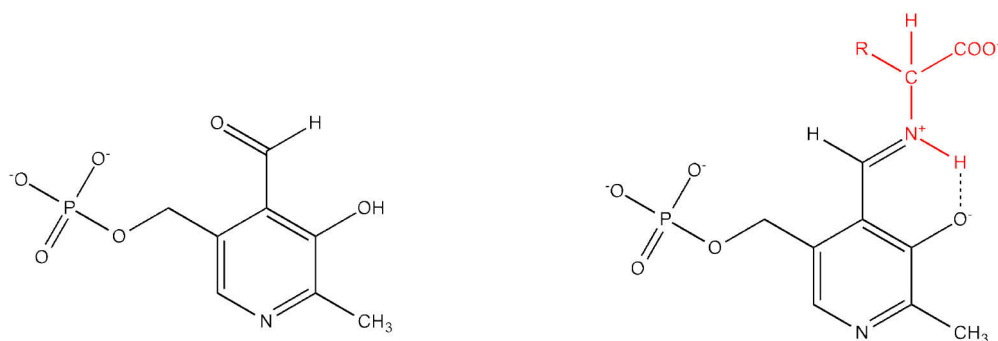
Although L-amino acids are predominant in living organisms, also D-amino acids play an important role, for example in bacterial cell walls, as already referred to in chapter 1.4. Most of them are produced by racemization from the corresponding L-amino acids by racemases (Scheme 10). Therefore, these enzymes, which belong to the group of isomerases (EC 5.1.X.X), play an important role in the D-amino acid metabolism of most living organisms. With the exception of phenylalanine racemase (EC 5.1.1.11), which requires ATP for catalysis, amino acid racemases can be divided into two major groups, differing in their catalytic mechanisms for racemization:

- pyridoxal-5'-phosphate-dependent racemases: racemization occurs *via* an unstable chiral Schiff-base intermediate (*e.g.* amino acid racemase, alanine racemase)
- pyridoxal-5'-phosphate-independent: racemization occurs *via* a two-base mechanism without a cofactor (*e.g.* glutamate racemase, proline racemase)



Scheme 10: Racemization of α -amino acid by amino acid racemase.

Pyridoxal-5'-phosphate (PLP, Scheme 11) is a biologically active phosphorylated derivative of vitamin B₆ and represents one of nature's most versatile cofactors (Schneider *et al.*, 2000).



Scheme 11, left: Pyridoxal-5'-phosphate (PLP). **Right:** PLP bound to an α -amino acid (red) as a Schiff-base.

According to the classification of Christen and coworkers, who classified PLP-dependent enzymes depending on the carbon atom involved in the reaction, amino acid racemases belong to the α -class of PLP-dependent enzymes (Alexander *et al.*, 1994). Another classification was proposed by Grishin (Grishin *et al.*, 1995) who classified PLP-dependent enzymes based on amino acid sequence alignments into 5 different fold types:

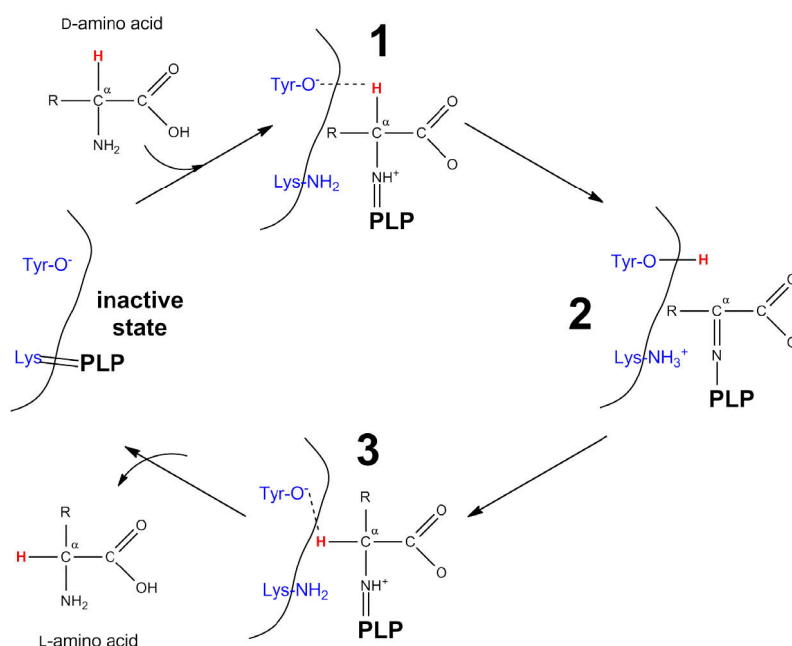
- Fold Type I: aspartate amino transferase family
- Fold Type II: tryptophan synthase family
- Fold Type III: alanine racemase family**
- Fold Type IV: D-amino acid aminotransferase family
- Fold Type V: glycogen phosphorylase

Since the amino acid racemases used in this work are PLP-dependent enzymes of Fold Type III, only this group of racemases will be described in more detail.

1.6.2 Structure, function and catalytic mechanism of PLP-dependent amino acid racemases

In this thesis two different amino acid racemases with broad substrate specificity from *Pseudomonas putida* strains KT2440 and NBRC12996 (EC 5.1.1.10) have been used. According to their origin they are entitled AArac2440 and AArac12996. Both enzymes share a AA sequence identity of 94 % and belong to Fold Type III. Each monomer consists of 409 amino acids (ca. 44 kDa per monomer). According to the crystal structure of alanine racemase from *Pseudomonas aeruginosa* (EC 5.1.1.1) each monomer consists of a classical α/β -barrel and a second β -strand domain. PLP is bound within the active center with the phosphate anchored to the N-terminus of an α -helix, H-bond interactions to the 3'-OH group, and is covalently bound to a lysine side chain *via* a Schiff-base (Schneider *et al.*, 2000; Eliot *et al.*, 2004).

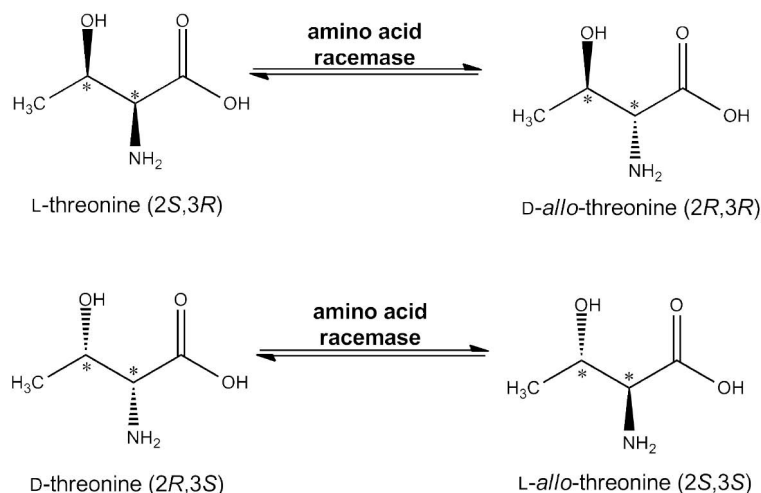
PLP mediates the base-catalyzed α -proton abstraction *via* an unstable chiral Schiff-base intermediate between the α -amino acid and the aromatic aldehyde. Thereby, racemization of the substrate can be divided into three major steps (Scheme 12).



Scheme 12: Catalytic mechanism of PLP-dependent amino acid racemases *via* a Schiff-base intermediate. Inactive state: internal Schiff-base; 1) external Schiff-base; 2) resonance-stabilized quinoid-type carbanion intermediate; 3) reprotonation of α -carbanion.

In the inactive state (absence of substrate) PLP is bound covalently to the ϵ -amino group of a lysine residue in the active center *via* an internal Schiff-base (aldimine). When the amino acid substrate enters the active center PLP is transferred from the lysine residue to the α -amino group of the amino acid to form an external Schiff-base (1). The α -proton of the substrate is then abstracted by a tyrosine residue in the active center to form a resonance-stabilized quinoid-type achiral carbanion intermediate (2). Racemization further proceeds *via* reprotonation of the α -carbanion which can occur from both sides yielding both enantiomers (3) (Reynolds *et al.*, 1991; Schnell *et al.*, 2003; Yoshimura *et al.*, 2010).

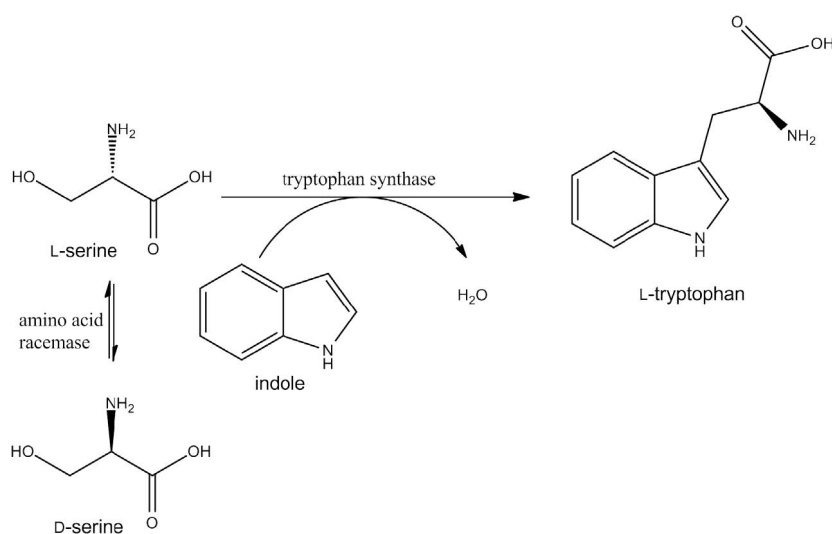
According to the stereochemical properties of the substrate, amino acid racemases can also catalyze the isomerization of diastereomers such as threonine (Scheme 13). Since only the stereoconformation of the α -amino group is affected by the amino acid racemase, while the β -hydroxy group remains unmodified, isomerization of L- and D-threonine yields the corresponding *allo*-forms.



Scheme 13: Isomerization of L- and D-threonine by amino acid racemase.

1.6.3 Applications of amino acid racemases

Racemases are increasingly used for dynamic kinetic resolutions (DKR) or as auxiliary enzymes in biocatalytic recycling processes. One noteworthy example is the biocatalytic synthesis of L-tryptophan performed by a coupled reaction of tryptophan synthase and an amino acid racemase starting from racemic serine and indole in a DKR process (Scheme 14). Under optimized conditions about 110 g/L of L-tryptophan was formed after 24 h of incubation in a 200 L reactor using whole cells of *E. coli* and *P. putida* (Ishiwata *et al.*, 1990). Further examples are the preparation of labeled aromatic amino acids such as L-tyrosine, L-DOPA and L-tryptophan using alanine racemase, the use of glutamate racemase in auxiliary processes for the production of D-phenylalanine and D-tyrosine, and the production of D-glutamate involving glutamate racemase (Schnell *et al.*, 2003).



Scheme 14: Synthesis of L-tryptophan in a DKR process using amino acid racemase. Tryptophan synthase enantioselectively catalyzes the β -substitution reaction of L-serine to form L-tryptophan, while the amino acid racemase catalyzes the simultaneous racemization of serine.

CHAPTER 2

AIM OF THE THESIS

2 Aim of the thesis

The general aim of this thesis is the development of processes for racemase supported crystallization of chiral amino acids (AA). To achieve this goal, two different approaches should be investigated starting from either racemic or enantiopure substrates:

1) *Enzyme-assisted preferential crystallization*

By the combination of preferential crystallization (crystallization of a single enantiomer from a racemic solution) with enzymatic racemization of the remaining enantiomer, yield limitations of classical chiral resolution processes, which are usually limited to a maximum yield of 50 %, should be overcome. This concept can only be applied to conglomerate forming racemates, since preferential crystallization from racemic solutions is limited to them. Due to only little information about conglomerate forming AA in literature, suitable substrates (racemic AA) for this process have to be identified beforehand. Therefore, crystallization properties (conglomerate forming system or racemic compound) and potential acceptance as substrate for enzymatic racemization have to be investigated. In order to set up an appropriate process, suitable substrate/enzyme pairs have to be characterized with regard to optimal process temperature, pH, stability and kinetic parameters (V_{\max} , K_m).

After successful identification and characterization of a suitable model substrate, a process for preferential crystallization of chiral AA with integrated enzymatic racemization for an increased maximum yield, should be established.

2) *Enzymatic production of chiral allo-threonine from bulk threonine*

Due to the limited substrate range for enzyme-assisted preferential crystallization, another approach for the production of chiral AA, by combination of crystallization and enzymatic isomerization, should be investigated. This approach focuses on the isomerization of diastereomers with sufficiently different solubility limits in the applied medium. A suitable substrate is the cheap bulk AA L-Thr which can be isomerized to the high-priced *allo*-Thr, a valuable intermediate for pharmaceutical applications, using amino acid racemases. The produced *allo*-Thr can be removed easily by crystallization.

After evaluation of racemases with sufficient activity for the isomerization of Thr, a lab-scale process for the production of chiral D- and L-*allo*-Thr should be developed.

Two related amino acid racemases (EC 5.1.1.10) with broad substrate range from *P. putida* KT2440 and *P. putida* NBRC12996 are available. For the application as biocatalyst during crystallization processes, these enzymes have to be overexpressed in *E. coli* and purified to homogeneity.

CHAPTER 3

PUBLICATIONS

3 Publications

Publication 1

Enzyme-assisted physicochemical enantioseparation processes - Part I: Production and characterization of a recombinant amino acid racemase

Würges, K., Petruševska, K., Serci, S., Wilhelm, S., Wandrey, C.,
Seidel-Morgenstern, A., Elsner, M. P. & Lütz, S.

Journal of Molecular Catalysis B: Enzymatic, 2009

Vol. 58, 10–16

DOI: 10.1016/j.molcatb.2008.10.006

Reproduced with the permission of Elsevier Ltd.



Enzyme-assisted physicochemical enantioseparation processes: Part I. Production and characterization of a recombinant amino acid racemase

Kerstin Würges^a, Katerina Petrusovska^b, Stephanie Serci^c, Susanne Wilhelm^c,
Christian Wandrey^a, Andreas Seidel-Morgenstern^b, Martin P. Elsner^b, Stephan Lütz^{a,*}

^a Institute of Biotechnology 2, Research Centre Juelich, D-52425 Juelich, Germany

^b Max Planck Institute for Dynamics of Complex Technical Systems, Magdeburg, Germany

^c Institute of Molecular Enzyme Technology, University of Duesseldorf, Germany

ARTICLE INFO

Article history:

Received 20 March 2008

Received in revised form 9 October 2008

Accepted 16 October 2008

Available online 30 October 2008

Keywords:

Amino acid racemase

Enzyme purification

Integrated enantioseparation process

Chiral chromatography

Preferential crystallization

ABSTRACT

The demand for enantiopure substances, e.g. for pharmaceutical applications or fine chemical production, continues to increase. This has led to the development of numerous stereoselective synthesis methods. Nevertheless a large number of chemical syntheses still result in racemic mixtures making a subsequent enantioseparation step necessary and thus are restricted to a maximum yield of 50%. Our work focuses on strategies to overcome this limitation by combining physicochemical separation processes with enzymatic racemization of the unwanted enantiomer in order to produce enantiopure amino acids. This paper deals with the production and characterization of a suitable amino acid racemase with broad substrate specificity (EC 5.1.1.10) from *Pseudomonas putida* which we cloned into *Escherichia coli*. Two enzyme lyophilizates of different purity were obtained from which the crude (CL) was sufficient for the racemization of methionine (Met) and the pure (PL) was used for asparagine (Asn). Racemization reactions of *D*-/*L*-Asn in H₂O and *D*-/*L*-Met in 95 vol.% 100 mM KP₁-buffer, 5 vol.% methanol (MeOH) at different pH values and temperatures were characterized. The studied range of reaction parameters was chosen in dependency on planned enantioseparation processes. We found increasing V_{max} values when temperature was risen stepwise from 20 to 40 °C for both systems and when pH was shifted from 6 to 8 for the Met system. The presented results provide the basis for engineering enzyme-assisted physicochemical enantioseparation processes.

© 2008 Elsevier B.V. All rights reserved.

1. Introduction

Chirality in nature and living systems is of great impact for a variety of active compounds interacting with them. The molecular building blocks of life, such as amino acids and sugars that form peptides, proteins and polysaccharides exist of chiral structures. Thus, optically pure enantiomers are of great interest for the fine chemical and pharmaceutical industry [1,2]. Despite an increasing number of stereoselective synthesis there are still a lot of reactions

that lead to racemic mixtures of the desired homochiral products. The scientific and economic relevance of homochiral substances has led to the development of numerous separation techniques based for example on chromatography [3–5], crystallization [6,7] and stereoselective biotransformations [8,9] just to mention a few. A major drawback of these resolutions is the yield which is principally limited to a maximum of 50%. An attractive solution to overcome this limitation is the combination of a physicochemical separation process e.g. chromatography [10] or preferential crystallization (PC) [11] with an enzymatic process to racemise the unwanted enantiomer [12,13]. In contrast to stereoselective biotransformations, such as the reduction of prochiral ketones to optically active alcohols [14,15] where only one enantiomer can be produced by a single biocatalyst, here *L*- and *D*-enantiomers can be obtained according to the chosen process route.

Since enantiopure amino acids (AA) are of great industrial relevance, e.g. *L*-Met for infusion solutions or food additives (ca. 600 t/year), AA are an interesting substance group for this approach.

* Corresponding author. Tel.: +49 2461 614388; fax: +49 2461 613870.

E-mail addresses: k.wuerges@fz-juelich.de (K. Würges),
petrusovska@mpi-magdeburg.mpg.de (K. Petrusovska),
s.serci@fz-juelich.de (S. Serci), s.wilhelm@fz-juelich.de (S. Wilhelm),
c.wandrey@fz-juelich.de (C. Wandrey),
seidel-morgenstern@mpi-magdeburg.mpg.de (A. Seidel-Morgenstern),
mpelsner@mpi-magdeburg.mpg.de (M.P. Elsner), s.luetz@fz-juelich.de (S. Lütz).

Table 1
Bacterial strains and plasmids used for cloning of AA racemase 5.1.1.10 and transformation into competent cell line.

Strains/plasmids	Genotype/phenotype	Reference/source
<i>P. putida</i> KT2440 DSM6125		Nelson et al., 2002 [26]
<i>E. coli</i> DH5 α	supE44 Δ (lacZYA-argF)U196 (ϕ 80 Δ lacZM15) hsdR17 recA1 endA1 gyrA96 thi-1 relA1	Woodcock et al., 1989 [27]
<i>E. coli</i> BL21 (DE3)	F ⁻ ompT hsdSB(r_B^- m_B^-) gal dcm (λ clts857 ind1 Sam7 nin5 lacUV5-T7 gene1)	Studier and Moffat, 1986 [28]
pET22b	T7-expression vector for <i>E. coli</i> , PelB signal sequence, Ap ^r	Novagen

Therefore we chose to use an already well known amino acid racemase with a broad specificity (EC 5.1.1.10) [16] as biocatalyst which was cloned into *E. coli* BL21 (DE3). We analyzed kinetic properties of two differently pure enzyme preparations with respect to racemization of the enantiomers of methionine (Met) and asparagine (Asn). Met, which is a racemic compound forming system and thus can be enantioseparated by PC [7], has been chosen as possible substrate for the application in an integrated enzymatic racemization process with chromatographic enantioseparation; Asn has been chosen because it is a suitable substance for enantioseparation by PC. Bechtold and coworkers [17] recently presented a detailed characterization of an amino acid racemase from *Pseudomonas putida* DSM 3263 (which is identical to the one used in our study) in which they concentrated on the racemization of *D*- and *L*-Met in organic-aqueous solutions. Our work is focusing on two different reaction systems: (1) racemization of *D*- and *L*-Met in 95 vol.% 100 mM KP_i-buffer (pH 7.0), 5 vol.% MeOH, which has been chosen suitable for the combination with chromatographic enantioseparation of methionine. (2) Racemization of *D*- and *L*-Asn in H₂O which can be separated by PC. PC can be an interesting and highly efficient method for the optical resolution of conglomerate forming substances. In contrast to racemic compounds where both enantiomers coexist in one unit cell, a conglomerate is defined as a mechanical mixture of crystals of both enantiomers [18]. Nevertheless, only a few natural amino acids do belong to the group of conglomerates such as threonine (Thr) and asparagine [19]. PC of Thr in aqueous solutions has already been studied in detail by Elsner et al. [11] and others [20,21]. To the best of our knowledge so far there is neither published data about preferential crystallization nor about racemization of Asn.

2. Experimental

2.1. Materials

NaCl and (NH₄)₂SO₄ were obtained from KMF Laborchemie Handels GmbH (Lohmar, Germany), yeast extract and NaH₂PO₄ were purchased from Merck (Darmstadt, Germany). Isopropyl- β -D-thiogalactopyranosid (IPTG) and carbenicillin disodium salt were obtained from Carl Roth GmbH (Karlsruhe, Germany), pyridoxal-5'-phosphate (PLP) was obtained from Serva Feinbiochemica (Heidelberg, Germany). Diethylaminoethyl (DEAE) sepharose fast flow was purchased from Amersham Biosciences (UK). For SDS-polyacrylamid gel electrophoresis the NuPAGE test kit from Invitrogen (Carlsbad, CA, USA) and the Precision Plus Protein™ Standard Dual Color from Bio-Rad (Hercules, CA, USA) were used. Ultrapure water (Milli-Q by Millipore, Schwalbach, Germany) has been used exclusively during all procedures. All other chemicals were either purchased from Sigma-Aldrich or Fluka (Munich, Germany) and were of the highest available purity.

2.2. Cloning and transformation

Bacterial strains and plasmids. The strains and plasmids used are listed in Table 1. *P. putida* KT2440 and *E. coli* DH5 α were used for cloning experiments and *E. coli* BL21 (DE3) as a heterologous expression host for plasmid-encoded racemase (orf PP3722).

Media and growth conditions. LB medium was routinely used to cultivate *E. coli* strains. Precultures for all experiments were prepared overnight in 5 ml LB medium in glass tubes at 37 °C. Plasmid-carrying *E. coli* cells were selected with 100 μ g/ml ampicillin.

DNA manipulation and PCR. DNA fragments were amplified by PCR standard methods. DNA modifying enzymes (Fermentas, St. Leon-Rot, Germany) were used according to manufacturer's instructions. Plasmid DNA was prepared using the "HiSpeed Plasmid Midi" kit (Qiagen, Hilden, Germany).

PCR amplification, cloning and expression of racemase. Genomic DNA was isolated from *P. putida* KT2440 by using the DNeasyTissue-Kit (Qiagen). The gene was amplified by PCR. The PCR conditions used with Primers aaRaz NdeI up 5'-CAA CAT ATG CCC TTT CGC CGT ACC-3' and aaRaz XhoI down 5'-TTT CTC GAG TCA GTC GAC GAG TAT CTT-3' were as follows: initial denaturation 5 min at 98 °C, 35 cycles of 98 °C for 45 s, 56 °C for 45 s, 72 °C for 60 s and a final elongation 10 min at 72 °C.

TripleMaster polymerase used in PCR was purchased from Eppendorf (Hamburg, Germany). PCR was performed according to the manufacturer's recommendations. The size of the PCR product was checked on a 1% agarose gel and the product was excised from the gel and purified with a "Perfect Gel-Cleanup-Kit" (Eppendorf) used according to the manufacturer's protocol. The fragment was digested with NdeI/XhoI and ligated in pET22b which was hydrolyzed by the same restriction enzymes. *E. coli* DH5 α was transformed with the resulting ligation.

Recombinant plasmids were identified and further characterized by restriction enzyme digestion. The DNA sequence of the amplified racemase was verified by DNA sequencing (Sequiseive, Vaterstetten, Germany).

E. coli BL21 (DE3) was transformed with the expression plasmid. A single colony was inoculated to LB medium containing 0.4% (w/v) glucose and 100 μ g/ml ampicillin and grown at 37 °C on a shaking incubator until an optical density at 580 nm of 0.5 was reached. IPTG was then added to a final concentration of 0.4 mM for induction of expression. The induced cells were incubated at 37 °C for 2 h and harvested by centrifugation at 14,000 rpm for 15 min. The expression was analyzed by SDS-PAGE.

2.3. Fermentation of recombinant *E. coli* BL21 (DE3)

E. coli BL21 (DE3) was grown in a modified LB medium containing 0.5% (w/w) trypton, 0.25% (w/w) yeast extract, 0.25% (w/w) NaCl, 0.025% (w/w) MgSO₄ heptahydrate, 0.013% (w/w) NaH₂PO₄, 0.5% (w/w) *D*(+)-glucose monohydrate and 50 μ g/ml carbenicillin disodium salt. A 50 mL preculture was grown for 6 h at 37 °C and 200 rpm in a 250-mL shaking flask after inoculation with 1 mL of the cryoculture (stored at -80 °C). 5 times 200 mL of aforementioned LB medium in 1 L shaking flasks were inoculated with 10 mL of the preculture to yield a volume of about 1 L starting culture for large scale fermentation. The starting culture was grown over night (18 h) at 27 °C and 200 rpm until it reached an OD₆₀₀ of 4.7. A fed-batch fermentation was performed in a process-controlled stainless steel bioreactor (Chemup, Richard Stühler GmbH & Co KG, Lahr, Germany) with a working volume of 30 L (pH 7.0, 500 rpm, 37 °C).

Table 2

Specific activities and yields of crude lyophilizate, resuspended precipitate and lyophilizate of pooled active DEAE chromatography fractions. Specific activities were measured at 35 °C and an initial substrate concentration of 200 mM *L*-Asn in H₂O.

Step	Mass/volume	Protein concentration	Specific activity [U/g _{prot}]	Total activity [U]	Yield
Crude lyophilizate	10,000 mg	77%	381	2940	100%
(NH ₄) ₂ SO ₄ -precipitation	27.5 mL	69.7 mg/mL	560	1074	37%
DEAE chromatography and lyophilization	175 mg	68%	3703	441	15%

Therefore 20 L of LB medium (as described above but containing 2% (w/w) *D*(+)-glucose monohydrate and 0.02 vol.% antifoam in addition) were fed into the reactor and inoculated with 1 L starting culture. The expression of the recombinant amino acid racemase was induced with 100 μmol/L IPTG after 3 h when the fermentation broth reached an OD₆₀₀ of about 5.5. After induction *D*(+)-glucose monohydrate was fed to the fermentation broth (ca. 30 g/h) and the temperature was decreased to 27 °C. After 24 h 750 g cells (biowet-mass, BWM) were harvested by centrifugation (20 min, 15,000g, 4 °C) and washed with 0.85% NaCl.

2.4. Purification of racemase

The overproduced racemase was released from the cytosol of *E. coli* BL21 (DE3) by ultrasonic cell-disruption in a continuous flow-cell sonifier (Branson W250, Danbury, CT, USA) from a 20% (w/w) cell suspension in 10 mM KP_i-buffer, pH 7.0 (containing 50 μM PLP and lysozyme from hen egg white) at 4 °C. Cell debris were removed by centrifugation (20 min, 20,000g, 4 °C), the supernatant was frozen portion wise at –20 °C, lyophilized for about 48 h and stored at 4 °C until it was used. A total mass of 93 g of crude lyophilizate (*CL*) could be obtained.

For further purification 10 g of *CL* were dissolved in 1000 mL of 10 mM KP_i, pH 7.0, and 176.0 g of (NH₄)₂SO₄ (30% saturation) were added to the solution. After 30 min the precipitate was removed by centrifugation (20 min, 10,000g, 4 °C) and additional 163.3 g of (NH₄)₂SO₄ (55% saturation) were added to the supernatant (1008 mL). The now forming precipitate was again removed by centrifugation; the pellet was resuspended in 100 mL of 10 mM KP_i, pH 7.0, and filtrated (pore size 0.8 μm). 111 mL of filtrate were washed with two volumes of H₂O in an Amicon-cell (membrane: Pall Omega 10kDa, A: 41.8 cm²) and afterwards concentrated to 30 mL (all steps were done in an ice bath for cooling).

The concentrate was then applied with a flow of 5 mL/min to a DEAE-sepharose column (5 × 25 cm, operated by ÄKTApurifier from Amersham Biosciences, Uppsala, Sweden) which had been equilibrated with 5 column volumes of 10 mM KP_i, pH 7.0. After the column had been washed (10 mL/min) with 2 volumes of the same buffer but containing 50 mM NaCl, the enzyme was eluted with the buffer supplemented with 100 mM NaCl. The active fractions, which have a specific absorption maximum at 420 nm, emerged at the beginning of elution and were pooled. The pooled fractions were washed with 3 × 90 mL of 10 mM KP_i, pH 7.0, in an Amicon-cell (membrane: Pall Omega 10kDa, A: 41.8 cm²) and concentrated to 10 mL. The enzyme solution was then frozen in liquid nitrogen and lyophilized. 175 mg of pure lyophilizate (*PL*) (light yellow powder) were obtained. To prevent a loss of the cofactor PLP during purification all buffers contained 20 μM of PLP.

2.5. Analytics

Enzyme assays were done at 650 rpm in 1.5 mL Eppendorf reaction vials which were placed in an Eppendorf Thermomixer. Calibrations were performed under assay conditions in the range of estimated analyte concentrations.

Methionine. Activities for racemization of Met solutions were measured by following the enantiomeric composition of the reaction medium via HPLC (Crownpak CR(+)) column (0.4 cm × 15 cm), Daicel Chem. Ind.; HClO₄, pH 2; T = 25 °C; 0.6 mL/min, V_{inj} = 5 μL; λ_{abs} = 200 nm). For kinetic studies activities of *CL* were measured as follows: 0.1 mg/mL of *CL* were added to 95 vol.% 100 mM KP_i-buffer, 5 vol.% MeOH, containing *L*- and *D*-Met ranging from about 7 to 200 mM. Initial reaction rates were determined by taking samples at three points of time. Therefore 100 mg reaction solution were diluted with 900 mg of HClO₄, pH 1.0, to stop the reaction and analyzed by HPLC to determine their enantiomeric composition. The slope of product formation, which was calculated by linear regression using Microsoft Excel, represents the initial reaction rates for the particular substrate concentration. (All samples were taken in duplicate, results represent mean values.)

Asparagine. Kinetic studies of *PL* were performed in aqueous *L*- and *D*-Asn solutions containing approximately between 20 and 250 mM Asn (depending on solubility at certain temperature) with concentrations of 0.1 mg *PL* per mL. Activity assays were done as described above but analyzed under different HPLC conditions (HClO₄, pH 1; T = 0 °C; 0.4 mL/min).

A control showed that neither methionine nor asparagine racemize spontaneously after dilution with HClO₄, pH 1 (done by HPLC analysis after 1 h incubation time).

Protein determination. Protein concentrations of both enzyme preparations were determined at 30 °C by a standard Bradford assay [22] using a Shimadzu UV-1601 photometer.

SDS-PAGE. Gel electrophoresis was performed according to the manufacturer's instructions using the NuPAGE test kit by Invitrogen. A total protein loading of about 1 μg for *CL* and about 0.1 μg for *PL* each were applied to a gel pocket. A protein standard solution was applied to a nearby pocket and electrophoresis was performed at 200 V for 45 min. After developing and incubating the gel, it was scanned with a desktop scanner.

3. Results and discussion

3.1. Enzyme purification

The recombinant amino acid racemase was purified from *E. coli* BL21 (DE3) in two independent steps leading to two differently pure enzyme preparations. Lyophilization of the cell-free protein extract (from 750 g BWM) gave 93 g of crude lyophilizate (*CL*) with a protein concentration of 77 wt%. While *CL* showed no other reactions on Met than racemization (constant mass balance over several days determined by HPLC) it exhibited a so far unidentified side reaction on Asn that lead to a degradation of the *L*-enantiomer. Therefore 10 g of *CL* were further purified as described resulting in 175 mg of pure lyophilizate (*PL*) with a protein concentration of 68 wt%. Table 2 summarizes specific activities and yields of the purification steps. The purified enzyme preparation did not show the aforementioned side reaction on *L*-Asn anymore. Fig. 1 shows the SDS-PAGE protein band patterns of both preparations. While *CL* is a mixture of all proteins present in the cytoplasm of *E. coli* BL21 (DE3), the band pattern for *PL* shows only one sharp band below 50 kDa which

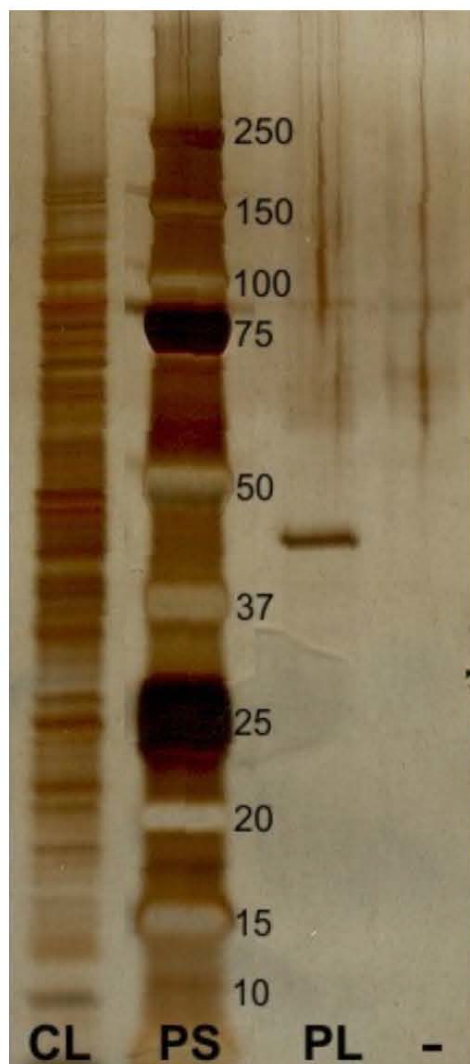


Fig. 1. SDS-PAGE of crude lyophilizate (CL), pure lyophilizate (PL) and protein standard (PS, molecular weights are given in kDa). The protein loading was about 1 μg for CL and 0.1 μg for PL. PL exhibits only one sharp band below 50 kDa, while CL shows a composition of all intracellular proteins. The right lane (-) represents an empty lane without any protein loading.

matches the MW of the cloned amino acid racemase (homodimer of $2 \times$ ca. 45 kDa).

3.2. Enzyme kinetics

The amino acid racemase which has been used for this work follows a reversible three-step Michaelis–Menten mechanism and uses PLP as cofactor. While no substrate is present, PLP is bound to a lysine residue in the active site via an internal Schiff-base. When a substrate molecule enters the active site, PLP is transferred from Lys to the α -amino group of the substrate to form an external Schiff-base. Racemization proceeds then via abstraction of the α -hydrogen atom to form a quinoid-type carbanion intermediate and subsequent reprotonation on the opposite or the original side. A more detailed description of the catalytic mechanism can be found elsewhere [12,23,24].

The racemization can be described by a reversible three-step mechanism where the conversion of the *L*- to the *D*-substrate

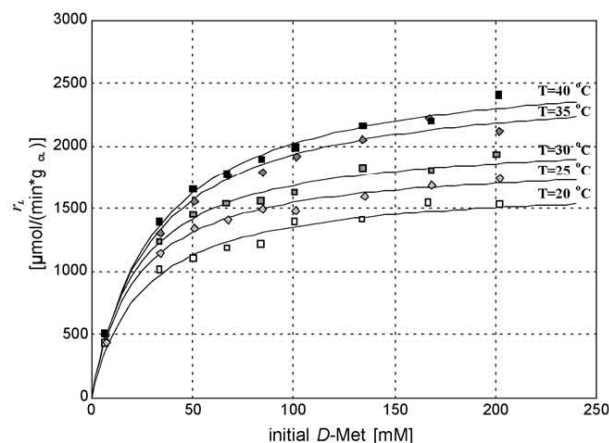
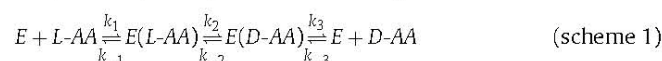


Fig. 2. Experimental data for *D*-methionine racemization with CL shown by symbols. Lines show data calculated by non-linear fitting for racemization of *D*-Met using K_m and V_{max} shown in Table 3. Solvent: 95 vol.% 100 mM KP_i -buffer (pH 7.0), 5 vol.% MeOH.

enzyme complex is pooled into one step:



with

$$K_{m,L} = \frac{k_{-1}k_{-2} + k_{-1}k_3 + k_2k_3}{k_1(k_{-2} + k_2 + k_3)}; \quad K_{m,D} = \frac{k_{-1}k_{-2} + k_{-1}k_3 + k_2k_3}{k_{-3}(k_{-1} + k_{-2} + k_2)}$$

where E is the racemase, k_i are the reaction rate constants for the single reactions and $K_{m,L/D}$ are the dissociation constants for the substrate/product binding to the enzyme for forward and backward reactions (under assumption that complex formation is not the rate limiting step).

From (scheme 1) the reaction rate can be derived as

$$r_L = C_E \cdot \frac{(V_{max,D}/K_{m,D}) \cdot C_D - (V_{max,L}/K_{m,L}) \cdot C_L}{1 + (C_L/K_{m,L}) + (C_D/K_{m,D})}, \quad r_D = -r_L, \quad (1)$$

where r_D and r_L are the reaction rates for the formation of *D*-AA and *L*-AA respectively, C_E is the enzyme concentration and $V_{max,L/D}$ are the maximum mass specific reaction rates (in $\mu\text{mol min}^{-1} \text{g}^{-1} \text{enzyme preparation}$) for the racemization of either *L*- or *D*-AA. With approaching the equilibrium condition (racemic composition) the driving force of the reaction (numerator in Eq. (1)) becomes 0. The Haldane relationship (Eq. (2)) describes the relation between the equilibrium constant K_{eq} of a reaction and the forward and backward kinetic constants of the catalyzed reaction. Under equilibrium conditions K_{eq} must be 1:

$$K_{eq} = \frac{C_L}{C_D} = \frac{V_{max,D}}{K_{m,D}} : \frac{V_{max,L}}{K_{m,L}} = 1 \quad (2)$$

3.2.1. Methionine

K_m and V_{max} values were determined for the racemization of *D*- and *L*-Met solutions with CL in 95 vol.% 100 mM KP_i -buffer (pH 7.0), 5 vol.% MeOH at $T=20$ – 40 °C (with step of 5 °C) as well as at pH 6, 7 and 8 at 25 °C. Figs. 2–4 show the results of the kinetic studies for *D*- and *L*-Met racemization. Initial rates were measured as described above. In all cases less than 5% of the initial enantiomer concentration was isomerized to allow for initial rate conditions.

V_{max} values increase for *D*- and *L*-Met racemization with rising temperature (about 1.5-fold for *L*-Met from 20 to 40 °C) and pH values (about 2.5-fold for *L*-Met from pH 6 to pH 8). Noticeable here is the switch of V_{max} values for *D*- and *L*-Met at pH 8. While at pH 6 and 7 $V_{max(L-Met)}$ is slightly higher than $V_{max(D-Met)}$, at pH

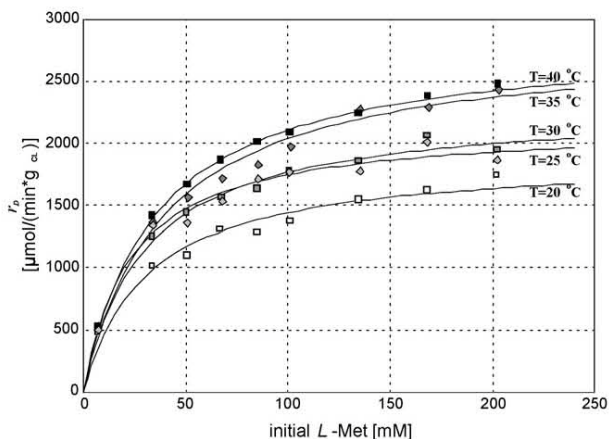


Fig. 3. Experimental data for *L*-methionine racemization with *CL* shown by symbols. Lines show data calculated by non-linear fitting for racemization of *L*-Met using K_m and V_{max} shown in Table 3. Solvent: 95 vol.% 100 mM KP_i -buffer (pH 7.0), 5 vol.% MeOH.

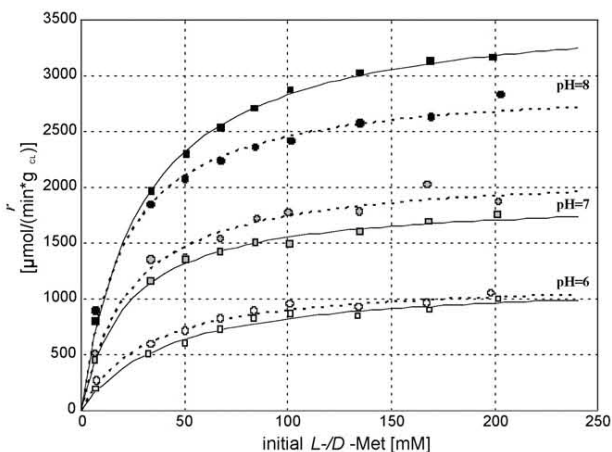


Fig. 4. Experimental data for *L*- (circles) and *D*- (squares) methionine racemization with *CL*. Lines show data calculated by non-linear fitting for racemization of *L*-Met (dotted) and *D*-Met (full) using K_m and V_{max} shown in Table 3. Solvent: 95 vol.% 100 mM KP_i -buffer, 5 vol.% MeOH, $T=25^\circ\text{C}$.

$8 V_{max(D-Met)}$ is significantly higher (23%) than $V_{max(L-Met)}$ (Table 3). K_m values increase only slightly when rising the temperature from 20 to 40 °C (follow *van't Hoff* relation, [25]) and fell with risen pH values.

3.2.2. Asparagine

Kinetic parameters were determined for the racemization of *D*- and *L*-Asn with *PL* in H_2O at $T=20$ – 40°C (with step of 5 °C). Figs. 5 and 6 show the results of the kinetic studies for *D*- and *L*-Asn racemization which were determined as described for methion-

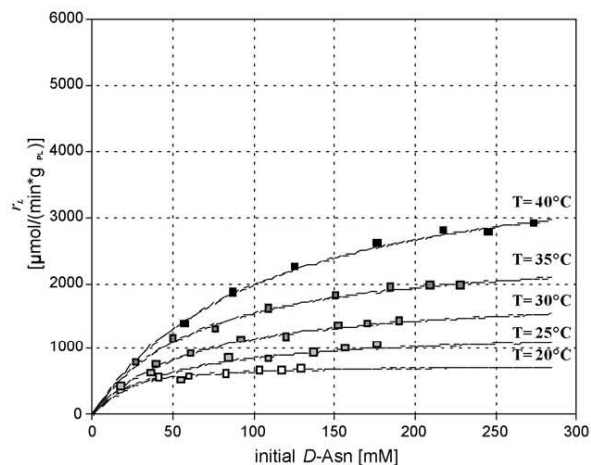


Fig. 5. Experimental data for *D*-asparagine racemization with *PL* shown by symbols. Lines show data calculated by non-linear fitting for racemization of *D*-Asn using K_m and V_{max} shown in Table 4. Solvent: 100% H_2O .

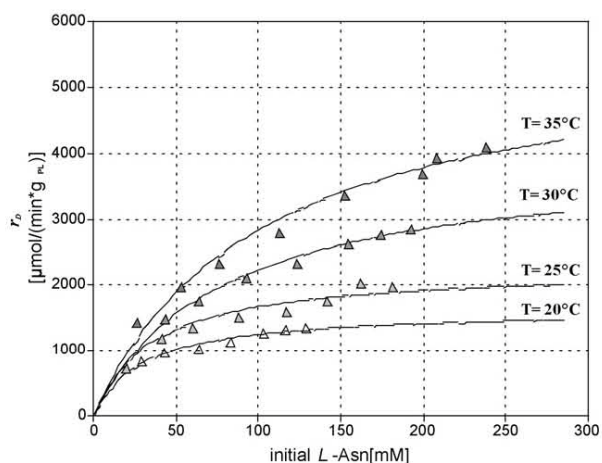


Fig. 6. Experimental data for *L*-asparagine racemization with *PL* shown by symbols. Lines show data calculated by non-linear fitting for racemization of *L*-Asn using K_m and V_{max} shown in Table 4. Solvent: 100% H_2O .

ine. Similar to methionine racemization V_{max} values increase with higher temperatures (about 3.5-fold for *L*-Asn from 20 to 35 °C and 5.2-fold for *D*-Asn from 20 to 40 °C). K_m values also increase significantly with rising temperatures which indicates a reduced substrate affinity (follow *van't Hoff* relation). Values for $V_{max(L-Asn)}$ and $V_{max(D-Asn)}$ strongly differ from each other. This apparent imbalance should be adjusted by a consistent difference of K_m values (Eq. (2)). Here this requirement can only be met (excluding values determined at 30 °C) when considering the broad error ranges (Table 4). A reasonable explanation for this might be the relatively

Table 3

Kinetic data for racemization of *D*- and *L*-methionine with *CL* at different temperatures and pH values. K_m and V_{max} were calculated by non-linear regression. Solvent: 95 vol.% 100 mM KP_i -buffer, 5 vol.% MeOH.

Temperature [°C]	pH	$K_m(D-Met)$ [mM]	$V_{max(D-Met)}$ [U/g _{CL}]	$K_m(L-Met)$ [mM]	$V_{max(L-Met)}$ [U/g _{CL}]
20	7	25 (±13.0%)	1696 (±3.1%)	31 (±17.0%)	1889 (±4.5%)
25	7	22 (±11.5%)	1892 (±2.6%)	23 (±14.7%)	2150 (±3.3%)
30	7	23 (±10.6%)	2075 (±2.4%)	30 (±15.7%)	2296 (±4.0%)
35	7	30 (±8.9%)	2512 (±3.9%)	39 (±11.6%)	2833 (±3.5%)
40	7	32 (±8.4%)	2668 (±2.3%)	35 (±11.4%)	2847 (±3.2%)
25	6	42 (±14.6%)	1160 (±4.5%)	30 (±22.3%)	1174 (±5.9%)
25	8	28 (±4.5%)	3627 (±1.1%)	20 (±8.7%)	2951 (±1.9%)

Table 4Kinetic data for racemization of *D*- and *L*-asparagine with *PL* at different temperatures. K_m and V_{max} were calculated by non-linear regression. Solvent: 100% H_2O .

Temperature [°C]	$K_m(D-Asn)$ [mM]	$V_{max}(D-Asn)$ [U/gPL]	$K_m(L-Asn)$ [mM]	$V_{max}(L-Asn)$ [U/gPL]
20	18 ($\pm 26.1\%$)	770 ($\pm 4.8\%$)	30 ($\pm 19.3\%$)	1626 ($\pm 5.6\%$)
25	50 ($\pm 33.3\%$)	1299 ($\pm 11.4\%$)	47 ($\pm 19.6\%$)	2427 ($\pm 6.3\%$)
30	62 ($\pm 8.9\%$)	1881 ($\pm 3.1\%$)	76 ($\pm 10.0\%$)	3930 ($\pm 3.9\%$)
35	66 ($\pm 8.2\%$)	2585 ($\pm 2.8\%$)	101 ($\pm 17.5\%$)	5683 ($\pm 7.1\%$)
40	103 ($\pm 8.8\%$)	4032 ($\pm 3.3\%$)	a	a

^a Due to the high racemization activity for *L*-Asn at 40 °C it was not possible to detect an activity at a substrate concentration where it is close to the expected V_{max} (at least 70%) and therefore was not determinable with a tolerable error.

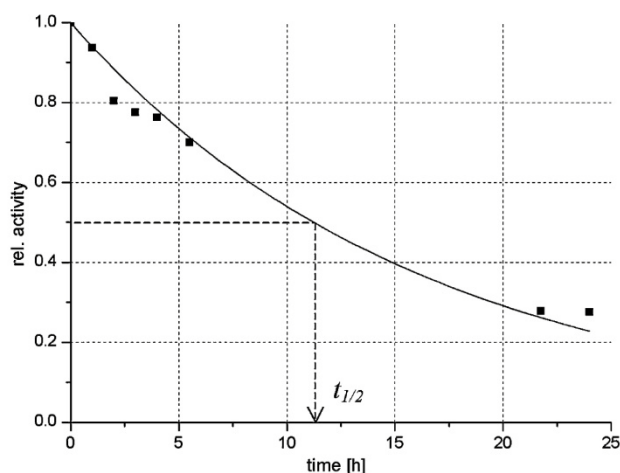


Fig. 7. Relative activity of *CL* in 95 vol.% 100 mM KP_1 -buffer (pH 7.0), 5 vol.% MeOH at 35 °C over a period of 24 h.

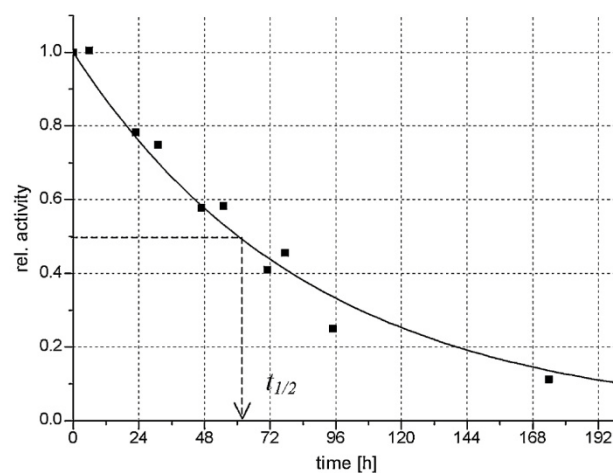


Fig. 8. Relative activity of *PL* in 500 mM *DL*-Asn solution at 35 °C over a period of 7 days.

poor solubility of *D*-/*L*-Asn (ca. 290 mM each at 35 °C). Due to this, kinetic measurements could not be carried out under substrate saturation conditions (V_{max} region) which lead to wide error ranges. Due to the very high racemization activity for *L*-Asn at 40 °C (about 5000 $\mu\text{mol}/(\text{min g}_{PL})$) at initial substrate concentration of 260 mM it was not possible to perform a measurement at a substrate concentration where the activity is even close to the expected V_{max} (at least 70% of V_{max}). In this case determined data was afflicted with an intolerable error and therefore is not included in the data analysis. Another reason for aforementioned broad error ranges, namely side reactions that might have led to an enantiospecific degradation of

one enantiomer, could be ruled out due to constant mass balances. Therefore the calculated kinetic parameters can only be considered as approximate values. All kinetic parameters are summarized in Table 4.

3.3. Enzyme stability

To investigate the enzyme stability in the presence of 5 vol.% MeOH, 5 mg *CL* were incubated at 35 °C in 1 mL 95 vol.% 100 mM KP_1 -buffer (pH 7), 5 vol.% MeOH over a period of 24 h. At defined times 100 μL of this solution were added to 100 μL of 300 mM *L*-

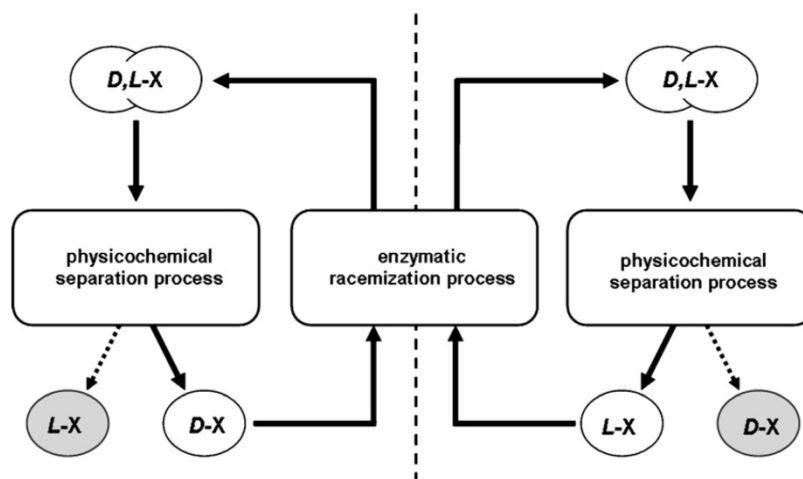


Fig. 9. Combination of a physicochemical separation process with enzymatic racemization of the unwanted counterenantiomer. Either *L*-enantiomers (left side) or *D*-enantiomers (right side) can be obtained from this process. A cyclic operation enables a theoretical yield of 100% of the target enantiomer (grey).

Met in 95 vol.% 100 mM KP_i -buffer (pH 7), 5 vol.% MeOH and initial reaction rates were determined by HPLC. Fig. 7 shows the relative activities fitted by non-linear regression using Eq. (3) where r_{rel} is the relative reaction rate giving an inactivation constant k_{time} of 0.0614 h^{-1} ($\pm 8\%$) and a half-life time $t_{1/2}$ of 11.3 h (Eq. (4)).

$$r_{rel}(t) = r_{rel}(0) \cdot e^{(-k_{time} \cdot t)} \quad (3)$$

$$t_{1/2} = \frac{\ln(0.5)}{-k_{time}} \quad (4)$$

To investigate the influence of highly concentrated Asn solutions on the enzyme activity 1 mg *PL* was incubated at 35°C in 1.5 mL aqueous 500 mM *DL*-Asn solution over a period of 7 days. Initial reaction rates were determined as described above but with 100 μL of 200 mM aqueous *D*-Asn solution as substrate (Fig. 8). Non-linear regression gave a k_{time} of 0.0115 h^{-1} ($\pm 5\%$) and a half-life time of 60.3 h.

The medium composition and temperature of both stability experiments were chosen in accordance to the planned reaction design for each enzyme preparation. Since *CL* will be applied in a process which implies chromatography for enantioseparation of methionine we determined the stability in the mobile phase (which also has to serve as reaction medium). An according experiment was performed with *PL*. In this case the reaction medium will be a highly concentrated asparagine solution with only a very small enantiomeric excess. We simulated this by storing the racemase in an aqueous 500 mM *DL*-Asn solution.

4. Conclusions

A plasmid containing an amino acid racemase gene was cloned into *E. coli* BL21 (DE3) and overexpressed during a 20-L fed-batch fermentation. The produced protein shall be used as biocatalyst in an integrated physicochemical separation process with enzymatic racemization. Two differently pure enzyme preparations were prepared from cell extract of which one was sufficient for methionine racemization but still had impurities which led to enzymatic asparagine degradation. Further purification yielded in a pure racemase lyophilizate with no side reactions concerning asparagine as substrate. We have investigated the kinetic parameters K_m and V_{max} for the racemization reactions of methionine in 95 vol.% 100 mM KP_i -buffer, 5 vol.% MeOH and of asparagine in H_2O at different temperatures and pH values with these two preparations. We showed that V_{max} and K_m values for both reaction systems increased with temperature. During stability studies we have determined half-life times of crude lyophilizate in 95 vol.% 100 mM KP_i -buffer (pH 7), 5 vol.% MeOH and of pure lyophilizate in 500 mM *DL*-Asn (each at 35°C). These reaction media and temperature were chosen for prospective reactor design. Further studies will concentrate on the reactor design for a combined enzymatic

racemization and physicochemical enantioseparation process as depicted in Fig. 9. One major benefit will be the theoretical possible yield of 100% of one enantiomer out of a racemic mixture.

Acknowledgements

Professor K.-E. Jaeger from the Institute of Molecular Enzyme Technology, University of Duesseldorf, is kindly acknowledged for the help in cloning the amino acid racemase used for this work. We also thank Prof. Tadao Oikawa from the Department of Biotechnology at the Kansai University for his initial help in starting this project.

References

- [1] N.M. Maier, P. Franco, W. Lindner, *J. Chromatogr. A* 906 (2001) 3–33.
- [2] M. Breuer, K. Dittrich, T. Habicher, B. Hauer, M. Keßeler, R. Stürmer, T. Zelinski, *Angew. Chem. Int. Ed.* 43 (2004) 788–824.
- [3] J. Dingenen, J.N. Kinkel, *J. Chromatogr. A* 666 (1994) 627–650.
- [4] E. Francotte, *J. Chromatogr. A* 666 (1994) 565–601.
- [5] K. Petrushevskaya, M.A. Kuznetsov, K. Gedidke, V. Meshko, S.M. Staroverov, A. Seidel-Morgenstern, *J. Sep. Sci.* 29 (2006) 1447–1457.
- [6] T. Vries, H. Wynberg, E. van Echten, J. Koek, W. ten Hoeve, R.M. Kellogg, Q.B. Broxterman, A. Minnaard, B. Kaptein, S. van der Sluis, L. Hulshof, J. Kooistra, *Angew. Chem. Int. Ed.* 37 (1998) 2349–2354.
- [7] H. Lorenz, A. Periberg, D. Sapounddjiev, M.P. Elsner, A. Seidel-Morgenstern, *Chem. Eng. Process.* 45 (2006) 863–873.
- [8] M. McCoy, *Chem. Eng. News* 77 (1999) 10–14.
- [9] S.C. Stinson, *Chem. Eng. News* 77 (1999) 101.
- [10] M. Bechtold, S. Makart, M. Heinemann, S. Panke, *J. Biotechnol.* 124 (2006) 146–162.
- [11] M.P. Elsner, D.F. Menendez, E.A. Muslera, A. Seidel-Morgenstern, *Chirality* 17 (2005) 183–195.
- [12] B. Schnell, K. Faber, W. Kroutil, *Adv. Synth. Catal.* 345 (2003) 653–666.
- [13] O. May, S. Verseck, A. Bommaris, K. Drauz, *Org. Process Res. Dev.* 6 (2002) 452–457.
- [14] K. Goldberg, K. Schroer, S. Lütz, A. Liese, *Appl. Microbiol. Biotechnol.* 76 (2007) 237–248.
- [15] K. Goldberg, K. Schroer, S. Lütz, A. Liese, *Appl. Microbiol. Biotechnol.* 76 (2007) 249–255.
- [16] H. Ikeda, Y. Yonetani, S.-i. Hashimoto, M. Yagasaki and K. Soda, WO 03/074690 A1, 2003, Japan.
- [17] M. Bechtold, S. Makart, R. Reiss, P. Alder, S. Panke, *Biotechnol. Bioeng.* 98 (2007) 812–824.
- [18] H.W.B. Roozeboom, *Z. Phys. Chem.* 28 (1899) 494–517.
- [19] J. Jacques, A. Collet, S.H. Wilen, *Enantiomers, Racemates and Resolutions*, Krieger, Malabar, 1994.
- [20] A.A. Rodrigo, H. Lorenz, A. Seidel-Morgenstern, *Chirality* 16 (2004) 499–508.
- [21] V.M. Proffir, M. Matsuoka, *Colloids Surf. A* 164 (2000) 315–324.
- [22] M.M. Bradford, *Anal. Biochem.* 72 (1976) 248–254.
- [23] A.C. Eliot, J.F. Kirsch, *Annu. Rev. Biochem.* 73 (2004) 383–415.
- [24] T. Yoshimura, N. Esaki, *J. Biosci. Bioeng.* 96 (2003) 103–109.
- [25] A. Cornish-Bowden, *Fundamentals of Enzyme Kinetics*, Portland Press Ltd, London, 2004.
- [26] K.E. Nelson, *Environ. Microbiol.* 4 (2002) 777–778.
- [27] D.M. Woodcock, P.J. Crowther, J. Doherty, S. Jefferson, E. Decruz, M. Noyer-weidner, S.S. Smith, M.Z. Michael, M.W. Graham, *Nucleic Acids Res.* 17 (1989) 3469–3478.
- [28] F.W. Studier, B.A. Moffatt, *J. Mol. Biol.* 189 (1986) 113–130.

Publication 2

Enzyme-assisted physicochemical enantioseparation processes - Part II: Solid-liquid equilibria, preferential crystallization, chromatography and racemization reaction

Petruševska-Seebach, K., Würges, K., Seidel-Morgenstern, A., Lütz, S. & Elsner, M. P.

Chemical Engineering Science, 2009

Vol. 64, 2473-2482

c

Reproduced with the permission of Elsevier Ltd.



Enzyme-assisted physicochemical enantioseparation processes—Part II: Solid–liquid equilibria, preferential crystallization, chromatography and racemization reaction

Katerina Petruševska-Seebach^a, Kerstin Würges^b, Andreas Seidel-Morgenstern^a, Stephan Lütz^b, Martin P. Elsner^{a,*}

^aMax Planck Institute for Dynamics of Complex Technical Systems, Magdeburg, Germany

^bInstitute of Biotechnology 2, Research Centre Jülich, Jülich, Germany

ARTICLE INFO

Article history:

Received 28 October 2008

Received in revised form 2 February 2009

Accepted 11 February 2009

Available online 27 February 2009

Keywords:

Amino acid racemase

Asparagine

Methionine

Integrated enantioseparation processes

Hybrid processes

Preferential crystallization

Chiral chromatography

Enzymatic reaction

Michaelis–Menten kinetics

ABSTRACT

This contribution addresses the design and investigation of two hybrid enantioseparation processes including an enzymatic racemization step in order to enhance the overall performance. Complementary to part I where the manufacturing and the characterization of an amino acid racemase (EC 5.1.1.10) was emphasized [Würges, K., Petruševska, K., Serci, S., Wilhelm, S., Wandrey, C., Seidel-Morgenstern, A., Elsner, M.P., Lütz, S., 2009. Enzyme-assisted physicochemical enantioseparation processes—part I: production and characterization of a recombinant amino acid racemase. *J. Mol. Cat. B* (in print), online available: doi:10.1016/j.molcatb.2008.10.006.], the work presented in this paper tends more towards developing a data base for potential process schemes for the manufacture of selected amino acids.

The first proposed process concept (P-I) couples preferential crystallization (PC) and racemization for the production of L-asparagine (L-Asn) using racemic mixture of dl-asparagine (conglomerate-forming system) as a starting material, while the second concept (P-II) integrates chromatography and racemization for the preparation of L-methionine (L-Met) starting with racemic mixture of dl-methionine (compound-forming system). As mentioned in part I, a racemization unit, where the unwanted enantiomer will be converted into racemate, is incorporated into the hybrid processes for the sake of 100% yield, theoretically. Besides the basic investigation according to the solid–liquid equilibria, PC and chromatography, the focus of this paper is mainly on the kinetic studies of the racemization reaction. Initially, the solubility ternary phase diagrams of both examined systems were determined, leading into the idea of combination of the proposed process schemes. For P-I the concept of PC of L-Asn was experimentally proven and the kinetics of the racemization was examined for d- and l-Asn in water using purified lyophilizate (PL). Concerning P-II, for the chromatographic unit the impact on the separation of dl-Met on eremomycin based stationary phase using KPi buffer and MeOH as mobile phase was evaluated in terms of resolution and selectivity at three different temperatures by varying the content of methanol (MeOH) in the mobile phase and the pH. The experiments for determination of the racemization kinetics were done for a compromised parameter set using crude lyophilizate (CL). In both cases a Michaelis–Menten three-step model was used to describe the enzymatic reaction.

© 2009 Elsevier Ltd. All rights reserved.

1. Introduction

Driven by the policy of regulatory authorities such as US Food and Drug Administration and the EU Committee for Proprietary Medical Products the manufacturing of pure enantiomers is distinguishably increasing in several industrial branches: pharmaceuticals, alimentary, etc. (Caner et al., 2004). As constituents of larger biomolecules with essential importance for the nutrition and health subsistence,

optically pure amino acids follow the same trend. The amino acid market and the perspectives, with special accent on their biotechnological production, are reviewed by Leuchtenberger et al. (2005). So far, most of the L-amino acids are produced using microbial methods. However, the way how and in which form an amino acid is going to be produced depends mainly on the process economics, available raw material and the market, e.g. methionine is usually produced as a racemic mixture (50/50 mixture of both enantiomers) (Scheper, 2003).

Regarding the basic approaches for the production of pure enantiomers, the resolution of a racemic mixture is considered as an attractive method since numerous preparative separation techniques

* Corresponding author. Tel.: +49 391 6110438; fax: +49 391 6110626.

E-mail address: mpelsner@mpi-magdeburg.mpg.de (M.P. Elsner).

can accompany the conventional organic synthesis as well as enzyme catalysis methods (Ahuja, 1996). The most often utilized methods and several novel resolution technologies are summarized in Sakai et al. (2007) and Fogassy et al. (2006), respectively.

Amino acids differ in terms of their phase diagram (Jacques et al., 1994) and that can predetermine the choice of a suitable separation technique. In case of conglomerate-forming systems (5–10% of all chiral substances belong to this group; Collet, 1999) the cost-effective and quite simple preferential crystallization (PC) holds great potential. Recently, PC in a cyclic operation mode for water–threonine system (conglomerate) was studied in detail by Elsner et al. (2005). Later on, an innovative configuration of coupled crystallizers was proposed by the same author outperforming the one-crystallizer mode by means of productivity and purity (Elsner et al., 2009). For compound-forming systems (>90% of the chiral substances are racemic compounds) the concept of PC is rather limited. Shiraiwa et al. (1997) have resolved DL-methionine (DL-Met; racemic compound) by converting DL-Met into DL-Met · HCl (conglomerate) and then performing PC. In fact, the first approval of applying PC for optical resolution of racemic compound in a frame of a hybrid process was done recently by Lorenz et al. (2006). Subsequently, they have shown that the enantiomers of methionine can also be preferably crystallized (Polenske and Lorenz, 2008; Kaemmerer et al., 2008). Concerning their study, before racemic compound solution undergoes PC, preliminary enantiomeric enrichment is required and usually, but not necessarily, the degree of enrichment can be correlated with the eutectic composition of the system.

The enrichment can be accomplished utilizing other methods for amino acid enantioseparation, e.g. chromatography-based techniques (HPLC, SMB) since among other conveniences, the development of new chiral stationary phases broadens their range of application (Petruševska et al., 2006; Zhang et al., 2007). On the other hand, those techniques are considered as quite expensive and their use has to be justified.

The issue of using PC, when highly enriched solutions are required, implies several questions like for instance if it is really necessary to combine sophisticated chromatography technique with PC or enantioseparation only by chromatography might be more reasonable? Is it more beneficial to combine less expensive techniques for enrichment and PC, etc.? However, a lot of physicochemical and economical parameters have to be taken into consideration before a decision of using a single or an integrated process is made. The potential of hybrid enantioseparation processes has been the subject of considerable scientific activities in the recent years, with an emphasis on the theoretical development of general design methods (Ströhlein et al., 2003) as well as on the experimental challenges emerging from the different operation windows of the single separation methods being combined (Fung and Ng, 2006). For the evaluation and design of a hybrid enantioseparation process using SMB and PC recently a shortcut method was proposed by Kaspereit et al. (2005).

Unfortunately, the separation techniques suffer with a general drawback of maximum 50% yield. Nevertheless, it is likely possible to overcome those limitations by performing racemization of the unwanted enantiomer, feed the racemate to the separation unit, and thus achieving 100% yield (Collet et al., 1980; May et al., 2002). Comprehensive overview of racemization methods is given by Ebberts et al. (1997). Due to the convenient reaction conditions, the development of biocatalysts and their rising industrial application (Bornscheuer and Buchholz, 2005), the use of an enzyme for racemization (racemase) is a challenging task for the development of efficient combined processes. So far, the functions on a molecular level and the applications of several amino acid racemases have been given by Yoshimura and Esaki (2003) and Schnell et al. (2003), respectively.

Regarding integrated processes including racemization, recently Bechtold et al. (2006a) introduced a novel process concept of coupling continuous chromatography and enzyme reactor. The general idea was analyzed in comprehensive studies with respect to the chromatographic part (Bechtold et al., 2006b) and the racemization (Bechtold et al., 2007).

Supplementing part I of this paper (Würges et al., 2009), based on an evaluation of the ternary phase diagrams of two systems (DL-Asn/water and DL-Met/solvent), two different process concepts for the production of pure enantiomers are proposed. Particularly with regard to manufacturing pure enantiomer of asparagine the integrated process consists of *crystallization* and *racemization*, whereas for methionine *chromatography* and *racemization* are coupled. Since the separation units are not the main subject of this work, we are going to present in this paper a preliminary assessment of the concept of PC for P-I and the chromatographic separation of DL-Met for P-II accompanied with a more detailed investigation about the influence of certain parameters (pH and MeOH amount in the solvent at different T) on the separation.

Distinct attention in this paper is paid on the reaction of racemization. In that manner, the impact of several parameters (the same as for the chromatographic part) was examined for the racemization of D-Met. For the racemization of D-Asn only the temperature was varied. Furthermore, for both systems the reaction kinetics was studied in detail. For that purpose the racemization was performed for different concentrations of the enantiomers and different enzyme concentrations. The experimental results were fitted into the Michaelis–Menten three-step mechanism model in order to determine the constants of the reaction.

The goal of this work is to offer a data base allowing evaluating and confirming the feasibility of combined processes for enantioseparation. The hybrid process concepts presented are not limited to amino acids. In principle, they could be extended to other chiral systems showing similar equilibrium characteristics.

2. Theory

2.1. Ternary phase diagram as a criterion for the choice of a separation technique

The general form of the ternary phase diagram for conglomerate-forming system is shown in Fig. 1a. As it was discussed before for this kind of systems the concept of PC is rather convenient for enantioseparation. Fig. 2 reveals a novel, promising and cost-effective process scheme for the manufacture of pure enantiomers by combining PC and racemization (P-I). The addition of a racemization unit results in an increase of the concentration of the wanted enantiomer and a decrease of the unwanted one in the liquid phase at the same time. Therefore, as long as the racemization is faster than the crystallization the composition moves directly towards the eutectic point belonging to the crystallization temperature T_{cryst} according to the straight trajectory in the ternary phase diagram (assigned by thick black arrow in the right-hand figure) increasing constantly the driving force for crystallization of the desired enantiomer and suppressing the occurrence of the counter enantiomer in comparison to the conventional PC process.

The choice of a separation technique is slightly more difficult for compound-forming systems. In this case the position of the eutectic points in the ternary diagram can predetermine the choice of a particular separation method or combination of few. When combined processes are used, special accent falls on the costs and the feasibility of the whole scheme. If the points tend to be more in the inner part of the triangle, i.e. not far away from the 50/50 mixture (Fig. 1b), poor enrichment is necessary in order to apply PC. In

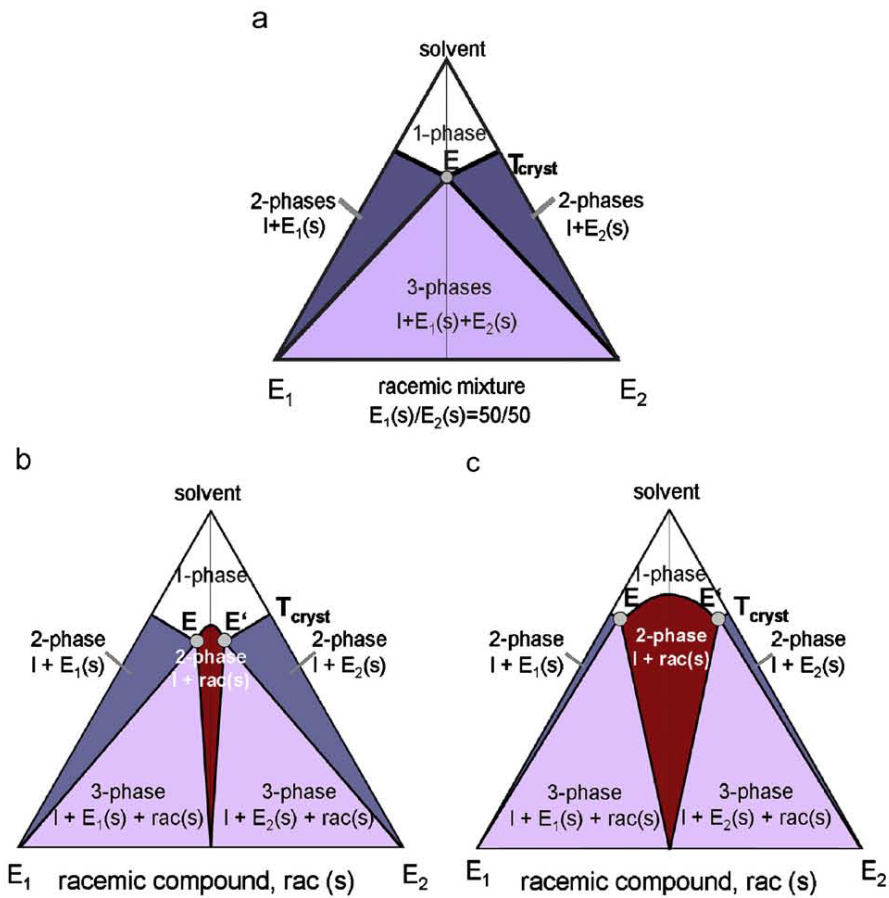


Fig. 1. Schemes of ternary phase diagrams for conglomerate-forming system (a) and two different compound-forming system (b) and (c).

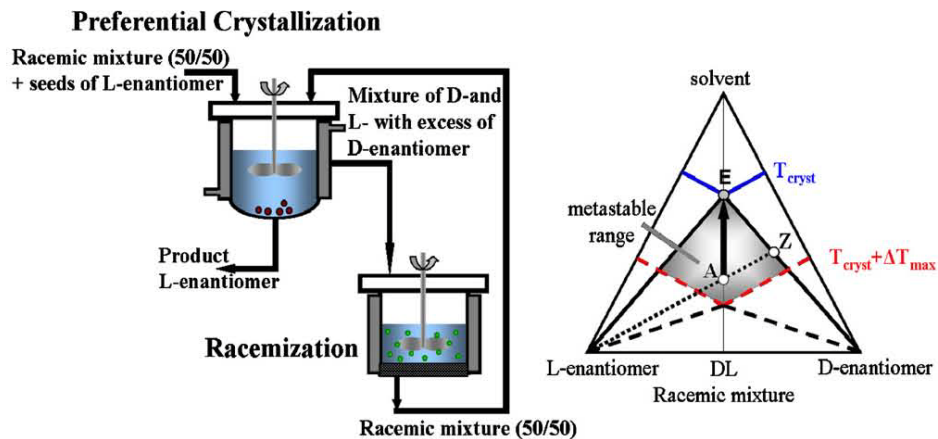


Fig. 2. Process scheme (P-I) for the production of pure enantiomers starting with racemic mixture of a conglomerate-forming system.

contrary, when the eutectica are close to the axis (Fig. 1c), highly enriched solution is required for PC separation. As mentioned before, when moderate excess of one of the enantiomers is required then the powerful but at the same time expensive chromatographic techniques can be coupled with PC. However, when high enantiomeric excess is needed then the use of only chromatography for the enantioseparation might be more reasonable. By upgrading the chromato-

graphic unit with racemization step of the unwanted enantiomer the process of production of pure enantiomer can be distinguishably improved (Fig. 3).

Since the presented process concepts consist of two process units a *compromised set of parameters* is required. In that manner, a profound investigation of the influence of the process parameters for each unit is necessary.

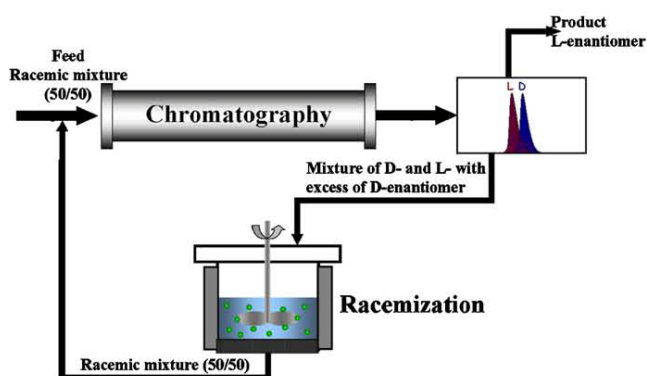
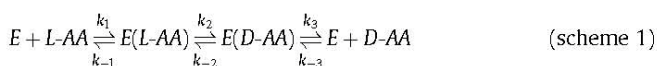


Fig. 3. Process scheme (P-II) for the production of pure enantiomer starting with racemic mixture of a compound-forming system with eutectic points close to the axes.

2.2. Kinetic model for the racemization reaction

As mentioned in the first part of the paper, by assuming that the applied amino acid racemase follows a reversible three-step Michaelis–Menten mechanism, the racemization reaction can be schematically presented as (Cornish-Bowden, 1995)



where E is the enzyme, $L-AA$ and $D-AA$ are L- and D-amino acids, respectively, and k_i and k_{-i} are the reaction constants for the forward and the backward reactions.

The reaction rate for the supposed scheme 1 can be derived as

$$r_L = C_E \frac{V_{\max,D} C_D - \frac{V_{\max,L}}{K_{m,L}} C_L}{1 + \frac{C_L}{K_{m,L}} + \frac{C_D}{K_{m,D}}} \quad \text{and} \quad r_D = -r_L \quad (1)$$

where

$$K_{m,L} = \frac{k_{-1}k_{-2} + k_{-1}k_3 + k_2k_3}{k_1(k_{-2} + k_2 + k_3)} \quad \text{and} \\ K_{m,D} = \frac{k_{-1}k_{-2} + k_{-1}k_3 + k_2k_3}{k_{-3}(k_{-2} + k_2 + k_{-1})} \quad (2)$$

In the relation given above r_L and r_D are reaction rates for the formation of L and D amino acid, respectively, C_E is the concentration of the enzyme preparation, $V_{\max,L/D}$ are the maximum (mass specific) reaction rates and $K_{m,L/D}$ are the dissociation constants for the substrate/product binding to the enzyme for the forward and backward reactions.

The equilibrium constant K_{eq} is 1 in case of racemization which is described by the Haldane relationship:

$$K_{eq} = \frac{C_L}{C_D} = \frac{V_{\max,D}}{K_{m,D}} / \frac{V_{\max,L}}{K_{m,L}} = 1. \quad (3)$$

By taking this constraint into consideration Eq. (1) can be rewritten as

$$r_L = C_E \frac{k(C_D - C_L)}{1 + \frac{C_L}{K_{m,L}} + \frac{C_D}{K_{m,D}}} \quad (4)$$

3. Experimental

3.1. Materials and equipment

Racemic mixtures and pure enantiomers of methionine and asparagine monohydrate were supplied by Sigma-Aldrich (Steinheim,

Germany). HPLC grade MeOH and K_2HPO_4 were purchased from ROTH (Karlsruhe, Germany) and KH_2PO_4 and $HClO_4$ from Merck (Darmstadt, Germany). The water used for all experiments was purified using Milli-Q gradient system (Millipore, Molsheim, France).

The basic chromatographic investigations and the analysis for the solubility of methionine were performed on analytical Diaspher-Chirasil-E column (eremomycin based CSP, BioChemMack S&T, Moscow, Russia), 10×0.46 cm, particle size $5 \mu\text{m}$. For the analysis of the solubility measurements for asparagine, Chirobiotic-T column, 250×4.6 mm, $5 \mu\text{m}$ particles (Astec, Whippany, NJ, USA) was used.

The enzyme preparation used in this work is an amino acid racemase (EC 5.1.1.10), described and characterized in Würges et al. (2009).

The quantity of CL from the first batch, specified in the first part of the paper, was able to satisfy the requirements for the kinetic experiments for the racemization of D- and L-Met, while for racemization of the enantiomers of asparagine a new batch of PL was prepared.

The chromatographic experiments and the analysis of the samples after solubility measurements and racemization were carried out using HP 1100 liquid chromatograph (Hewlett-Packard, Waldbronn, Germany). Enzyme assays were done at 850 rpm in 2 mL Eppendorf reaction vials placed in an Eppendorf Thermomixer (Hamburg, Germany).

3.2. Procedures

3.2.1. Solubility measurements and construction of the ternary phase diagrams

The solubility of different mixtures between D- and L-Asn monohydrate in water and D- and L-Met in solvent (0.1 M KPi buffer, pH = 7/MeOH = 95/5 v/v) was determined at 15, 25, 35, 40 and 45 °C. The mass fraction of L-enantiomer in the D-/L-mixture was changed from 0.5 to 1. The solutions with total mass of 10 g were placed in glass vessels and stirred by magnetic stirrer. The necessary isothermal conditions were achieved using thermostated double jacketed vessels in which the temperature was constantly measured with a PT-100 sensor. After complete dissolution of the solid phase, cooling down to a certain temperature, ensuring equilibrium state by providing several days for it and analysis of the liquid and the solid phase, the solubility of each composition of the enantiomers was determined. For both phases, high performance liquid chromatography (HPLC) analysis was carried out. The analysis of the experimental results for asparagine was carried out on the Chirobiotec-T column at $T = 25^\circ\text{C}$ using a mixture of ethanol/water = 30/70 v/v as mobile phase with flow rate of 0.5 mL/min. The calibration of the UV/VIS detector was performed at 210 nm. For analysis of the methionine samples the Diaspher-Chirasil-E column was used. The composition of the mobile phase was the same as the solvent for this system, $T = 25^\circ\text{C}$, the flow rate was 0.5 mL/min and the detection at 230 and 240 nm.

To validate the results of the HPLC analysis, additionally, the solubility concentrations were determined via measuring the density of the liquid phase using a density meter (density meter DE40, Mettler-Toledo, Gießen, Germany).

Based on the results obtained from the measurements of the solubility, the ternary phase diagrams were constructed for both systems.

3.2.2. PC runs

PC of L-Asn from aqueous solution of DL-Asn was carried out in a batch mode, i.e. in a stirred jacketed glass vessel of 450 mL total volume. Saturated solution (corresponding to a saturation temperature $T_{\text{sat}} = 36^\circ\text{C}$) was prepared and placed in the crystallizer, heated up approximately to 15° above the saturation temperature and maintained at this temperature for a while in order to assure complete

dissolution. Shortly after the solution was cooled down to T_{sat} regulated decrease of the temperature was applied using a cooling rate of 10 K/h until the crystallization temperature ($T_{\text{cryst}} = 30^\circ\text{C}$) was reached. After the assurance that primary nucleation has not occurred the PC was initiated by adding 0.6 g seeds of L-Asn. During the whole time crystal-free solution was pumped out of the crystallizer with a flow rate of 3.6 mL/min by a circulation pump (Heidolph PD 5201, SP Quick 1.6, Heidolph Electro GmbH & Co. KG, Kelheim, Germany) via insulated lines through the polarimeter and density meter and was led back to the vessel. Information about the process were obtained by in-line measurement of the temperature (PT-100 sensor), on-line monitoring of the optical rotation angle using polarimeter (POLARmonitor, IBZ Messtechnik, Hannover, Germany) and on-line measurements of the density of the liquid phase (density meter DE40, Mettler-Toledo, Gießen, Germany). In order to avoid re-crystallization the temperature of the analytical devices and the lines was about 10° higher than the crystallization temperature T_{cryst} .

3.2.3. Chromatographic separation of DL-Met (P-II)

For the chromatographic unit in P-II the separation of DL-Met was performed on the Diaspher-Chirasil-E column. The experiments were carried out at 25, 35 and 40°C for different MeOH amount in the solvent (0, 5, 10 and 20% at $\text{pH} = 7$) and different pH values (6, 7, 8 and 9 with 0% MeOH). To determine the influence of the examined parameters on the separation, the selectivities α and the quality of separation, i.e. the resolutions R_s were evaluated by injecting $1\ \mu\text{L}$ of solutions with $C_{\text{DL-Met}} = 1\ \text{g/L}$ in the column using flow rate of $0.5\ \text{mL/min}$.

3.2.4. Racemization kinetics

3.2.4.1. D-/L-Asparagine. The simplicity in terms of process conditions for P-I resulted in examination only of the influence of the temperature on racemization reaction. The rates of racemization for D-Asn were determined at $T = 20\text{--}50^\circ\text{C}$ with step of 5°C for $C_{\text{D-Asn}} = 25\ \text{g/L}$ and $C_{\text{PL}} = 0.5\ \text{g/L}$.

The kinetic studies were performed at a temperature of 30°C , predetermined by the conditions already chosen for the PC unit. The racemization of D- and L-Asn was done for different concentrations, $C_{\text{D-/L-Asn}} = 15, 25$ and $35\ \text{g/L}$ (the highest concentration is close to the solubility limit of D-/L-Asn for the examined system) for two PL concentrations ($C_{\text{PL}} = 0.5$ and $1\ \text{g/L}$) in a time range where no loss of the PL-activity can be taken into consideration.

3.2.4.2. D-/L-Methionine. Since the MeOH amount in the solvent, pH and the temperature played a major role on the chromatographic separation, the influence of the same parameters on the racemization reaction was investigated in order to determine a compromised set of parameters for P-II. In that manner the initial rates of the reaction were measured for the following conditions: 0%, 5%, 10% and 20% MeOH in the solvent ($\text{pH} = 7, 25^\circ\text{C}, C_{\text{D-Met}} = 15\ \text{g/L}, C_{\text{CL}} = 0.26\ \text{g/L}$); at $\text{pH} = 5\text{--}11$ with step 1 (0% MeOH, $25^\circ\text{C}, C_{\text{D-Met}} = 30\ \text{g/L}, C_{\text{CL}} = 0.26\ \text{g/L}$) and $T = 20\text{--}45^\circ\text{C}$ with step 5 ($\text{pH} = 7, 5\% \text{ MeOH}, C_{\text{D-Met}} = 20\ \text{g/L}, C_{\text{CL}} = 1\ \text{g/L}$). Besides that, for most of the mentioned conditions the stability of the CL was also examined. Concerning the kinetics, the racemization of D-Met in buffer (0.1 M, KPi, $\text{pH} = 7$)/MeOH = 95/5 v/v at 25°C was extensively studied for four different concentrations, $C_{\text{D-Met}} = 5, 10, 20$ and $30\ \text{g/L}$, and each one of them mentioned for three different CL concentrations, $C_{\text{CL}} = 0.5, 1$ and $2.5\ \text{g/L}$ (the results only for $C_{\text{CL}} = 1$ and $2.5\ \text{g/L}$ are shown). Furthermore, the racemization reaction was performed at $T = 20\text{--}45^\circ\text{C}$ with step 5 for $C_{\text{D-Met}} = 20\ \text{g/L}$ and $C_{\text{CL}} = 1\ \text{g/L}$. Additionally, L-Met was also racemized in the same solvent at 25°C using $C_{\text{L-Met}} = 5, 10, 20$ and $30\ \text{g/L}$ and $C_{\text{CL}} = 1\ \text{g/L}$.

4. Results and discussion

4.1. Ternary phase diagrams and feasibility of the process concepts

The correlation in terms of solubility between different mixtures of D-, L-Asn and water is presented in Fig. 4. In the ternary phase diagram five isotherms are shown. The ratio between the mass fraction of the racemic mixture and measured pure enantiomer is approximately 2, meaning, the system shows nearly ideal behavior, i.e. the solubility of one enantiomer is not going to be influenced by the presence of the other enantiomer. The system reveals behavior of a

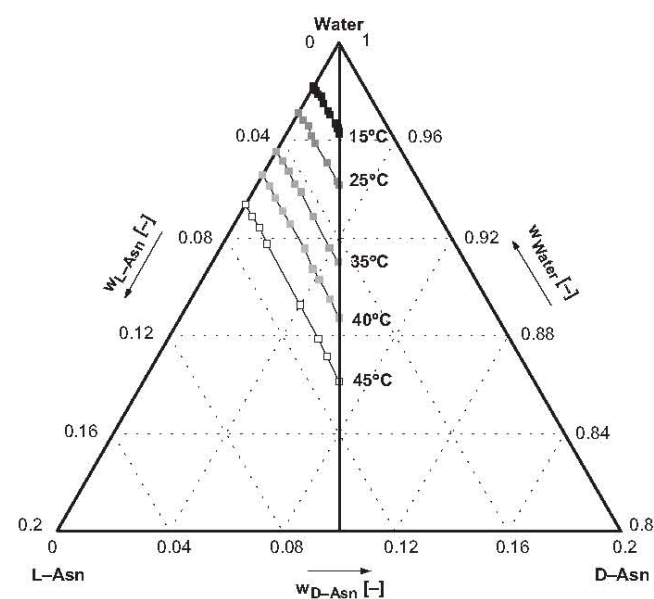


Fig. 4. Solubility ternary phase diagram for D-/L-Asn and water for different temperatures.

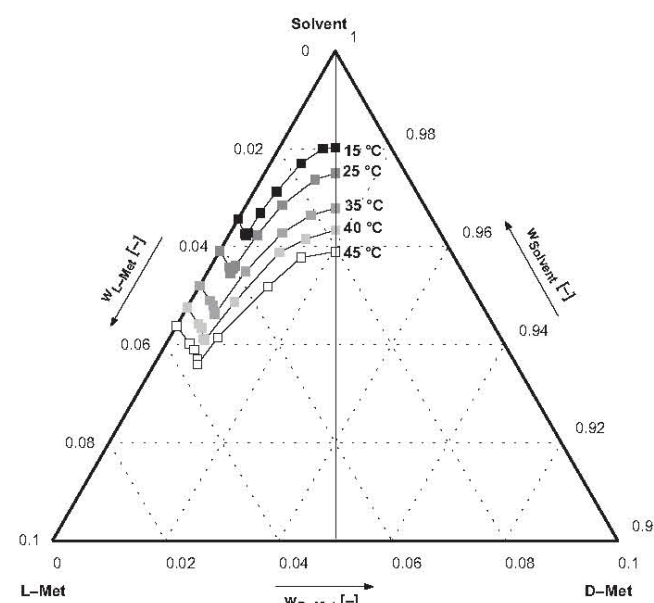


Fig. 5. Solubility ternary phase diagram for D-/L-Met and solvent (0.1 M KPi buffer, $\text{pH} = 7/\text{MeOH} = 95/5\ \text{v/v}$) for different temperatures.

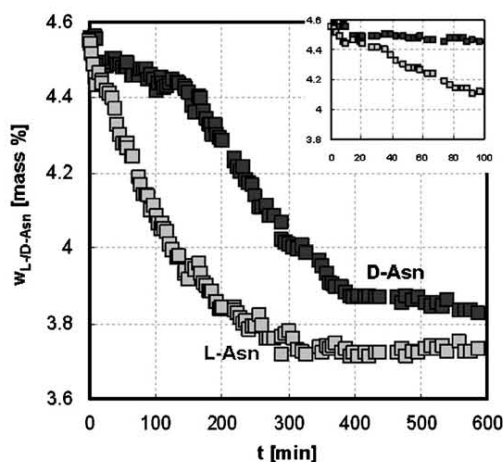


Fig. 6. Preferential crystallization of L-Asn from supersaturated aqueous solution of DL-Asn at 30°C (saturated solution at 36°C).

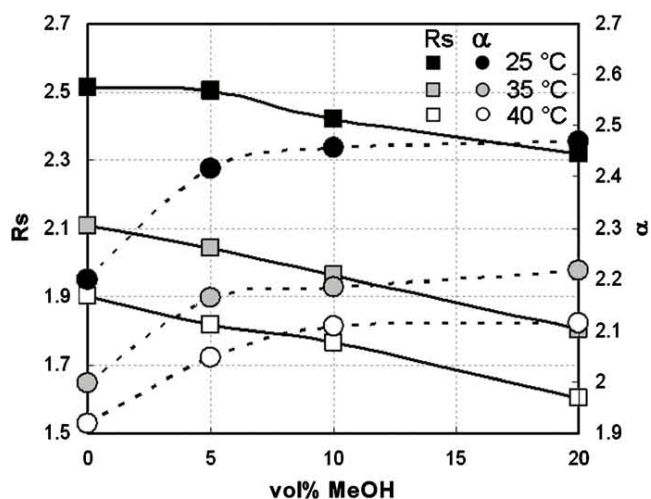


Fig. 7. Influence of different amounts of MeOH in the solvent on the chromatographic resolution and the selectivity at different temperatures and pH = 7.

conglomerate and the concept of the process scheme P-I presented in Fig. 2 seems convenient for production of pure enantiomers. Great advantage of this process is the possibility of performing PC and racemization in water. As an option, instead of utilizing two separate units, one-tank process might also hold potential in this case.

In Fig. 5 the ternary phase diagram of D-, L-Met and solvent (0.1 M KPi buffer, pH = 7/MeOH = 95/5 v/v) is shown. As it is presented, the eutectic points for this system are close to the axes (the ratio L-/D-Met is approx. 90/10) justifying the concept of P-I.

4.2. PC runs

The feasibility of isothermal PC can be considered as proven since one can clearly notice a decrease of the mass fraction of the wanted (seeded) L-Asn and constant concentration profile of D-Asn in the liquid phase in a period of approx. 150 min (Fig. 6). The decrease of the mass fraction of D-Asn designates the beginning of its crystallization and at the same time decrease of the product purity.

Several experiments have been performed and stopped after 80, 100 and 120 min in order to check the composition of the solid phase. HPLC analyses of the harvested products resulted in purities

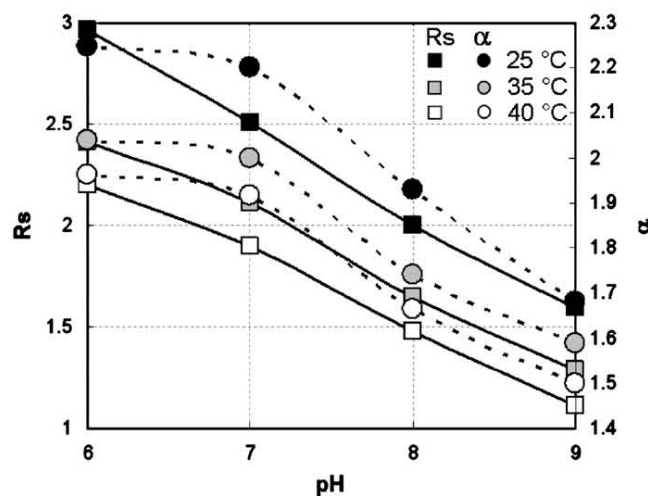


Fig. 8. Influence of pH on the chromatographic resolution and the selectivity at different temperatures for 0% MeOH in the mobile phase.

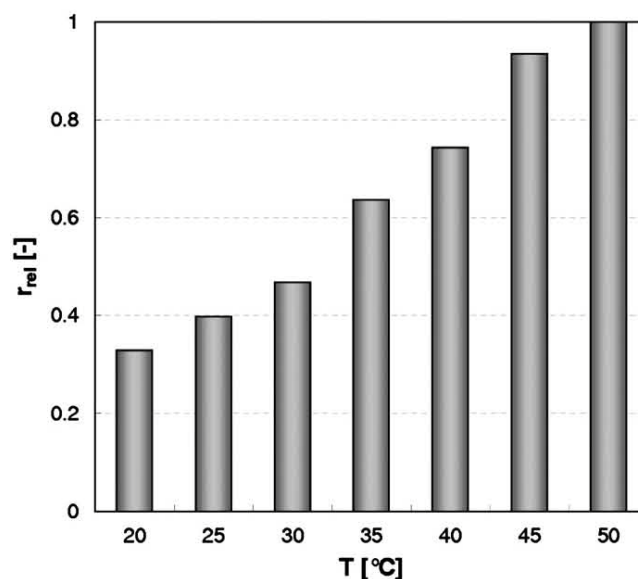


Fig. 9. Effect of the temperature on the initial rate of racemization of D-Asn in water, $C_{D-Asn} = 25 \text{ g/L}$, $C_{PI} = 0.5 \text{ g/L}$.

higher than 98% and confirmed the on-line measurements of the liquid phase composition.

4.3. Chromatographic separation of DL-Met (P-I)

Based on the previous studies for the enantioseparation of DL-Met on eremomycin-based stationary phase a buffer (in this case KPi) and MeOH were considered as main components of the mobile phase for the chromatographic separation. The concentration of the buffer was fixed to a value of 0.1 M since lower concentrations were not able to “buffer” high concentrations of methionine solutions in case of pH = 7.

In Fig. 7 the influence of different amounts of MeOH in the solvent on the resolution and the selectivity is presented for several temperatures. The results indicate that the separation is better when lower MeOH content is present, in contrary to the selectivity which shows opposite trend.

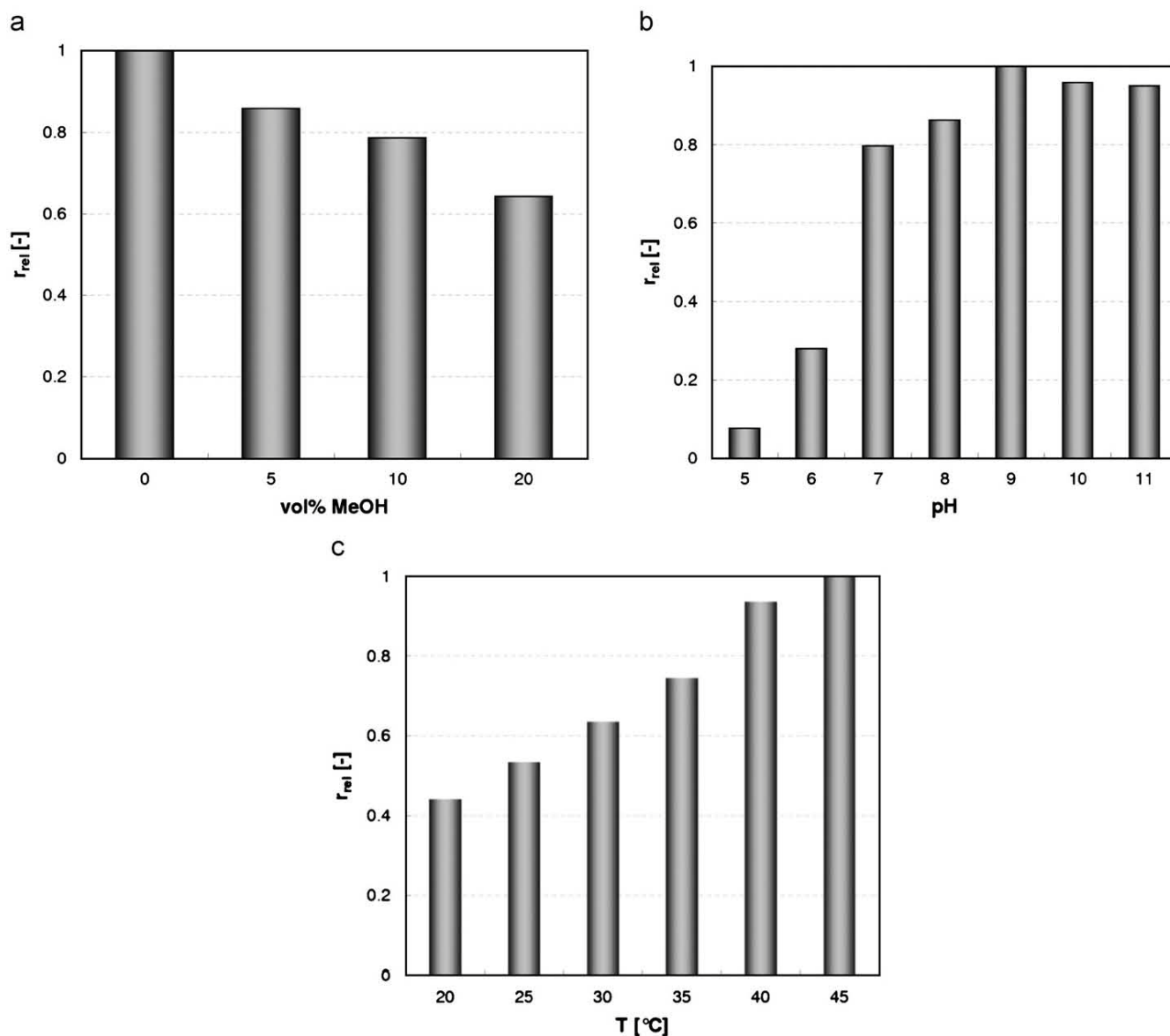


Fig. 10. Change of the initial rate of racemization of D-Met in dependence of: (a) MeOH content in the solvent for pH = 7, $C_{D-Met} = 15$ g/L, $C_{Cl} = 0.26$ g/L at 25 °C; (b) pH for 0% MeOH in the solvent, $C_{D-Met} = 30$ g/L, $C_{Cl} = 0.26$ g/L at 25 °C; (c) Temperature for pH = 7, 5% MeOH in the solvent, $C_{D-Met} = 20$ g/L and $C_{Cl} = 1$ g/L.

Besides the positive impact on the resolution, additionally low MeOH amount has other advantages, such as higher solubility of methionine and from common knowledge it is well known that enzymes do not tolerate MeOH.

In that manner, further investigations for the resolution of methionine were done for different pH values without presence of an organic modifier. The results depicted in Fig. 8 show that acetic conditions are preferable for the examined system.

In both cases the column performed better at 25 °C than at higher temperatures.

In order to check the reproducibility of the column after treatment with approx. 2L of buffer with pH 7 and without MeOH, several analytical injections of DL-Met were compared. Small difference in the resolution was noticed but no effect on the selectivity. Nevertheless, in order to stay in the safer range of the reproducibility, the amount of MeOH in the solvent was fixed to 5%.

4.4. Racemization kinetics

4.4.1. D-Asparagine

The results obtained from the influence of the temperature on the rate of racemization for D-Asn, depicted in Fig. 9, indicate higher rates for higher temperatures. In fact, at temperature of 30 °C the enzyme preparation performs with less than half of its capacity. Consequently, the temperature can be considered as a parameter of great potential for the optimization of the process.

4.4.2. D-Methionine

The results presented in Figs. 10a–c show better performances of the enzyme preparation at lower MeOH content and higher pH and temperatures, respectively.

Referring to some of the mentioned restrictions (buffer concentration and MeOH content) and the diverse trends for the effect

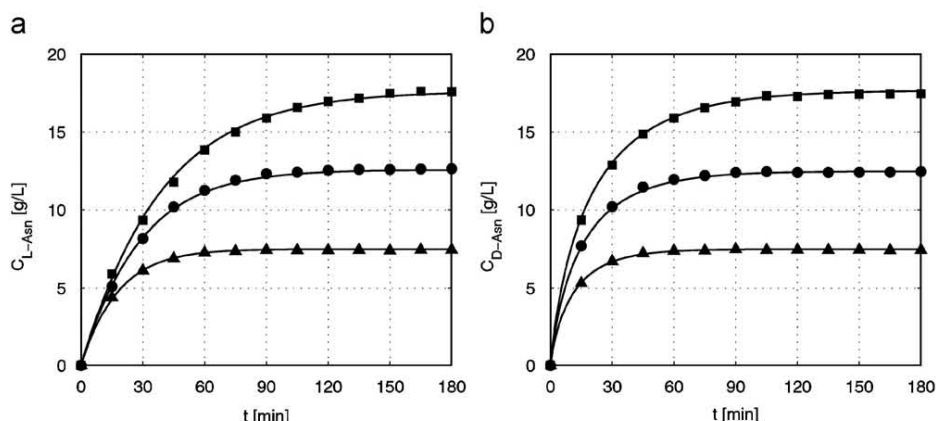


Fig. 11. Experimental (symbols) and fitted curves (lines) for racemization of: (a) D-Asn and (b) L-Asn in water for $C_{PL} = 0.5$ g/L and for different concentrations, $C_{D-L-Asn} = 15, 25$ and 35 g/L at 30°C .

Table 1

Estimated kinetic parameters and standard deviations for racemization of D-/L-Asn in water at 30°C and D-/L-Met in solvent at 25°C .

Racemization of	C_{PL} (g/L)	$K_{m,L}$ (g/L)	STDEV	$K_{m,D}$ (g/L)	STDEV	k (L/(g _{PL} min))	STDEV
D-Asn	0.5	2.44	1.17	2.19	0.67	0.436	0.13
L-Asn	0.5	18.57	1.56	3.22	0.19	0.219	0.01
Racemization of	C_{CL} (g/L)	$K_{m,L}$ (g/L)	STDEV	$K_{m,D}$ (g/L)	STDEV	k (L/(g _{PL} min))	STDEV
D-Met	1	2.11	0.22	3.4	0.34	0.122	0.01
L-Met	1	1.97	0.17	2.63	0.27	0.169	0.01

of T and pH for both units in P-II, a mixture of 0.1 M KPi buffer, $\text{pH} = 7/\text{MeOH} = 95/5$ v/v and temperature of 25°C was chosen as a compromised parameter set for further investigations.

The parameters of the racemization model (Eq. (4)) were determined using the parameter estimation tool *gEST*[®] incorporated in *gPROMS*[®] (Process Systems Enterprise Ltd., London, UK). The model was fitted to a set of experimental data by minimizing the maximum likelihood objective function sub-determined by the constant variance model. The following expression characterizes the maximum likelihood objective function:

$$\Phi = \frac{N}{2} \ln(2\pi) + \frac{1}{2} \min_{\Theta} \left\{ \sum_{i=1}^{NE} \sum_{j=1}^{NV_i} \sum_{k=1}^{NM_{ij}} \left[\ln(\sigma_{ijk}^2) + \frac{(z_{ijk} - \hat{z}_{ijk})^2}{\sigma_{ijk}^2} \right] \right\} \quad (5)$$

where N is the total number of experimental points, Θ is the set of model parameters to be estimated, NE is number of experiments, NV_i number of variables measured in the i -th experiment and NM_{ij} is the j -th variable in the i -th experiment. The variance of the k -th measurement of the variable j in the experiment i and its k -th measured and model predicted value in the i -th experiment are designated by σ_{ijk}^2 , \hat{z}_{ijk} and z_{ijk} , respectively.

As constraints in the constant variance model, where the measurement error is determined by constant standard deviation, the initial guess, the lower and the upper bounds of the standard deviation were set to 1×10^{-2} , 1×10^{-10} and 1×10^{-1} , respectively.

4.4.3. Racemization of D-/L-Asparagine

The model parameters for racemization of D- and L-Asn were estimated for each enantiomer separately by simultaneous fitting of the experimental data for $C_{D-L-Asn} = 15, 25$ and 35 g/L and $C_{PL} = 0.5$ g/L. The results are depicted in Fig. 11a, b, showing a remarkable match

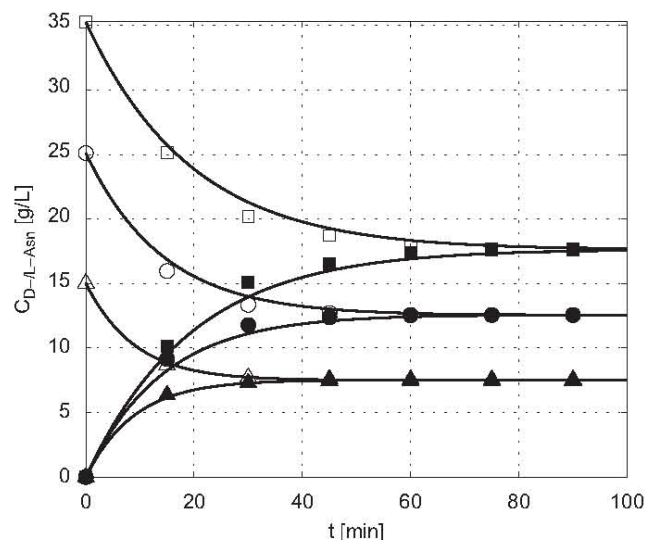


Fig. 12. Model validation for racemization of D-Asn in water for $C_{PL} = 1$ g/L and different concentrations of D-Asn (15, 25 and 35 g/L) at 30°C . Experimental data (black symbols: D-Asn; open symbols: L-Asn) and calculated curves (lines) obtained using the parameters shown in Table 1 for D-Asn.

between the experimental and fitted curves. The kinetic parameters are presented in Table 1. Namely, higher parameters were obtained for L-Asn in comparison to D-Asn, respectively, and rather diverse values for $K_{m,L}$ and $K_{m,D}$ for L-Asn. The experimentally noticeable difference of faster racemization for L-Asn, shown in Fig. 11, might be the result of different reaction mechanism for both enantiomers since side reactions could be excluded (Würges et al., 2009).

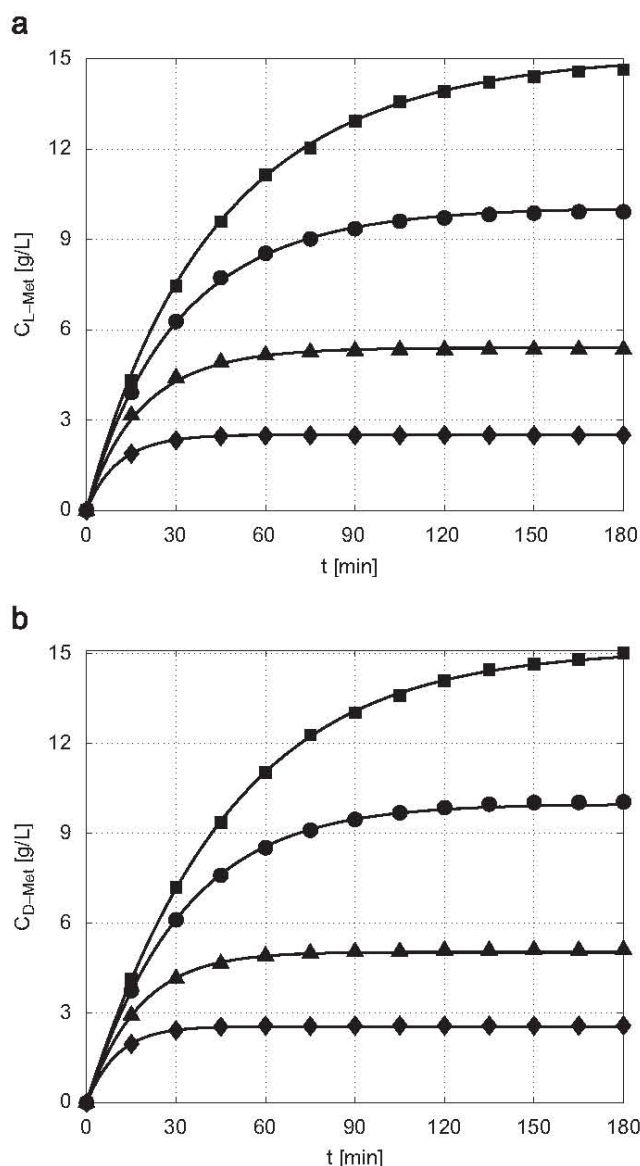


Fig. 13. Experimental (symbols) and fitted curves (lines) for racemization of : (a) D-Met and (b) L-Met in solvent for $C_{CL} = 1 \text{ g/L}$ and for different concentrations, $C_{D-L-Met} = 5, 10, 20$ and 30 g/L at 25°C .

Additionally, the difference in the dissociation constants for L-Asn may be explained by the restrictions given by the shape of the fitted concentration curves which usually allow a reliable prediction of maximum two parameters not being strongly correlated. However, the chosen model equation can sufficiently describe the enzymatic reaction in a wide concentration range (from diluted solutions up to solutions close to the solubility limit) and provides an adequate description of the racemization which is for engineering issues necessary for further process developments.

Since the racemization of D-Asn is of interest in this study, the validity of the model parameters was proven for $C_{D-Asn} = 15, 25$ and 35 g/L using $C_{PL} = 1 \text{ g/L}$ (Fig. 12).

4.4.4. Racemization of D-/L-methionine

The results of the experimental work and the model curves for racemization of D- and L-Met are presented in Fig. 13a, b. The simultaneous fitting of four different concentrations resulted with signifi-

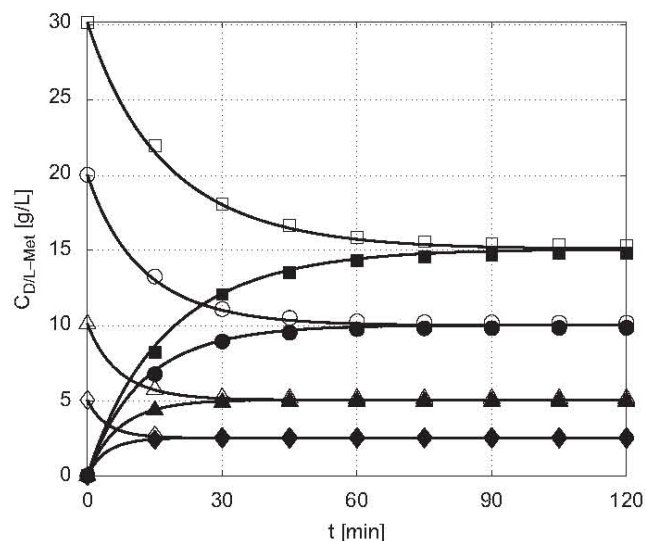


Fig. 14. Model validation for racemization of D-Met in solvent for $C_{CL} = 2.5 \text{ g/L}$ and different concentrations of D-Met (5, 10, 20 and 30 g/L) at 25°C . Experimental data (black symbols: D-Met; open symbols: L-Met) and calculated curves (lines) obtained using the parameters shown in Table 1 for D-Met.

cant predictions in the whole range of the examined system (starting from diluted up to solution close to the solubility limit of the enantiomer in the given solvent, $C_{CL} = 1 \text{ g/L}$). The values of the estimated kinetic parameters are summarized in Table 1. From the presented results, it is quite obvious that the dissociation constants are a bit smaller and the k value is higher for the racemization of L-Met in comparison to D-Met.

Like for the racemization of the enantiomers of asparagine the validation of the fitted model parameters was also confirmed in this case, i.e. the experimental results for racemization of D-Met were predicted satisfactorily for $C_{CL} = 2.5 \text{ g/L}$ (Fig. 14).

4.5. Feasibility of process schemes P-I and P-II

The experimental study presented in this work for two different examples provides a useful data base and allows to draw general conclusions about the feasibility of the process schemes P-I and P-II.

Concerning the working media and the time required for PC (slower process) and racemization (the purified enzyme preparation performs quite fast), the process scheme P-I seems to be quite promising and flexible. However, additional kinetic investigations have to be carried out in order to design PC. Before both units are integrated a choice of a proper reactor for racemization and optimization of the process scheme is required. One can even consider an attractive and simple one-tank process where the desired enantiomer is going to be preferably crystallized while the racemization reaction occurs in the liquid phase at the same time. On the other hand, several difficulties might appear when the enzyme preparation is present in the crystallizer. For instance, one of the major ones is the interruption of PC due to the presence of other components in the system influencing the form of the solubility ternary phase diagram.

Regarding the second examined (compound forming) system, the availability of chiral stationary phases as well as solvents which can be used as mobile phases for the chromatographic separation and as medium for racemization renders process scheme P-II to an attractive option. The experimental investigation shows that the enantioseparation as well as the racemization is feasible in a wider range of solvent compositions. Nevertheless, the authors are aware of the

changes in the solvent compositions due to dilution after chromatography and the complexity of the process scheme when a continuous process is intended to be performed.

5. Conclusion

Based on the determined solubility ternary phase diagrams for asparagine/water and methionine/solvent, two process concepts P-I and P-II were proposed for the production of pure enantiomers. For the conglomerate system (asparagine/water) the process scheme P-I consists of the cost-effective and moderately simple PC and racemization unit, while for the compound-forming system (methionine/solvent), due to the position of the eutectica, the combination of HPLC and racemization (process scheme P-II) was considered.

The feasibility of scheme P-I (just in pure water as solvent) led to an investigation only of the temperature influence on the racemization of D- and L-Asn, resulting in higher racemization rates at higher temperatures. Additionally, this process scheme holds a great potential of even greater simplification, since it can be realized as a one-tank process. This idea might be considered as an upgrade of the work presented in this paper.

For scheme P-II, the influence of particular process parameters, such as MeOH content in the solvent, pH and the temperature was studied for the chromatographic separation of DL-Met using eremomycin as chiral stationary phase as well as for the racemization of D- and L-Met. Lower MeOH amount in the solvent was found to be convenient for both units, while the effect of *T* and pH was diverse (diminished separation, but higher enzyme preparation performance for higher *T* and pH).

For the racemization of D-/L-Asn and D-/L-Met, a Michaelis–Menten three-step model was able to describe the experimental results. In all cases a highly satisfactory fit was obtained between the estimated and the experimental data. An experimentally distinguishable difference in the performance of the PL was observed for the racemization of D-Asn in comparison to L-Asn which is also noticeable in the values of their kinetic parameters. On the contrary, for the racemization of D- and L-Met only a slight difference was found between the kinetic constants. The validity of the utilized model was confirmed for both enantiomers for higher enzyme preparation concentrations.

Both process schemes need to be further optimized for efficient use.

Acknowledgments

The authors would like to acknowledge the contribution of Polina Peeva for the extensive measurements of the solubility data. The Diaspher-Chirasil-E column was a generous gift of Prof. Dr. S.M. Staroverov (Chemical Department, Lomonosov State University, Moscow, Russia).

References

- Ahuja, S., 1996. *Chiral Separations, Applications and Technology*. American Chemical Society, Oxford University Press, Washington DC, New York.
- Bechtold, M., Makart, S., Heinemann, M., Panke, S., 2006a. Integrated operation of continuous chromatography and biotransformations for the generic high yield production of fine chemicals. *Journal of Biotechnology* 124, 146–162.
- Bechtold, M., Heinemann, M., Panke, S., 2006b. Suitability of teicoplanin–aglycone bonded stationary phase for simulated moving bed enantioseparation of racemic amino acids employing composition-constrained eluents. *Journal of Chromatography A* 1113, 167–176.
- Bechtold, M., Makart, S., Reiss, R., Alder, P., Panke, S., 2007. Model-based characterization of an amino acid racemase from *Pseudomonas putida* DSM 3263 for application in medium-constrained continuous processes. *Biotechnology and Bioengineering* 98 (4), 812–824.
- Bornscheuer, U.T., Buchholz, K., 2005. Highlights in biocatalysis—historical landmarks and current trends. *Engineering in Life Sciences* 5 (4), 309–323.
- Caner, H., Groner, E., Levy, L., Agranat, I., 2004. Trends in the development of chiral drugs. *Drug Discovery Today* 9 (3), 105–110.
- Collet, A., Brienne, M.J., Jacques, J., 1980. Optical resolution by direct crystallization of enantiomer mixtures. *Chemical Reviews* 80 (3), 215–230.
- Collet, A., 1999. Separation and purification of enantiomers by crystallization methods. *Enantiomer* 4, 157–172.
- Cornish-Bowden, A., 1995. *Fundamental of Enzyme Kinetics*. Portland Press, London.
- Ebbers, E.J., Ariaans, G.J.A., Houbiers, J.P.M., Bruggink, A., Zwanenburg, B., 1997. Controlled racemization of optically active organic compounds: prospects for asymmetric transformation. *Tetrahedron* 53 (28), 9417–9476.
- Elsner, M.P., Fernández Menéndez, D., Alonso Muslera, E., Seidel-Morgenstern, A., 2005. Experimental study and simplified mathematical description of preferential crystallization. *Chirality* 17, S183–S195.
- Elsner, M.P., Ziomek, G., Seidel-Morgenstern, A., 2009. Efficient separation of enantiomers by preferential crystallization in two coupled vessels. *AIChE Journal* 55 (3), 640–649.
- Fogassy, E., Nögrádi, M., Kozma, D., Egri, G., Pálóvics, E., Kiss, V., 2006. Optical resolution methods. *Organic and Biomolecular Chemistry* 4, 3011–3030.
- Fung, K.Y., Ng, K.M., 2006. Experimental study of the effect of buffer on chromatography and crystallization hybrid processes. *Industrial and Engineering Chemistry Research* 45 (25), 8393–8399.
- Jacques, J., Collet, A., Wilen, S.H., 1994. *Enantiomers, Racemates and Resolutions*. Malabar, Florida.
- Kaemmerer, H., Polenske, D., Lorenz, H., Seidel-Morgenstern, A., 2008. Selection and application of chiral resolution strategies for compound forming systems on the basis of solubility isotherms. In: *Proceedings 15th International Workshop on Industrial Crystallization (BIWIC 2008)*, Magdeburg, pp. 1–8.
- Kaspereit, M., Gedicke, K., Zahn, V., Mahoney, A.W., Seidel-Morgenstern, A., 2005. Shortcut method for evaluation and design of a hybrid process for enantioseparations. *Journal of Chromatography A* 1092, 43–54.
- Leuchtenberger, W., Huthmacher, K., Drauz, K.S., 2005. Biotechnological production of amino acids and derivatives: current status and prospects. *Applied Microbiology and Biotechnology* 69, 1–8.
- Lorenz, H., Polenske, D., Seidel-Morgenstern, A., 2006. Application of preferential crystallization to resolve racemic compounds in a hybrid process. *Chirality* 18, 828–840.
- May, O., Verdeck, S., Bommarius, A., Drauz, K., 2002. Development of dynamic kinetic resolution processes for biocatalytic production of natural and nonnatural L-amino acids. *Organic Process Research & Development* 6, 452–457.
- Petruševska, K., Kuznetsov, M.A., Gedicke, K., Meshko, V., Staroverov, S.M., Seidel-Morgenstern, A., 2006. Chromatographic enantioseparation of amino acids using a new chiral stationary phase based on a macrocyclic glycopeptide antibiotic. *Journal of Separation Science* 29, 1447–1457.
- Polenske, D., Lorenz, H., 2008. Einfluss der Lage der eutektischen Linie im ternären Phasendiagramm auf das Potenzial der Bevorzugten Kristallisation zur Enantiomerengewinnung. Poster presented at GVC-Fachausschuss Kristallisation, Halle, 05.03–07.03.2008.
- Sakai, K., Hirayama, N., Tamura, R., 2007. *Novel Optical Resolution Technologies*. Springer, Berlin, Heidelberg.
- Scheper, T., 2003. *Advances in Biochemical Engineering/Biotechnology; Microbial Production of L-Amino Acids*, 79. Springer, Berlin, Heidelberg.
- Schnell, B., Faber, K., Kroutil, W., 2003. Enzymatic racemization and its application to synthetic biotransformations. *Advanced Synthesis and Catalysis* 345, 653–666.
- Shiraiwa, T., Miyazaki, H., Watanabe, T., Kurokawa, H., 1997. Optical resolution by preferential crystallization of DL-methionine hydrochloride. *Chirality* 9, 48–51.
- Ströhlein, G., Schulte, M., Strube, J., 2003. Hybrid processes: design method for optimal coupling chromatography and crystallization units. *Separation Science and Technology* 38 (14), 3353–3383.
- Würges, K., Petruševska, K., Serçi, S., Wilhelm, S., Wandrey, C., Seidel-Morgenstern, A., Elsner, M.P., Lütz, S., 2009. Enzyme-assisted physicochemical enantioseparation processes—part I: Production and characterization of a recombinant amino acid racemase. *J. Mol. Cat. B* (in print), available online: doi:10.1016/j.molcatb.2008.10.006.
- Yoshimura, T., Esaki, N., 2003. Amino acid racemases: functions and mechanisms. *Journal of Bioscience and Bioengineering* 96 (2), 103–109.
- Zhang, L., Gedicke, K., Kuznetsov, M.A., Staroverov, S.M., Seidel-Morgenstern, A., 2007. Application of an eremomycin–chiral stationary phase for the separation of DL-methionine using simulated moving bed technology. *Journal of Chromatography A* 1162, 90–96.

Publication 3

Enzyme-assisted physicochemical enantioseparation processes - Part III: Overcoming yield limitations by dynamic kinetic resolution of asparagine via preferential crystallization and enzymatic racemization

Würges, K., Petruševska-Seebach, K.,
Elsner, M. P. & Lütz, S.

Biotechnology and Bioengineering, 2009

Vol. 104, No. 6, 1235-1239

DOI 10.1002/bit.22498

Reproduced with the permission of Wiley Periodicals, Inc.

Enzyme-Assisted Physicochemical Enantioseparation Processes—Part III: Overcoming Yield Limitations by Dynamic Kinetic Resolution of Asparagine Via Preferential Crystallization and Enzymatic Racemization

Kerstin Würges,¹ Katerina Petruševska-Seebach,² Martin P. Elsner,² Stephan Lütz¹

¹Institute of Biotechnology 2, Research Centre Juelich, Juelich, Germany; telephone: 49-2461-61-4388; fax: 49-2461-61-3870; e-mail: s.luetz@fz-juelich.de

²Max Planck Institute for Dynamics of Complex Technical Systems, Magdeburg, Germany

Received 12 May 2009; revision received 20 July 2009; accepted 27 July 2009

Published online 4 August 2009 in Wiley InterScience (www.interscience.wiley.com). DOI 10.1002/bit.22498

ABSTRACT: The application of enantioseparation methods alone can only yield up to 50% of the desired chiral product. Thus enantioseparation becomes more attractive when accompanied by the racemization of the counter-enantiomer. Here we present first results of dynamic kinetic resolution of L-asparagine (L-Asn) via preferential crystallization and enzymatic racemization from a racemic, supersaturated solution on a 20 mL scale. An enzyme lyophilisate (WT amino acid racemase from *P. putida* KT2440 (E.C. 5.1.1.10), overexpressed in *E. coli* BL21(DE3)) was used for in situ racemization (enzyme concentrations varying from 0 to 1 mg/mL). When preferential crystallization was applied without any enzyme, a total of 31 mg of L-Asn monohydrate could be crystallized, before crystal formation of D-Asn started. Crystallization experiments accompanied by enzymatic racemization led to a significant increase of crystallized L-Asn (198 mg L-Asn monohydrate; >92%ee) giving the first experimental proof for this new process concept of dynamic kinetic resolution via preferential crystallization and enzymatic racemization. Measurements of the racemase activity before and after the crystallization process showed no significant differences, which would allow for enzyme recovery and recycling.

Biotechnol. Bioeng. 2009;104: 1235–1239.

© 2009 Wiley Periodicals, Inc.

KEYWORDS: amino acid racemase; dynamic kinetic resolution; preferential crystallization; integrated enantioseparation process; asparagine; in situ racemization; production of L-amino acids

Introduction

The demand of enantiopure substances, for example, as intermediates for the synthesis of optically active ingredients

for pharmaceutical applications or fine chemicals, has grown continuously during the last decades (Breuer et al., 2004). So has the market for amino acids as synthetic building blocks with annual growth rates of 5–7% (Leuchtenberger et al., 2005). Chiral compounds may be obtained via many different methods, for example, by biocatalysis or by catalytic asymmetric synthesis (Katsuki and Sharpless, 1980; Knowles and Sabacky, 1968). Nevertheless, the majority of chemical syntheses still leads to racemates so that the development of quite diverse approaches for chiral separation of optically active molecules has become a growing field of research (Fogassy et al., 2006). For the development and synthesis of pharmaceutical compounds, technically complex and expensive chiral separation techniques, such as preparative HPLC or supercritical fluid chromatography are often applied. Detailed treatises can be found elsewhere (McConnell et al., 2007).

Separation processes can roughly be divided into physicochemical and biocatalytic methods. While chromatography, which belongs to the first mentioned group, offers a plentitude of very selective and easy to control applications, its use particularly in preparative scale (e.g., in the form of simulated moving bed chromatography (Makart et al., 2008)) is still limited by high costs. Optical resolution by crystallization (either with or without chiral resolving agents) on the other hand, in some cases may be an inexpensive choice for the production of enantiopure substances on a large scale (Faigl et al., 2008). Noorduin et al. (2008) recently published a new method for the emergence of enantiopure crystals from nearly racemic solutions by grinding of the growing crystals and chemically induced solution-phase racemization. Enantioseparation via biocatalytic resolution on the other hand is based on

S. Lütz's present address is Novartis, CH-4056 Basel, Switzerland.
Correspondence to: S. Lütz

enantioselective transformation of the unwanted enantiomer to a product which is easy to separate from the remaining chiral educt. An example is the production of L-methionine from racemic *N*-acetyl-methionine by enzymatic deacetylation with aminoacylase from *Aspergillus niger* and subsequent crystallization (Chenault et al., 1989). Since all of these separation methods are aimed at producing enantiopure products, they all suffer from the fact of being limited to a maximum yield of 50%. In order to overcome this barrier, it becomes necessary to recycle the unwanted enantiomer by racemization.

A new strategy to overcome this yield limitation could be the dynamic kinetic resolution via preferential crystallization and enzymatic racemization (DPE) of the desired enantiomer from a racemic solution (Fig. 1), for which we already presented the process scheme (Petruševska-Seebach et al., 2009). Preferential crystallization (PC) relies on the property of dissolved chiral substances to form crystals of only one single enantiomer per unit cell. Starting from a racemic supersaturated solution, this holds only true for substances belonging to the group of conglomerate forming systems (Jacques et al., 1994). The utilization of enzymes for racemization instead of chemicals or high temperature treatment (Drauz et al., 1997) as well as the spontaneous crystallization from a supersaturated solution without evaporation of the solvent, makes this process an environmentally friendly approach. To demonstrate the advantage of in situ racemization with PC, we chose to use an aqueous solution of the proteinogenic amino acid asparagine (Asn). Enzymatic racemization was carried out by a well-characterized amino acid racemase from *Pseudomonas putida* (E.C. 5.1.1.10). In order to prevent undesired side reactions caused by other enzymes expressed in *E. coli*, the amino acid racemase was used in the form of a purified lyophilisate (Würges et al., 2009). This paper presents the proof of principle for a new approach suitable for the production of chiral substances from their racemates by DPE. It is not meant to give a detailed investigation on optimized reaction conditions and process parameter.

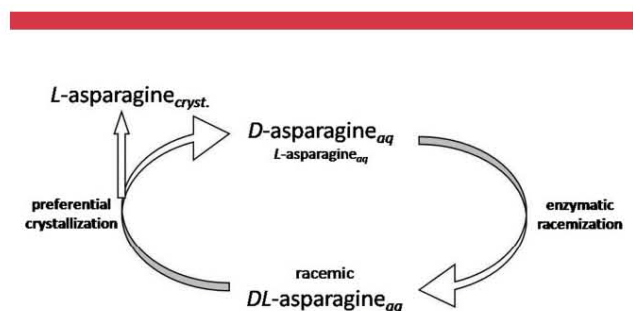


Figure 1. Principle of dynamic kinetic resolution of L-asparagine (Asn) via preferential crystallization and enzymatic racemization from a racemic solution. While L-Asn is removed from the system by crystallization, the resulting D-Asn excess is racemized enzymatically.

Materials and Methods

D-asparagine monohydrate ($\geq 99\%$) and L-asparagine monohydrate ($\geq 99\%$) were obtained from Sigma-Aldrich (Taufkirchen, Germany), racemic asparagine monohydrate ($\geq 99\%$) was obtained from Alfa Aesar (Karlsruhe, Germany) and perchloric acid (70%) was obtained from Fluka (Steinheim, Germany). Ultra pure water (Milli-Q by Millipore; Schwalbach, Germany) was used exclusively whenever H₂O is mentioned. A purified lyophilisate of the amino acid racemase (PL) was prepared as described previously (Würges et al., 2009). For crystallization experiments a double jacket glass vessel ($V = 25$ mL, glass workshop, Research Centre Juelich, Germany) with a mounted overhead stirrer (type: RW20.n, IKA Labortechnik, Staufen, Germany) was used. Furthermore, the reactor setup consisted of a peristaltic pump (type: ISM828, Ismatec SA, Zurich, CH), a convective benchtop incubator (Heraeus, Hanau, Germany), a flow-through polarimeter (type: P-2000, Jasco, Gross-Umstadt, Germany) and a water thermostat (type: F25-MH, Julabo Labortechnik GmbH, Seelbach, Germany). All components were connected via PTFE-tubing (1/16" OD \times 1.0 mm ID, CS-Chromatographie Service GmbH, Langerwehe, Germany). Syringe filters with a pore size of 0.2 μm (CS GmbH, Langerwehe, Germany) were used for sample purification. Enzyme assays were carried out in 1.5 mL reaction vials and incubated in a Thermostat Plus[®] (both Eppendorf, Hamburg, Germany). Enantiomeric compositions of samples were determined with an HPLC-system (Agilent Series 1100, Agilent Technologies, Inc., Santa Clara, CA) equipped with a chiral column (Crownpak CR(+)) 4×15 cm², Daicel Chem. Ind., Illkirch Cedex, France) using HClO₄ (pH 1) as mobile phase.

PC is an interesting method for the optical resolution of racemic solutions which is applicable to conglomerate forming systems. In contrast to racemic compounds, where both enantiomers coexist in 1 U cell, a conglomerate is defined as a mechanical mixture of crystals of both enantiomers. A third type of racemates are the so-called solid solutions. A detailed description can be found elsewhere (Jacques et al., 1994). Due to the attempt of a system to reach its thermodynamic equilibrium, there is an attractive possibility for direct crystallization of enantiopure crystals from a conglomerate forming system. The principle of this kinetically controlled crystallization is shown in Figure 2. To provide the driving force for PC, the racemic solution has to be supersaturated. This can be achieved most easily by cooling the solution from a temperature T_1 , at which the solution is unsaturated, to a temperature T_2 , at which it is supersaturated but still within the metastable zone (region in which no spontaneous crystallization is likely to occur). Within this zone the solution will return delayed to its thermodynamic equilibrium at which the liquid phase is racemic and the solid phase consists of a mixture of crystals of both enantiomers. By seeding the supersaturated solution with enantiopure crystals, a homochiral surface area for crystal growth is offered. Therefore the

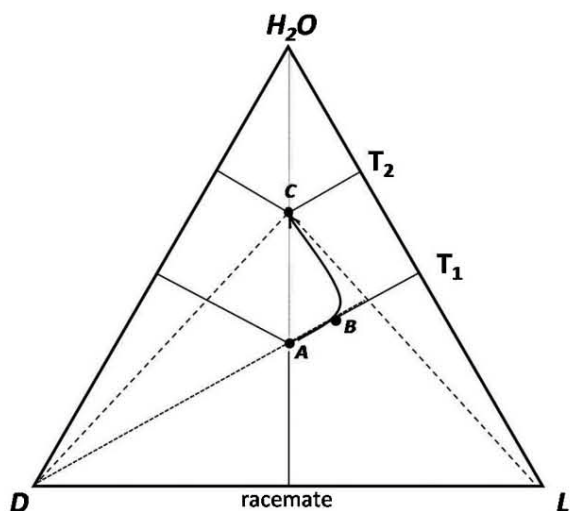
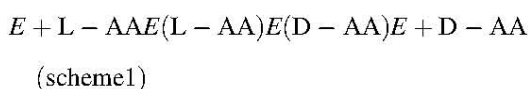


Figure 2. Principle of preferential crystallization (PC) for conglomerate forming systems in a ternary phase diagram. By subcooling the solution from T_1 to T_2 , the system becomes supersaturated and PC can be initiated by seeding with enantiopure crystals. The arrow represents the course of solution composition during PC until it has reached equilibrium conditions for T_2 .

liquid phase composition does not move directly from the starting composition (A) to the equilibrium composition (C) but follows a trajectory from (A) over (B) to (C). As long as the trajectory does not alter its linear direction, it is possible to collect enantiopure crystals. Detailed treatises of this process can be found in literature (Collet, 1999; Jacques et al., 1994; Lorenz et al., 2006; Rodrigo et al., 2004). Unfortunately, the occurrence of conglomerate forming systems is rather rare and can be estimated at about 10% of all racemates (Collet, 1999). Asn is one of the very few proteinogenic amino acids belonging to this group and was therefore chosen to demonstrate the yield increase achieved by DPE.

PL of amino acid racemase was used as biocatalyst for all described experiments. The enzyme follows a reversible three-step Michaelis–Menten kinetic (uses pyridoxal-5'-phosphate as cofactor) where the conversion of the L- to the D-amino acid/enzyme complex ($E(L-AA)$ and $E(D-AA)$) is pooled into one step:



with

$$K_{m,L} = \frac{k_{-1}k_{-2} + k_{-1}k_3 + k_2k_3}{k_1(k_{-2} + k_2 + k_3)}$$

$$K_{m,D} = \frac{k_{-1}k_{-2} + k_{-1}k_3 + k_2k_3}{k_{-3}(k_{-1} + k_{-2} + k_2)}$$

where E is the enzyme, k_i are the reaction rate constants for the single reactions and $K_{m,L/D}$ are the dissociation constants

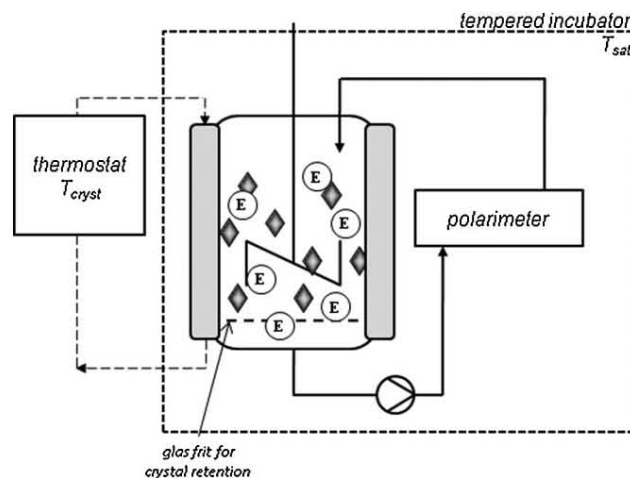


Figure 3. Reactor setup for dynamic kinetic resolution via preferential crystallization and enzymatic racemization (E: enzyme, T_{sat} : saturation temperature, T_{cryst} : crystallization temperature).

for the substrate/product binding to the enzyme for forward and backward reactions (under assumption that complex formation is not the rate limiting step). Detailed descriptions of the catalytic mechanism can be found elsewhere (Eliot and Kirsch, 2004; Schnell et al., 2003; Yoshimura and Esaki, 2003).

For crystallization studies a reactor setup was used as depicted in Figure 3. It consisted of a double jacket glass vessel with a polarimeter-bypass in which the optical rotation of the crystallization solution was determined continuously. The glass vessel, which served as crystallizer, was equipped with a glass frit (pore size of 16–40 μm) at its outlet to hold back crystals and with an overhead mixer for homogeneous mixing of the crystals in solution. The temperature of the crystallizer was controlled by a water-filled thermostat. The crystallization solution was pumped with a peristaltic pump (0.9 mL/min; 0.3 mm ID silicon tubing) through a polarimetric cell ($\lambda = 436 \text{ nm}$; 35°C) and back into the crystallizer. To prevent nucleation in tubings, all units were placed in an incubator and tempered to the saturation temperature of 35°C . A saturated Asn solution was prepared by dissolving racemic Asn H_2O (in excess) in H_2O for 1 h at 35°C (solubility of DL-Asn H_2O in water at 35°C : 99.6 g/L; solubility of DL-Asn H_2O in water at 32°C : 85.9 g/L). Undissolved crystals were removed by filtration with a 0.2 μm syringe filter and 20 mL of the saturated solution were transferred into the crystallizer that was tempered to 35°C . For DPE experiments, different amounts of PL (as indicated in Fig. 4) were dissolved in 20 mL solution, which was filtered before transferring it to the crystallizer. By pumping the solution through the bypass all air was displaced from the polarimetric cell. To provide the driving force for crystallization, the crystallizer was cooled down to the crystallization temperature of 32°C . By seeding

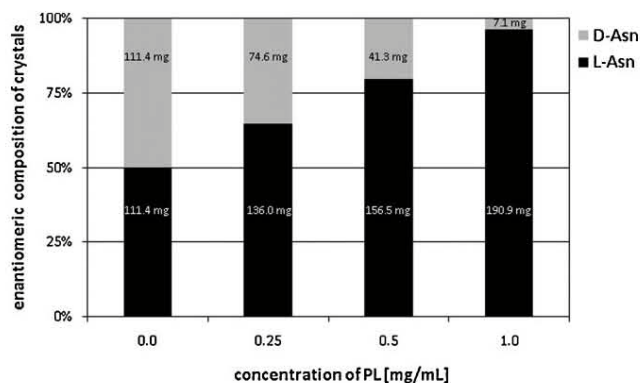


Figure 4. Increase of L-Asn fraction during EPC with rising enzyme concentration (PL). Numbers in bars are masses of crystallized Asn H₂O. Difference between theoretical crystal yield (273 mg, $T_{\text{sat}} = 35^{\circ}\text{C}$, $T_{\text{cryst}} = 32^{\circ}\text{C}$, $V = 20\text{ mL}$) and determined crystal yield is due to loss during harvest and crystal washing.

with 5 mg L-Asn H₂O (crystal fraction of 315–500 μm) PC was started. The experiments were terminated either after complete crystallization (meaning complete degradation of supersaturation) or at a defined time during initial enantioselective crystallization. At the end all crystals were removed from the solution by vacuum filtration over a paper filter, washed once with 5 mL of ice-cold H₂O and dried over night at 60°C. To determine the overall enantiomeric composition of the dried crystals, they were dissolved in H₂O and analyzed via chiral HPLC (mobile phase: HClO₄ pH 1.0, flow = 0.8 mL/min, $T = 0^{\circ}\text{C}$, inj $V = 5\ \mu\text{L}$, $\lambda = 200\text{ nm}$). Retention times were 2.1 min for D-Asn and 2.7 min for L-Asn, respectively. To determine enzyme activities before and after crystallization, 100 μL of crystallization solution were filtered through a 0.2 μm syringe filter and incubated with 100 μL of a 200 mM L-Asn substrate solution at 35°C and 650 rpm in a thermomixer. In intervals of 5 min, 10 μL were diluted with 990 μL of HClO₄ (pH 1) to terminate the reaction. The amount of converted product was determined via chiral HPLC. Initial slopes of product concentration over time (linear regression function of *MS Excel*[®] 2007) represent the enzyme activities. Calibration was performed for L- and D-Asn within the range of analyzed concentrations.

In the following paragraphs we present the results of PC experiments of L-Asn from a racemic supersaturated solution with and without enzymatic in situ racemization. Asn was identified as a conglomerate forming system by determination of the solubility ratio α with [rac] and [ep] representing the solubilities of racemic and enantiopure mixtures. Ideal conglomerates exhibit an α value of 2 ($\alpha = [\text{rac}]/[\text{ep}]$). In Petruševska-Seebach et al. (2009) we already reported on the nearly ideal behavior of Asn in water meaning the solubility of the racemic mixture is approximately twice as high as the solubility of pure enantiomer. It should be mentioned that in case of DPE the added enzyme

may have an impact on the solubility data of Asn in water. But since the molarity of added enzyme is very small compared to D- and L-Asn (about 1:30,000:30,000 for $c_{\text{PL}} = 1\text{ mg/mL}$ in saturated DL-Asn solution at 35°C) here it is seen as negligible.

To characterize the crystallization behavior in the system described above, L-Asn was crystallized from a saturated racemic solution without any addition of enzyme, and the enantiomeric composition of the solution was monitored via a polarimeter. A maximum excess of D-Asn of about 15 mM was reached after 150 min ($\Delta T = -3^{\circ}\text{C}$, $m_{\text{seed}} = 5\text{ mg}_{\text{L-Asn}}\text{H}_2\text{O}$). Another experiment was terminated after 120 min to gain as much as possible of enantiopure L-Asn. All formed crystals were filtered and dried over night at 60°C. A total mass of 31 mg of L-Asn H₂O ($\geq 99.5\%$ ee, determined by HPLC) could be collected. An end time of 120 min was found to be a good compromise between maximum crystal yield and purity.

A preliminary experiment showed that enzymatic in situ racemization could fully dissipate an excess of D-Asn in solution. All following DPE experiments were thus performed in a 25 mL crystallizer as described above but without the polarimeter bypass. The bypass was omitted to simplify the reactor and therefore minimize possible perturbations of the crystallization experiment. To determine the influence of different enzyme concentrations on the enantiomeric composition of the crystallization product, a series of experiments with different amounts of PL was performed under the conditions described above. Formed crystals were filtered after 20 h, washed with ice-cold H₂O and dried over night at 60°C. The enantiomeric composition was determined by dissolving the crystals in H₂O and subsequent HPLC analysis. As Figure 4 shows, the L-Asn fraction increased from 50.0% when no PL was added to 96.4% when 1 mg_{PL}/mL was added. The maximum yield of L-Asn H₂O ($\geq 92\%$ ee) gained during PC could thus be raised more than sixfold from 31 to 198 mg by in situ racemization with 1 mg_{PL}/mL.

For a cost efficient process enzyme recovery and recycling is always of great benefit. To check a potential activity loss, which might have occurred during the process, activities of the utilized PL were determined before and after each crystallization experiment as described. Remaining racemase activities of four independent runs showed no activity loss when compared to the initial activities but stayed rather constant (average remaining racemase activity after PC: $v_{\text{rel after}} = 107 \pm 17\%$).

We have presented an experimental proof, that DPE can improve the crystallization yield of L-Asn ($\geq 92\%$ ee) from a racemic solution. We developed a reactor concept for crystallization experiments of up to 20 mL reaction volume equipped with a polarimeter for online monitoring of the crystallization process. The reproducibility of the process was confirmed under chosen conditions (data not shown here) and a maximum yield of 31 mg nearly pure L-Asn H₂O ($\geq 99.5\%$ ee) was achieved by PC without enzymatic racemization. By adding the enzyme, an

accumulation of D-Asn in solution could be avoided which led to a sixfold yield-increase of L-Asn H₂O ($\geq 92\%$ ee) up to 198 mg. Furthermore, it was shown that the yield is dependent on the enzyme concentration during DPE. The use of higher enzyme concentrations kept the enantiomeric composition in solution closer to the racemic composition and thus prolonged the time until D-Asn crystallization affected PC. Nevertheless, the crystal yield is rather low (1.6% without racemization; 9.9% with 1 mg_{PL}/mL) when it is related to the initial mass of racemic Asn in the overall reaction volume of 20 mL which was 1.992 g. This might be circumvented by continuous feeding of racemic Asn into the process, which provides steady state conditions and thus allows a continuous process with 100% yield with respect to the Asn feed. Measurements of racemase activity in solution before and after crystallization experiments revealed no decrease, which is advantageous for a prolonged process and a potential reuse of the enzyme. For an efficient use, this promising integrated process needs to be further optimized with regard to crystallization and saturation temperatures, seed-crystal properties as well as reactor design.

References

- Breuer M, Ditrich K, Habicher T, Hauer B, Kefeler M, Stürmer R, Zelinski T. 2004. Industrial methods for the production of optically active intermediates. *Angew Chem Int Ed* 43(7):788–824.
- Chenault HK, Dahmer J, Whitesides GM. 1989. Kinetic resolution of unnatural and rarely occurring amino acids: Enantioselective hydrolysis of N-acetyl amino acids catalyzed by acylase I. *J Am Chem Soc* 111:6354–6364.
- Collet A. 1999. Separation and purification of enantiomers by crystallisation methods. *Enantiomer* 4(3–4):157–172.
- Drauz K, Bommarius A, Karrenbauer A, Knaup M, Degussa AG, assignee. 1997. 19.06.1997. Process for racemization of N-acetyl-D(L)-alpha-aminocarboxylic acids. Germany patent WO/1997/021650.
- Eliot AC, Kirsch JF. 2004. Pyridoxal phosphate enzymes: Mechanistic, structural, and evolutionary considerations. *Annu Rev Biochem* 73:383–415.
- Faigl F, Fogassy E, Nógrádi M, Pálovics E, Schindler J. 2008. Strategies in optical resolution: A practical guide. *Tetrahedron: Asym* 19:519–536.
- Fogassy E, Nógrádi M, Kozma D, Egri G, Palovics E, Kiss V. 2006. Optical resolution methods. *Org Biomol Chem* 4:3011–3030.
- Jacques J, Collet A, Wilen SH. 1994. *Enantiomers, racemates and resolutions*. Malabar: Krieger.
- Katsuki T, Sharpless KB. 1980. The first practical method for asymmetric epoxidation. *J Am Chem Soc* 102:5974–5976.
- Knowles WS, Sabacky MJ. 1968. Catalytic asymmetric hydrogenation employing a soluble optically active rhodium complex. *Chem Commun* 22:1445.
- Leuchtenberger W, Huthmacher K, Drauz K. 2005. Biotechnological production of amino acids and derivatives: Current status and prospects. *Appl Microbiol Biotechnol* 69(1):1–8.
- Lorenz H, Perlberg A, Sapoundjiev D, Elsner MP, Seidel-Morgenstern A. 2006. Crystallization of enantiomers. *Chem Eng Process* 45(10):863–873.
- Makart S, Bechthold M, Panke S. 2008. Separation of amino acids by simulated moving bed under solvent constrained conditions for the integration of continuous chromatography and biotransformation. *Chem Eng Sci* 63:5347–5355.
- McConnell O, Bach A, Balibar C, Byrne N, Cai Y. 2007. Enantiomeric separation and determination of absolute stereochemistry of asymmetric molecules in drug discovery—building chiral technology toolboxes. *Chirality* 19:658–682.
- Noorduyn WL, Izumi T, Millemaggi A, Leeman M, Meekes H, Enckevort WJP, Kellogg RM, Kaptein B, Vlieg E, Blackmond DG. 2008. Emergence of a single solid chiral state from a nearly racemic amino acid derivative. *J Am Chem Soc* 130:1158–1159.
- Petruševska-Seebach K, Würges K, Seidel-Morgenstern A, Lütz S, Elsner MP. 2009. Enzyme-assisted physicochemical enantioseparation processes—part II: Solid-liquid equilibria, preferential crystallization, chromatography and racemization reaction. *Chem Eng Sci* 64:2473–2482.
- Rodrigo AA, Lorenz H, Seidel-Morgenstern A. 2004. Online monitoring of preferential crystallization of enantiomers. *Chirality* 16:499–508.
- Schnell B, Faber K, Kroutil W. 2003. Enzymatic racemisation and its application to synthetic biotransformations. *Adv Synth Catal* 345(6–7):653–666.
- Würges K, Petruševska K, Serci S, Wilhelm S, Wandrey C, Seidel-Morgenstern A, Elsner MP, Lütz S. 2009. Enzyme-assisted physicochemical enantioseparation processes—part I: Production and characterization of a recombinant amino acid racemase. *J Mol Catal B: Enzymatic* 58:10–16.
- Yoshimura T, Esaki N. 2003. Amino acid racemases: Functions and mechanisms. *J Biosci Bioeng* 96(2):103–109.

Publication 4

An efficient route to both enantiomers of *allo*-threonine by simultaneous amino acid catalyzed isomerization of threonine and crystallization

Würges, K., Mackfeld, U., Pohl, M.,
Wiechert, W. & Kubitzki, T.

Advanced Synthesis & Catalysis, 2011

DOI: 10.1002/adsc.201100051

Copyright Wiley-VCH Verlag GmbH & Co. KGaA. Reproduced with permission.

Note: This manuscript represents the author's version of the peer-reviewed manuscript and is thus not identical to the copyedited version of the article available on the publisher's website.

DOI: 10.1002/adsc.200((will be filled in by the editorial staff))

An efficient route to both enantiomers of *allo*-threonine by simultaneous amino acid racemase catalyzed isomerization of threonine and crystallization

Kerstin Würges^a, Ursula Mackfeld^a, Martina Pohl^{a*}, Stephan Lütz^{a,b}, Susanne Wilhelm^c, Wolfgang Wiechert^a and Tina Kubitzki^a^a IBG-1: Biotechnology, Forschungszentrum Jülich GmbH, 52425 Jülich, Germany^b Novartis Institutes for BioMedical Research, Basel, Switzerland^c Institute of Molecular Enzyme Technology, University of Düsseldorf, Germany

Fax: +49 (2461) 61-3870; phone: +49 (2461) 61-4388; email: ma.pohl@fz-juelich.de

Received: ((will be filled in by the editorial staff))

Supporting information for this article is available on the WWW under <http://dx.doi.org/10.1002/adsc.200#####>. ((Please delete if not appropriate))

Abstract. We present an efficient method for the production of D- and L-*allo*-threonine (*allo*-Thr) with very high purity by enzymatic isomerization of L- or D-threonine (Thr) and simultaneous crystallization. Isomerization of Thr to *allo*-Thr is catalyzed by a purified amino acid racemase (AARac12996) from *Pseudomonas putida* NBRC12996, which can easily be obtained from a recombinant *E. coli* strain by secretion into the medium and subsequent anion exchange chromatography. Crystallization of D- and L-*allo*-Thr was performed in a repetitive batch mode over a period of up to 55 days at 30 °C. Total amounts of 30.8 g D-*allo*-Thr and 32.4 g L-*allo*-Thr were obtained with a very good diastereomeric excess of $de_{D-*allo*}$ >99.2 % and $de_{L-*allo*}$ >98.4 %, respectively, and in good yields (D-*allo*-Thr: 83 %, L-*allo*-Thr: 79 %). The enzyme's remarkable high stability

under process conditions resulted in enzyme specific yields of 2.56 g D-*allo*-Thr per mg AARac12996 and 1.62 g L-*allo*-Thr per mg AARac12996.

In contrast to chemical multi-step syntheses of *allo*-Thr, our process consists of only one enzyme catalyzed reaction step with simultaneous product crystallization. The process is performed under low energy consumption (30 °C, atmospheric pressure) in water and avoids the use and production of any toxic or harmful compounds. Recovery of the enantiomerically pure products is performed by simple filtration which reduces downstream processing significantly compared to chromatographic methods which are usually applied.

Keywords: *allo*-threonine, amino acid racemase, crystallization

1 Introduction

allo-threonine (*allo*-Thr) is part of many biologically active peptides such as naturally occurring antibiotics as well as other therapeutic chiral molecules.^[1-7] For example D-*allo*-Thr is used for chemical syntheses of key intermediates for the production of thienamycin, which is a potent antibiotic used against gram-positive and gram-negative bacteria.^[8,9] Further, *allo*-Thr is used as starting material in the chemical synthesis of lysobactin, an antibiotic used against methicillin-resistant *Staphylococcus aureus* (MRSA).^[10]

Several methods for the chemical as well as enzymatic synthesis of *allo*-Thr have been described.^[11-15] Kataoka *et al.*^[2] reported a stereoselective C-C bond formation between glycine and acetaldehyde using L-*allo*-Thr aldolase from *Aeromonas jandaei* DK-3. The same reaction can be performed using the serine hydroxymethyltransferase GlyA from *E. coli*.^[16] Lim *et al.*^[17] reported on an amino acid racemase from *Pseudomonas putida* ATCC 17642

with a threonine- α -epimerase activity (EC 5.1.1.6), which, to our knowledge, is the first and only reference about an enzymatic isomerization of threonine (Thr) in the literature. Although several amino acid racemases show broad substrate specificity such as arginine racemase from *P. graveolens*^[18] and amino acid racemases from *A. punctata*^[19] and *P. striata*^[20], they do not act on amino acids with substituted β -methylene groups such as threonine, isoleucine and valine. We could demonstrate that the amino acid racemase from *Pseudomonas putida* NBRC12996 (AARac12996) also catalyzes the isomerization of these amino acids. Nevertheless, chemical methods^[11-15] clearly outnumber the described enzymatic approaches. However, they consist of multi-step reaction cascades with only low yields. For example Blaskowich *et al.*^[12] described an 8-step synthesis of D- or L-*allo*-Thr starting from the respective threo-isomer with a total yield of 38 %. Although both enantiomers of *allo*-Thr are commercially available, they are extremely

expensive and, hence, not useful as starting material for large-scale syntheses.^[21]

Here we describe an easy and inexpensive method for the production of high-priced *allo*-Thr starting from cheap Thr using AArac12996. This enzyme was chosen since Kino *et al.*^[22] reported an activity on L-Thr, although it is very low compared to the preferred substrate L-lysine (0.1 %). Separation of *allo*-Thr from Thr in our approach is performed by simultaneous crystallization in a simple batch reactor. In contrast to replacing crystallization^[23, 24] or dynamic kinetic resolution processes, where enzymatic racemization is combined with preferential crystallization of single enantiomers from a saturated racemic solution,^[25] the crystallization of *allo*-Thr is based on its lower solubility limit compared to Thr in water.

AArac12996 has a broad substrate specificity which is comparable to other pyridoxal-5'-phosphate (PLP)-dependent amino acid racemases.^[26] This group of enzymes catalyzes the isomerization of the α -C atom. For amino acids with the α -C atom as the only chiral center this means interconversion of the L- and D-forms, whereas diastereomers with two chiral centers in α - and β -positions, such as Thr, are converted to their diastereomeric forms (figure 1).

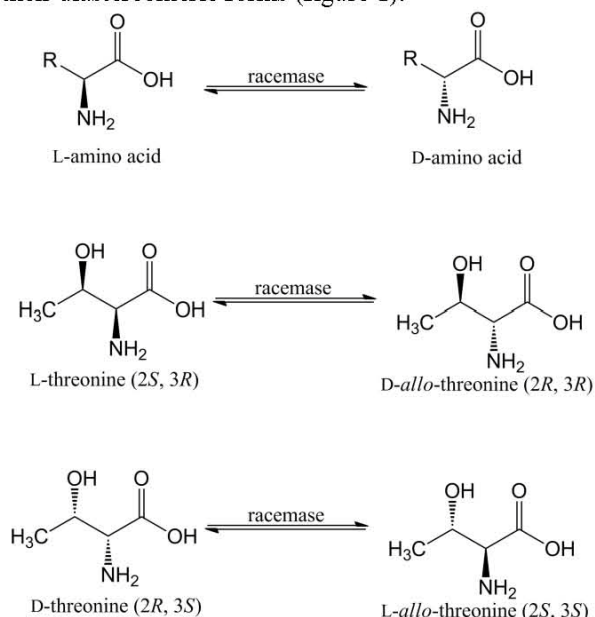


Figure 1: Isomerization of α -C atom catalyzed by amino acid racemase. Top: amino acids with only one chiral center are converted to their counterenantiomer. Middle and bottom: isomerization of α -C atom so that L-Thr is converted to its diastereomer D-*allo*-Thr and D-Thr to its diastereomer L-*allo*-Thr.

2 Results and Discussion

Cloning, overexpression and purification of AArac12996

The coding gene of AArac12996 from *P. putida* NBRC12996 was cloned into pET22b+ and overexpressed in *E. coli* BL21(DE3).

Surprisingly, our studies on protein expression resulted in a progressive accumulation of racemase activity in the extracellular medium over time (Table 1), indicating an intrinsic signal sequence in the coding gene. The full amino acid sequence (Supplementary Material) of AArac12996 was analyzed for a corresponding signal sequence using the program SignalP 3.0^[27] and a specific cleavage site was found between Ala24 and Ala25. This signal sequence shows the typical tripartite structure of signal peptides, consisting of a hydrophobic core region (h-region) flanked by a positively charged n-region and a polar c-region that contains the signal peptidase cleavage site.^[28] The subsequent release of periplasmic racemase through the outer cell membrane is supposed to be an autolytic response to the stress caused by overexpression and secretion of a foreign protein.^[29] Matsui *et al.*^[30] proposed a translocation mechanism for an amino acid racemase ArgR from *P. taetrolens*, which has an amino acid sequence identity of 73 % compared to AArac12996. ArgR is thought to be translocated via the Sec pathway by cleavage of an N-terminal signal peptide. According to the physiological role of alanine racemase^[31] it is assumed that also amino acid racemase plays an important role for the synthesis of D-alanine and D-glutamate in the murein layer. Cultivation of the recombinant *E. coli* in 2 L LB-medium yielded a total activity of 5900 U. Purification of the secreted enzyme from the medium by ultrafiltration and subsequent anion exchange chromatography resulted in pure enzyme (according to SDS-PAGE) with a specific activity of 8.6 U mg⁻¹. The freeze-dried protein (320 mg, protein concentration of ~73 %) was stored at -20 °C.

Table 1: Development of the intracellular and extracellular activity of AArac12996 during expression in *E. coli* BL21(DE3) cells in a 2 L cultivation. Activity was assayed using the standard assay as described in the experimental section.

expression time	activity in medium	activity in cells
[h]	[U]	[U]
20.0	300	1225
42.5	419	2361
67.0	3504	527

Characterization of AArac12996

AArac12996 is a PLP-dependent dimeric enzyme with a molecular weight of 44.2 kDa per monomer. While AArac12996 shows maximum activity for L-lysine (100 % relative activity), the activity for L-Thr isomerization is rather low (0.1 %). The enzyme was initially characterized by following the isomerization of L-asparagine (Asn), which was chosen because the i. Isomerization of Thr cannot be followed polarimetrically for easy activity measurements. ii. Activity for L-Asn is ca. 20fold higher than for L-Thr. The pH-optimum was found in the range of pH

8.6 - 9.7 (Figure 2). Investigation of the temperature dependency yielded a maximum initial rate activity at 31 °C (Figure 3). For isomerization of Asn the activation energy E_a was calculated as 48.4 kJ mol⁻¹, which is comparatively high compared to related racemases, such as alanine racemases from *P. fluorescens*^[32] (29.2 kJ mol⁻¹ for L-alanine) and *B. stearothermophilus*^[33] (7.54 kJ mol⁻¹ for D-alanine). The stability of AArac12996 was studied over 7 days by following the residual activity of liquid enzyme samples between 20 °C and 47 °C (Figure 4). The enzyme is stable for 7 days at 20 and 30 °C, whereas a rapid decay of activity was observed at 40 °C (6% residual activity in initial rate studies, Figure 3). Nevertheless, stability investigations at 40 °C (which assayed the residual activity at 30 °C) still showed a residual activity of about 16 % after 3 days. These results indicate a reversible inactivation of AArac12996 at temperatures between 31 °C and 40 °C. At 47 °C AArac12996 was inactivated irreversibly and showed no residual activity after an incubation of 2 h. The influence of supplemented PLP, which is covalently bound as cofactor to the active site of AArac12996, was investigated in the concentration range between 0 and 50 μM. Within this concentration range PLP had no influence on the enzyme activity; thus, it was omitted during biotransformations.

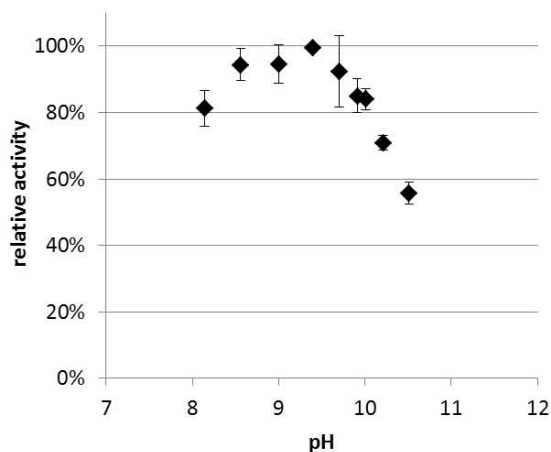


Figure 2: Determination of pH-optimimum for AArac12996 (0.1 mg mL⁻¹) in glycine/NaCl buffer (90 mM) at 30 °C. Relative activities were determined polarimetrically by following the isomerization of L-Asn (25 mM) for 5 minutes.

Kinetic parameters were determined for the isomerization of Thr. While the maximal velocities for the isomerization of both Thr-enantiomers are identical, their K_m values differ by a factor of 2 with L-Thr being the preferred enantiomer (Table 2). Based on these parameter studies, AArac12996 was characterized in detail for its application in the production of *allo*-Thr.

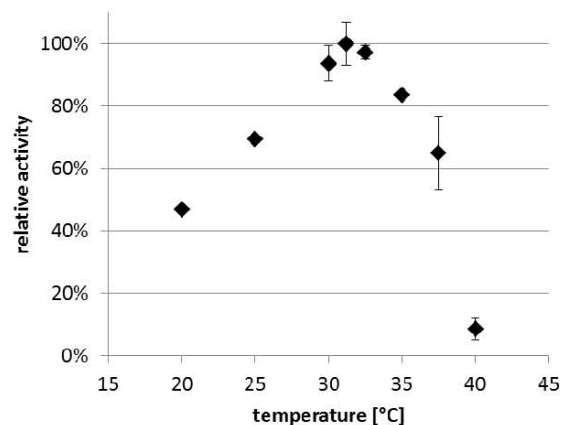


Figure 3: Determination of the temperature dependency for AArac12996 (0.1 mg mL⁻¹) in water. Residual activity was determined polarimetrically at 30 °C for the isomerization of L-Asn (90 mM) for 5 minutes.

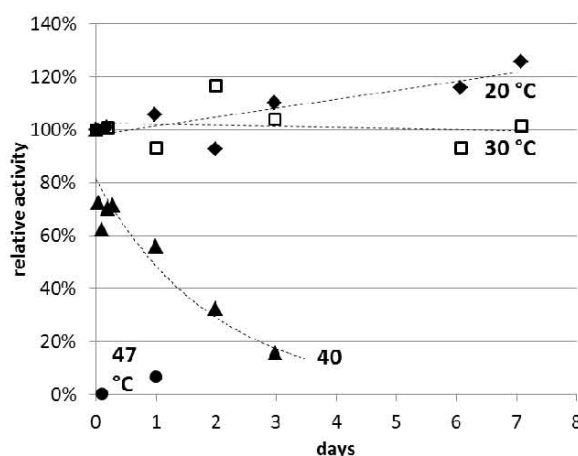


Figure 4: Stability of AArac12996 in water. Enzyme solutions (1 mg mL⁻¹) were stored at 20 °C – 47 °C. Aliquots were taken for polarimetric determination of residual activity (isomerization of L-Asn (90 mM) at 30 °C for 5 minutes).

Table 2: Kinetic parameters for the isomerization of Thr catalyzed by AArac12996 at 30 °C in water. Initial rate activities were determined by chiral HPLC. V_{max} values were calculated per mg of protein in the lyophilizate. k_{cat} corresponds to the turnover number per monomer.

reaction	V_{max} [U mg ⁻¹ _{AArac12996}]	K_m [mM]	k_{cat} [s ⁻¹]
L-Thr →	1.865 ± 0.154	92.5 ± 18.4	1.37
D- <i>allo</i> -Thr			
D-Thr →	1.866 ± 0.069	185.5 ± 11.9	1.37
L- <i>allo</i> -Thr			

Repetitive batch crystallization of *allo*-threonine

Both enantiomers of *allo*-Thr were produced and crystallized with very high purity starting from either D- or L-Thr. The process was performed in a repetitive batch mode, in which enzymatic isomerization of Thr to *allo*-Thr and crystallization of *allo*-Thr took place simultaneously in one single reaction vessel at 30 °C (Figure 5). Depending on the desired *allo*-Thr enantiomer, either L- or D-Thr was used as the substrate. The process consists of three main steps:

I) Start of the first batch by addition of AArac12996 to a saturated Thr solution (119 g L⁻¹ at 30 °C in water, pH was titrated to 8.5 using 10 n NaOH) containing undissolved excess Thr: Thr is converted to *allo*-Thr until the saturation limit of *allo*-Thr (83 g L⁻¹ at 30 °C in water, pH 8.5) is reached. The concentration of Thr remains constant (due to progressive solubilization of excess Thr).

II) Crystallization of *allo*-Thr: *allo*-Thr starts to crystallize spontaneously upon exceeding the solubility limit. The composition of the solution is 42 % D-*allo*-Thr and 58 % L-Thr due to different solubilities. This process is driven by the conversion of Thr to *allo*-Thr until depletion of excess Thr.

III) Complete conversion of excess Thr to *allo*-Thr: The process stops when all excess Thr is dissolved and converted. *allo*-Thr crystals are separated by filtration and dried at 60 °C. The next batch can be started by the addition of fresh Thr.

Steps II and III are repeated for a repetitive batch crystallization.

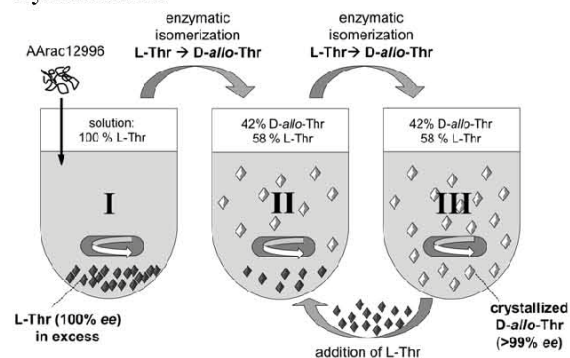


Figure 5: Repetitive batch crystallization (20 mL) of D-*allo*-Thr in one single reaction vessel. I: AArac12996 is added to a saturated L-Thr solution (starting condition) II: dynamic process of crystallization (D-*allo*-Thr), solubilization (L-Thr) and isomerization (L-Thr → D-*allo*-Thr) III: addition of fresh L-Thr when excess has depleted. Steps II and III are repeated for repetitive batch crystallization.

Repetitive batch processes (20 mL scale) were performed for the production of D- and L-*allo*-Thr, respectively. Process data and yields for both enantiomers are summarized in Tables 3 and 4. Production of D-*allo*-Thr was performed over 55 days and consisted of 12 batches with yields of 1.6 to

4.4 g D-*allo*-Thr per batch and a diastereomeric excess (de_{allo}) between 96.9 and 100 %. A space time yield (STY) of 28 g L⁻¹ d⁻¹ and a final yield of 30.8 g D-*allo*-Thr ($de_{allo} > 99.2$ %) were achieved. An initial amount of 10 mg AArac12996 was applied and additional 2 mg of AArac12996 were added after 13 days.

Production of L-*allo*-Thr was performed over 56 days and consisted of 12 batches with yields of 1.5 to 4.0 g L-*allo*-Thr per batch and a de_{allo} between 94.6 and 100 %. A STY of 28.8 g L⁻¹ d⁻¹ and a final yield of 32.2 g L-*allo*-Thr ($de_{allo} > 98.4$ %) were obtained using a total amount of 20 mg AArac12996.

The enzyme showed a remarkable high stability under process conditions yielding 2.56 g D-*allo*-Thr and 1.62 g L-*allo*-Thr per mg AArac12996, respectively.

The activity of AArac12996 in the crystallization solution was monitored throughout the process. Figure 6 shows the relative activities of AArac12996 during D-*allo*-Thr crystallization over a period of 55 days. The deactivation constant k_d was calculated from

$$v = v_0 \cdot e^{(-k_d t)}$$

where v_0 is the initial enzyme activity.

$$k_d = 0.0218 \text{ d}^{-1} (\pm 0.0035 \text{ d}^{-1})$$

Half-life $t_{1/2}$ of the enzyme was derived from

$$t_{1/2} = \frac{\ln(0.5)}{-k_d} = 31.8 \text{ d}$$

Table 3: Production of D-*allo*-Thr by repetitive batch crystallization and enzymatic isomerization of L-Thr (V= 20 mL, 30°C, pH 8.5, initial amount of AArac12996: 10 mg, addition of 2 mg AArac12996 after 13 days).

batch no.	process time [d]	added L-Thr [g]	batch time [h]	yield ^{a)} [g]	de_{allo} ^{b)} [%]
1	5.9	7	141	3.05	100.0
2	8.8	2	69	1.68	100.0
3	13.8	4	120	3.55	98.0
4	16.0	2	53	1.97	96.9
5	19.9	3	94	3.08	98.3
6	23.8	3	93	2.84	100.0
7	26.8	2.5	74	2.08	99.7
8	30.8	3	94	2.6	99.3
9	34.0	2	77	1.83	100.0
10	37.0	2	73	1.63	99.4
11	47.8	4	258	4.41	99.9
12	54.8	2.5	168	2.10	99.7
sums	54.8	37.0	1314	30.82	99.2

a) yield of crystallized D-*allo*-Thr, b) diastereomeric excess of D-*allo*-Thr in crystals

Table 4: Production of L-*allo*-Thr by repetitive batch crystallization and enzymatic isomerization of D-Thr ($V=20$ mL, 30°C , $\text{pH } 8.5$, AArac12996: 20 mg).

batch no.	process time [d]	added D-Thr [g]	batch time [h]	yield ^{a)} [g]	de_{allo} ^{b)} [%]
1	9.8	9	236	3.94	99.6
2	12.7	2	70	1.98	99.0
3	15.8	3	74	2.98	98.6
4	19.9	3	99	3.10	99.6
5	22.8	3	70	2.55	98.4
6	27.0	4	99	3.32	94.6
7	30.8	3	92	2.80	95.8
8	34.0	2	77	2.06	100.0
9	37.1	2	73	1.79	99.7
10	47.8	4	258	4.04	99.8
11	50.9	2.5	75	1.54	99.7
12	55.8	3	117	2.32	96.5
sums	55.8	40.5	1339	32.42	98.4

a) yield of crystallized L-*allo*-Thr, b) diastereomeric excess of L-*allo*-Thr in crystals

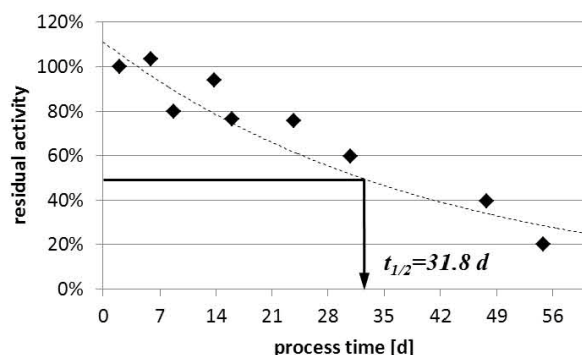


Figure 6: Deactivation and half life ($t_{1/2}$) of AArac12996 during repetitive batch crystallization of D-*allo*-Thr. Activities were determined using the standard assay. $k_d=0.0218$ d^{-1} (± 0.0035 d^{-1}).

3 Conclusion

Enantiopure L- and D-*allo*-Thr were produced by enzymatic isomerization of either D- or L-Thr and simultaneous crystallization. Recovery of the enantiomerically pure products was performed by simple filtration which reduced downstream processing significantly compared to e.g. chromatographic methods.^[34]

The reaction was catalyzed by AArac12996 from *P. putida*, which was cloned and overexpressed in *E. coli*. As the enzyme was secreted into the medium, its purification is easy. V_{max} and K_m values were

determined for both Thr enantiomers. V_{max} was found to be similar for both reactions (1.87 U mg^{-1} AArac12996), whereas the K_m value, which is a measure for the affinity for both enantiomers, differs by a factor of 2 (table 2), indicating a higher affinity for L-Thr ($K_{m,L\text{-Thr}}=92.5$ mM, $K_{m,D\text{-Thr}}=185.5$ mM). AArac12996 shows highest initial rate activity at a pH of about 9 and a temperature of 31°C . Surprisingly, the enzyme was completely stable at 30°C for at least 7 days. Thus, this temperature was chosen for the production of D- and L-*allo* Thr.

D- and L-*allo*-Thr were crystallized with high purities in repetitive batch processes starting from saturated Thr solutions. Total amounts of 30.8 g D-*allo*-Thr and 32.4 g L-*allo*-Thr were obtained with a very good diastereomeric excess of $de_{D\text{-allo}}>99.2\%$ and $de_{L\text{-allo}}>98.4\%$, respectively, and in good yield (D-*allo*-Thr: 83 %, L-*allo*-Thr: 79 %). Final space time yields of 28.0 $\text{g L}^{-1} \text{d}^{-1}$ for D-*allo*-Thr and 28.8 $\text{g L}^{-1} \text{d}^{-1}$ for L-*allo*-Thr were reached. A conversion of almost 100 % could easily be achieved by additional batches. The enzyme's remarkable high stability under process conditions resulted in enzyme specific yields of 2.56 g D-*allo*-Thr per mg AArac12996 and 1.62 g L-*allo*-Thr per mg AArac12996.

Compared to chemical synthesis methods for *allo*-Thr, which contain several reaction steps each followed by chromatographic purification of the intermediate,^[13] our process consists of only one enzyme catalyzed reaction (isomerization of bulk Thr) and simultaneous crystallization in one single reaction vessel. The process was carried out at moderate temperature (30°C) in water and avoids any toxic or harmful compounds. Product recovery was performed by simple filtration of the crystallization solution and subsequent crystal drying, which made downstream processing very comfortable. In contrast to other biocatalytic production and separation methods for *allo*-Thr^[34] we could achieve very high purities with $de_{\text{allo}}>99\%$ and theoretically approach complete conversion of the substrate.

4 Experimental Section

Cloning of AArac12996

The AArac12996 gene was amplified by standard PCR from the genomic DNA of *Pseudomonas putida* NBRC12996 which was kindly provided by the Department of Biotechnology, Kansai University (Japan). Genomic DNA was isolated from an overnight culture grown at 30°C in LB-Medium using the DNeasy Blood & Tissue Kit (Qiagen). Following primers (Eurofins MWG Operon, Ebersberg, Germany) have been used for cloning:

*NdeI*_AArac_fw:

5'-AAAACATATGCAATTTAGCCGTACCCTCCTGG-3'

NdeI start

*XhoI*_AARac_rev:

5'-AAACTCGAGTCAGTCGACGAGAATCTTCGG-3'

XhoI stop

The PCR-fragment was purified on an agarose gel (1%) and digested with *NdeI* and *XhoI* (Fermentas, St. Leon-Rot, Germany). Subsequently the AARac12996 gene was ligated into the *NdeI/XhoI* digested vector pET22b+ (Novagen®, Merck KGaA, Darmstadt, Germany) yielding the final construct pET22b-AARac12996. The expression host *E. coli* BL21(DE3) was transformed with pET22b-AARac12996 by electroporation. Sequence identity was verified by DNA sequencing (Agowa, Berlin, Germany). For protein and DNA-sequences see Supplementary Material.

Expression and purification

Cultivation of the recombinant *E. coli* BL21(DE3) strain was performed in 5 x 400 mL of LB medium (10 g L⁻¹ peptone, 5 g L⁻¹ yeast extract, 10 g L⁻¹ NaCl) at 37 °C and 100 rpm in 2 L shaking flasks. Each flask was inoculated with 4 mL of an overnight pre-culture. At OD₆₀₀~0.6 protein expression was induced by addition of IPTG (100 µM) and the temperature was decreased to 27 °C. After 67 h cells were separated from the racemase containing medium by centrifugation (15000 g, 20 min, 4 °C). Separation of AARac12996 from low molecular weight medium components was performed by ultrafiltration (ultrafiltration device manufactured by mechanical workshop of IBT, Forschungszentrum Jülich GmbH, Germany; membrane cutoff: 10 kDa) by concentrating the medium to 10 % of its initial volume three times and refilling with potassium phosphate buffer (10 mM KPi, 10 µM PLP, pH 7). Occurring precipitates were separated by centrifugation and the supernatant was filtered (syringe filter, 0.4 µm) before applying onto an anion-exchange column (DEAE-Sepharose FF, 5 x 25 cm, column volume (CV): 500 mL, equilibrated with 10 mM KPi (10 µM PLP, pH 7)). Unbound proteins were washed from the column with 2 CV of 10 mM KPi (10 µM PLP, pH 7). AARac12996 was eluted with 10 mM KPi (10 µM PLP, pH 7) containing 100 mM NaCl after about 3.8 CV at a flow rate of 10 mL min⁻¹. Enzyme containing fractions were detected at 280 nm (absorption of aromatic side chains of proteins) and 420 nm (absorption of PLP). A total volume of 850 mL was desalted by ultrafiltration using 10 mM KPi (10 µM PLP, pH 7) as described above, concentrated to a final volume of 120 mL, frozen in liquid nitrogen and lyophilized for 24 h (freeze-dryer: Christ Alpha 2-4, Germany). The freeze-dried enzyme (320 mg, 73 % protein content) was stored at -20 °C.

Activity assay

The specific activity of AARac12996 was investigated by determination of the initial reaction rate for the isomerization of L-Asn. Therefore, the linear slope of

product (D-Asn) formation was determined within a conversion range <10%. Specific activities were determined using a standard activity assay and following the increase of D-Asn by chiral HPLC.

One unit of activity was defined as the amount of AARac12996 which catalyzes the isomerization of 1 µmol L-Asn to D-Asn per minute under standard conditions (190 mM L-Asn in water, 35 °C). Relative activities for investigation of pH-optimum and temperature dependency as well as for stability investigations were determined by following the decrease of optical rotation with a polarimeter. In order to allow optimal solubility and crystallization in the *allo*-Thr production process, all measurements (except for the determination of the pH-optimum) were performed in water without buffer salts.

Assay conditions HPLC: 950 µL L-Asn in water (200 mM), 50 µL AARac12996 containing solution. To stop the reaction 10 µL of assay solution were diluted with 990 µL HClO₄ (pH 1) prior to injection. Column: Daicel Crownpak CR(+) 0.4 x 15 cm; mobile phase: HClO₄ (pH 1); flow: 0.6 mL min⁻¹; column temperature: 0 °C. HPLC-system: Agilent Series 1100.

Assay conditions polarimeter: 1 mL L-Asn solution in water (90 mM if not indicated otherwise), 110 µL AARac12996 solution (1 mg mL⁻¹). Polarimeter: Jasco P-2000; cell length = 100 mm, λ = 365 nm, t = 5 min, 30 °C (varying temperatures for determination of temperature dependency).

Kinetic parameters

V_{max} and K_m for the isomerization reaction of Thr to *allo*-Thr were calculated by non-linear regression using Origin 7G (OriginLab Corporation, Northampton, USA). The turnover number k_{cat} was derived from V_{max} for a single monomer. All kinetic parameters are related to the relative protein mass determined (according to Bradford) in the enzyme preparation. The identity of *allo*-Thr was verified by ¹H-NMR spectroscopy (Bruker, Avance DR X 600) in D₂O (600 MHz, ppm: δ= 1.14-1.15 (d, 3H, J =6.42, CH₃), 3.77-3.78 (d, 1H, J =3.77, CH), 4.28-4.32 (m, 1H, CH)).

Determination of protein concentration

Protein concentrations were determined according to Bradford^[35] using BSA as standard.

Investigation of temperature dependency and pH-optimum

The temperature dependency of the initial rate activity of AARac12996 (0.1 mg mL⁻¹) was determined for L-Asn (90 mM) in water between 20 °C and 40 °C. Initial reaction rates were measured polarimetrically.

The pH-optimum of AARac12996 (0.1 mg mL⁻¹) was determined polarimetrically by initial rate measurements in glycine/NaCl buffer (90 mM each, titrated with NaOH) in the range of pH 8.1 to 12.6

using L-Asn (25 mM) as a substrate. It has to be noted that the substrate concentration (25 mM) was significantly lower than the K_m -value for L-Asn (>100 mM). However, higher concentrations of Asn could not be applied, because the capacity of the buffer was exceeded otherwise. Reaction rates were determined only from the linear part of the conversion curve. Since the activities were not obtained under V_{max} conditions, initial reaction rates at different pH values are given as relative activities. All measurements were performed twice and relative activities were calculated as mean values.

The activation energy E_a of AArac12996 was derived from the Arrhenius plot ($\ln(v)$ vs. T^{-1}) as the product of the slope m and the negative gas constant R ($8.314 \text{ J K}^{-1} \text{ mol}^{-1}$): $E_a = -m \cdot (-R)$.

Stability investigations

Enzyme stabilities were investigated for AArac12996 (1 mg mL^{-1}) in water at temperatures between 20 and 47 °C. Aliquots were taken over up to 7 days and residual activities were determined polarimetrically at 30 °C for 5 min using L-Asn (90 mM) as a substrate.

Repetitive batch crystallization

Repetitive batch crystallization was performed for L- and D-*allo*-Thr. Here we describe the process for the crystallization of D-*allo*-Thr, which is similar to the one for L-*allo*-Thr but starting from the other Thr enantiomer. Experiments were performed in a double jacketed 50 mL glass reactor which was tempered by a water thermostat to 30 °C. A saturated L-Thr solution was prepared by the addition of 5 g L-Thr to 20 mL water and the pH was adjusted to 8.5 with 10 n NaOH. Excess L-Thr remained as sediment. The conversion of L-Thr to D-*allo*-Thr was performed by 12 mg AArac12996 (for L-*allo*-Thr crystallization 20 mg AArac12996 were used). Crystallization of D-*allo*-Thr started upon exceeding the solubility limit. The crystallization process was monitored by HPLC as described below. After complete solubilization of excess L-Thr, D-*allo*-Thr crystals were harvested by filtration, washed with 2 mL of ice cold water and dried for 1 h at 60 °C. The next batch was started by addition of fresh L-Thr to the remaining solution (Figure 5).

Monitoring of the crystallization process

The composition of solution during *allo*-Thr crystallization and the diastereomeric excess (de_{allo}) of crystals were determined by HPLC employing an HP 1100 series equipped with a chiral column (Daicel Crownpak CR(+)) 0.4 x 15 cm; mobile phase: HClO_4 (pH 1); flow: 0.8 mL min^{-1} ; column temperature: 5 °C). de_{allo} was calculated from $de_{allo} = ([allo\text{-Thr}] - [Thr]) / ([allo\text{-Thr}] + [Thr])$ where $[allo\text{-Thr}]$ and $[Thr]$ are the crystal fractions of the respective diastereomer. Space time yields (STY) were calculated from $STY = \text{yield} / (t \cdot V)$ where t is the process time and V is the reaction volume. The

remaining activity of AArac12996 during *allo*-Thr crystallization was determined as described above with 50 μL of enzyme containing crystallization solution.

Acknowledgements

We kindly thank Prof. Tadao Oikawa from the Department of Biotechnology of Kansai University (Japan) for providing the *Pseudomonas putida* strain NBRC12996.

References

- [1] L. A. Flippin, K. Jalali-Araghi, P. A. Brown, H. R. Burmeister, and R. F. Vesonder, *J. Org. Chem.* **1988**, *54*, 3006-3007.
- [2] M. Kataoka, W. Masaru, M. Ikemi, T. Morikawa, T. Miyoshi, and S. Shimizu, *Ann. N. Y. Acad. Sci.* **1998**, *864*, 318-322.
- [3] M. J. Miller, *Acc. Chem. Res.* **1986**, *19*, 49-56.
- [4] T. Nagahara and T. Kametani, *Heterocycles* **1987**, *25*, 729-806.
- [5] J. Burke, Terrence R., M. Knight, and B. Chandrasekhar, *Tetrahedron Lett.* **1989**, *30*, 519-522.
- [6] P. J. Maurer, C. G. Knudsen, A. D. Palkowitz, and H. Rapoport, *J. Org. Chem.* **1985**, *50*, 325-332.
- [7] J. L. Morell, P. Fleckenstein, and E. Gross, *J. Org. Chem.* **1977**, *42*, 355-356.
- [8] M. Shiozaki, N. Ishida, H. Maruyama, and T. Hiraoka, *Tetrahedron* **1983**, *39*, 2399-2407.
- [9] M. Shiozaki, N. Ishida, T. Hiraoka, and H. Maruyama, *Tetrahedron* **1984**, *40*, 1795-1802.
- [10] A. Guzman-Martinez, R. Lamer, and M. S. VanNieuwenhze, *J. Am. Chem. Soc.* **2007**, *129*, 6017-6021.
- [11] P. L. Beaulieu, *Tetrahedron Lett.* **1991**, *32*, 1031-1034.
- [12] M. A. Blaskovich and G. A. Lajoie, *Tetrahedron Lett.* **1993**, *34*, 3837-3840.
- [13] G. Cardillo, L. Gentilucci, A. Tolomelli, and C. Tomasini, *J. Org. Chem.* **1998**, *63*, 3458-3462.
- [14] P. Lloyd-Williams, N. Carulla, and E. Giralt, *Tetrahedron Lett.* **1997**, *38*, 299-302.
- [15] D. Pons, M. Savignac, and J.-P. Genet, *Tetrahedron Lett.* **1990**, *31*, 5023-5026.
- [16] S. Makart, M. Bechtold, and S. Panke, *J. Biotechnol.* **2007**, *130*, 402-410.
- [17] Y.-H. Lim, K. Yokoigawa, N. Esaki, and K. Soda, *J. Bacteriol.* **1993**, *175*, 4213-4217.
- [18] T. Yorifuji, K. Ogata, and K. Soda, *J. Biol. Chem.* **1971**, *246*, 5085-&.
- [19] K. Inagaki, K. Tanizawa, H. Tanaka, and K. Soda, *Agric. Biol. Chem.* **1987**, *51*, 173-180.
- [20] K. Soda and S. Osumi, *Methods Enzymol.* **1971**, *17B*, 629-236.
- [21] G. M. Coppola and H. F. Schuster, *Asymmetric Syntheses, Construction of Chiral Molecules Using Amino Acids*, John Wiley & Sons, New York, **1987**.

- [22] K. Kino, M. Sato, M. Yoneyama, and K. Kirimura, *Appl. Microbiol. Biotechnol.* **2007**, *73*, 1299-1309.
- [23] H. Miyazaki, H. Morita, T. Shiraiwa, and H. Kurokawa, *Bull. Chem. Soc. Japan* **1994**, *67*, 1899-1903.
- [24] T. Shiraiwa, K. Fukuda, and M. Kubo, *Bull. Chem. Pharm. Bull.* **2002**, *50*, 287-291.
- [25] K. Würges, K. Petrussevska-Seebach, M. P. Elsner, and S. Lütz, *Biotechnol. Bioeng.* **2009**, *104*, 1235-1239.
- [26] E. J. Ebberts, G. J. A. Ariaans, J. P. M. Houbiers, A. Bruggink, and B. Zwanenburg, *Tetrahedron* **1997**, *53*, 9417-9476.
- [27] J. D. Bendtsen, H. Nielsen, G. von Heijne, and S. Brunak, *J. Mol. Biol.* **2004**, *340*, 783-795.
- [28] H. Nielsen and A. Krogh, *Proceedings of the Sixth International Conference on Intelligent Systems for Molecular Biology* **1998**, *6*, 122-130.
- [29] I. Suominen, M. Karp, M. Lahde, A. Kopio, T. Glumoff, P. Meyer, and P. Mantsala, *Gene* **1987**, *61*, 165-176.
- [30] D. Matsui, T. Oikawa, N. Arakawa, S. Osumi, F. Lausberg, N. Stäbler, R. Freudl, and L. Eggeling, *Appl. Microbiol. Biotechnol.* **2009**, *83*, 1045-1054.
- [31] T. Uo, T. Yoshimura, N. Tanaka, K. Takegawa, and N. Esaki, *J. Bacteriol.* **2001**, *183*, 2226-2233.
- [32] K. Yokoigawa, Y. Okubo, H. Kawai, N. Esaki, and K. Soda, *J. Mol. Catal. B: Enzym.* **2001**, *12*, 27-35.
- [33] K. Inagaki, K. Tanizawa, B. Badet, C. T. Walsh, H. Tanaka, and K. Soda, *Biochemistry* **1986**, *25*, 3268-3274.
- [34] S. Makart, M. Bechthold, and S. Panke, *Chem. Eng. Sci.* **2008**, *63*, 5347-5355.
- [35] M. M. Bradford, *Anal. Biochem.* **1976**, *72*, 248-254.

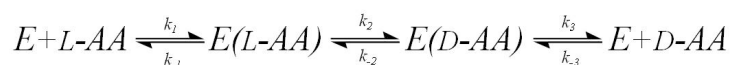
Corrections

Publication 1:

- Introduction (page 10): The annual production rate of L-Met is given with ca. 600 t/year which must be corrected to ca. 600000 t/year (Eggeling *et al.*, 2006).
- Introduction (page 11): “Met, which is a racemic compound forming system and thus can be enantioseparated by PC, ...” must be corrected to: “Met, which is a racemic compound forming system and thus **cannot** be enantioseparated by PC, ...”

Publication 3:

- Materials and Methods (page 1236): “In contrast to racemic compounds, where both enantiomers coexist in 1 U cell, ...” must be corrected to “In contrast to racemic compounds, where both enantiomers coexist in 1 **unit** cell, ...”
- Scheme 1 (page 1237): Arrows and reaction rate constants k_i are missing. Corrected scheme must be:



CHAPTER 4

DISCUSSION

4 Discussion

Context of publications

The publications, which will be discussed in the following, have been prepared in the course of a doctoral thesis performed at the Institute of Bio- and Geosciences 1 (former Institute of Biotechnology 2) at the Forschungszentrum Jülich. **Publications 1, 2 and 3** focus on strategies to overcome yield limitations in chiral resolutions by the combination of physicochemical separation processes and enzymatic racemization. They were published as a series, as the contents and results build up on each other. **Publication 4** deals with enzymatic isomerization of Thr, a modified application of amino acid racemases, together with stereoselective crystallization of a single diastereomer. The results presented in **publication 2** were mainly prepared by Katerina Petruševska-Seebach at the Max Planck Institute for Dynamics of Complex Technical Systems in Magdeburg, whereas the work presented in **publications 1, 3 and 4** was done almost exclusively by Kerstin Würges.

Publication 1 describes cloning, overexpression and characterization of an amino acid racemase from *Pseudomonas putida* KT2440 (AArac2440). Kinetic parameters for the racemization of methionine and asparagine were determined. The reaction conditions were chosen according to two different applications: I) the racemization of D- and L-methionine (Met) in combination with chromatographic enantioseparation, and II) the racemization of D- and L-asparagine (Asn) in combination with preferential crystallization (PC).

Publication 2: This paper addresses the design and theoretical investigation of the two enantioseparation processes introduced in **publication 1** in order to enhance the overall performance. Besides basic investigations with respect to the solid-liquid equilibria of Met and Asn, PC as well as chromatography, the focus is mainly on the kinetic studies of AArac2440. It has to be noted that this paper does not describe classical enzyme kinetics in terms of Michaelis-Menten kinetics but models various racemization reactions at different initial substrate concentrations. The chosen model equation sufficiently describes the reaction of AArac2440 in a wide concentration range (from diluted up to nearly saturated substrate solutions). It provides an adequate description of the racemization, which for engineering issues, is necessary for further process development.

Publication 3: A new method for the dynamic kinetic resolution of racemic AA is presented, which is able to overcome the usual yield limitation of 50 % of simple enantioseparation processes. This method applies PC for chiral resolution instead of a biocatalytic asymmetric transformation step. Racemization is performed enzymatically using AArac2440. An experimental proof for increasing the product yield of the chosen model substrate L-Asn from a racemic solution (compared to PC without racemization) is given.

Publication 4: The last paper investigates a novel process for biocatalytic production of chiral *allo*-Thr by enzyme catalyzed isomerization of Thr and stereoselective crystallization of *allo*-Thr. This approach is a modification of the enzyme-assisted PC presented in **publication 3**. Due to the diastereomeric character of Thr, isomerization occurs as epimerization instead of racemization. The formed *allo*-Thr was separated by simple crystallization, thus offering an efficient method for the production of D- and L-*allo*-Thr with very high purities. In contrast to **publications 1, 2 and 3**, a different but related amino acid racemase AArac12996 was used, which originates from *Pseudomonas putida* NBRC12996.

4.1 Amino acid racemases AArac2440 and AArac12996

4.1.1 Overexpression and secretion

AArac2440 and AArac12996 from different *Pseudomonas putida* strains (KT2440 and NBRC12996) were cloned into pET-22b(+) as described in **publications 1 and 4** and overexpressed in *E. coli* BL21(DE3). During expression studies, a progressive secretion of both enzymes into the cultivation medium was observed (Table 2). Sequence analyses demonstrated respective N-terminal signal peptides (see Appendix, section III). These results suggest that the enzymes are naturally secreted into the periplasmic space (chapter 4.1.4).

Table 2: Development of the intracellular and extracellular activity of AArac2440 and AArac12996 during expression in *E. coli*. Standard activity assay was carried out using 190 mM L-Asn at 35 °C.

expression [h]	AArac2440		AArac12996	
	medium [U/mL]	cells [U/g]	medium [U/mL]	cells [U/g]
20.0	0.6	99	0.15	58
42.5	1.5	145	0.21	78
67.0	1.9	168	1.75	44

Similar results have been discussed for amino acid racemase ArgR from *Pseudomonas taetrolens*, where a translocation mechanism *via* the Sec pathway over the inner cell membrane into the periplasm by cleavage of the N-terminal signal peptide was proposed (Matsui *et al.*, 2009). The Sec pathway is a membrane associated pathway over the inner cell membrane for the secretion of unfolded proteins (Driessen *et al.*, 1998). As the signal peptide as well as the size of ArgR are comparable to AArac2440 and AArac12996, a similar secretion pathway can be assumed. The release of periplasmic racemase through the outer cell membrane into the medium is supposed to be an autolytic response to the stress caused by overexpression and secretion of a foreign protein (Suominen *et al.*, 1987). A similar protein secretion system using bacterial strains derived from *E. coli* K12 called ESETEC[®] was presented by Wacker Biotech GmbH (Muecke *et al.*, 2009). It uses the Sec pathway for active

protein transport from the cytosol across the inner cell membrane. After cleavage of the signal peptide by a signal peptidase, the premature protein is folded in the periplasm and transferred over the outer cell membrane (Leonhartsberger *et al.*, 2009).

About the physiological role of the racemase secretion into the medium can only be speculated, as no further investigations have been done and no literature concerning the secretion of amino acid racemase EC 5.1.1.10 is available. However, it is well known that other racemases (*e.g.* alanine racemase) play an important role in the bacterial growth by providing D-Ala and D-Glu, which are central compounds of the murein layer (Figure 5) of all bacterial cell walls (Yoshimura *et al.*, 2003), as was already described in the introduction. Therefore, it is likely that periplasmic amino acid racemase is involved in the isomerization of the respective proteinogenic L-AA in the periplasmic space.

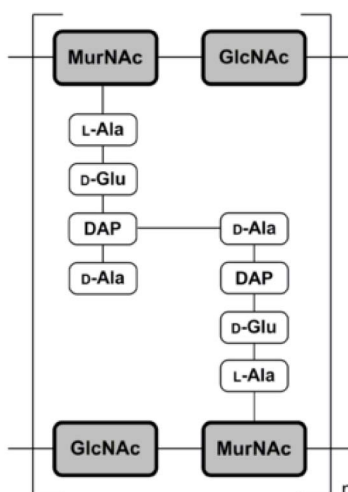


Figure 5: Schematic drawing of murein layer (*E. coli*). GlcNAc (N-acetylglucosamine) and MurNAc (N-acetylmuramic acid) are cross-linked by AA-tetramers. Besides DAP (diaminopimelic acid), D-Ala and D-Glu are main components of these tetramers.

4.1.2 Purification from cell extract and medium

Enzyme purification was performed using two different methods starting from either cell extract or medium. Figure 6 gives an overview about the enzyme sources, the purity of the enzyme samples and their applications. Different purity grades were necessary due to side reactions that occurred using the crude cell extract. While this unpurified enzyme sample was sufficient for Met racemization, it led to enzymatic degradation processes of Asn and Thr that were identified by decreasing overall concentrations of Asn and Thr, respectively. Degradation of Asn and Thr was not characterized any further, but could be avoided by purification of the applied enzyme sample.

- a) Purification from cell extract (publication 1).** The harvested cells were disrupted by sonication. After separation of cell debris by centrifugation the clear racemase containing cell extract was either directly lyophilized or subjected to further purification *via* fractionated precipitation using ammonium sulfate, desalting and subsequent ion exchange chromatography. The crude racemase preparation, which additionally contained an undefined variety of the host cells' metabolic enzymes, is termed CL (Crude cell extract Lyophilisate), whereas the pure racemase preparation PL (Pure Lyophilisate) contained no protein impurities.
- b) Purification from medium (publication 4).** Due to the secretion of the enzyme into the cultivation medium, the second approach for enzyme purification was developed based on the medium. After protein expression, the cells were separated from the racemase containing medium by centrifugation and all low molecular weight components were removed by ultrafiltration. The medium was exchanged against potassium phosphate buffer (KPi) prior to applying the concentrated racemase solution to DEAE column chromatography. The racemase containing fractions were pooled, desalted and lyophilized.

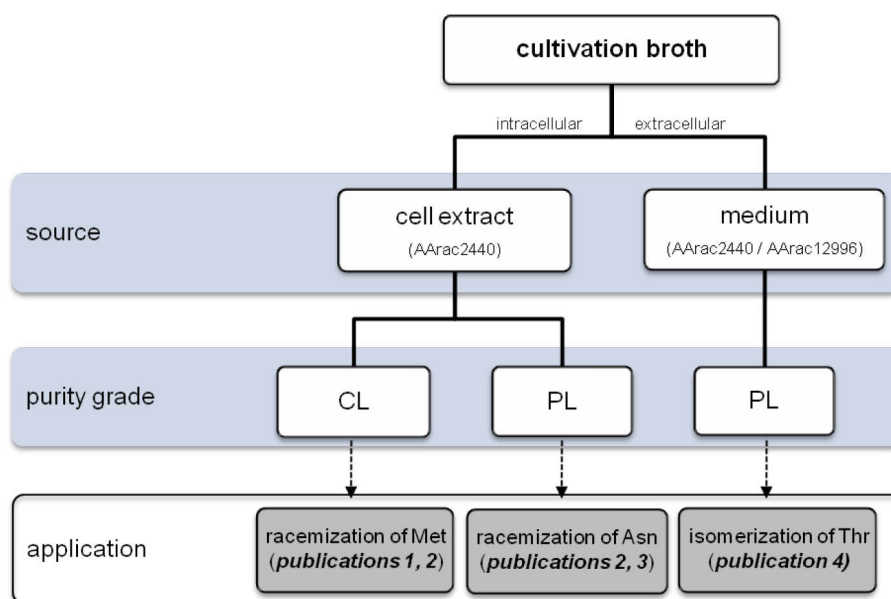


Figure 6: Overview of racemase purification procedures applied in this thesis, classified by source, purity grade (CL: lyophilisate of crude cell extract; PL: lyophilisate of purified racemase) and application.

As can be seen in Figure 7 the distribution of racemase activity between cells and medium after 67 hours of expression is almost equivalent. For enzyme purification from the cells only soluble racemase within the cell extract is accessible. However, the major part of racemase activity (ca. 80 % of initial cell activity) was found in the cell debris indicating some kind of membrane association. Attempts to solubilize this racemase fraction, *e.g.* by using detergents like Tween 20, have not been successful. Direct purification from the cultivation medium

(final yield ca. 21 %) was much more efficient than purification from the cell extract (final yield ca. 1 %; Tables 3 a and b). The purity of this racemase preparation was demonstrated by SDS-PAGE analysis (Figure 8).

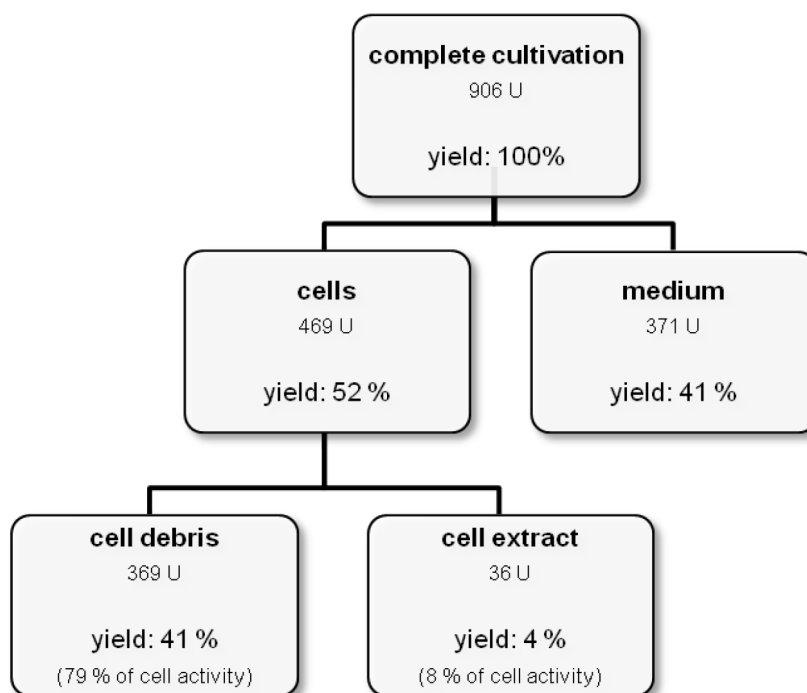


Figure 7: Distribution of racemase activity during a cultivation of AArac2440-expressing *E. coli* (shaking flask, V=200 mL, expression for 67 h at 27 °C). Activity was determined using standard activity assay (190 mM L-Asn, 35 °C; **publication 4**).

Tables 3 a) and b): Yields of AArac2440 purified from medium (a) and cell extract (b). Activity was determined using the standard activity assay (190 mM L-Asn, 35 °C; **publication 4**).

a) 200 mL shaking flask, 70 h expression			b) 20 L biostat, 24 h expression		
	activity [U]	yield		activity [U]	yield
complete cultivation	5043	100.0%	complete cultivation	513641	100.0%
medium	2003	39.7%	cell extract	10957	2.1%
concentrated medium*	2559	50.7%	concentrated cell extract*	6268	1.2%
active fraction**	1559	30.9%	active fraction**	6384	1.2%
lyophilisate	1056	20.9%	lyophilisate	5348	1.0%

*before chromatography, **after chromatography

*before chromatography, **after chromatography

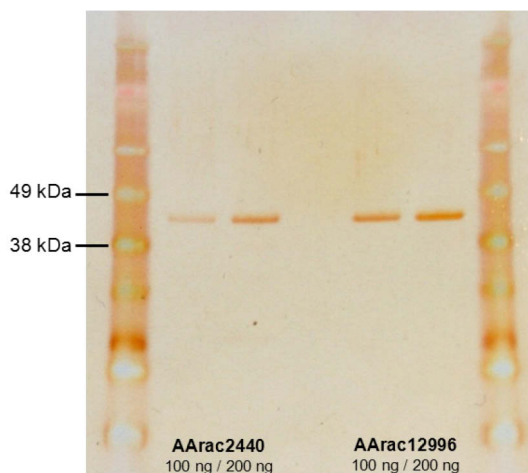


Figure 8: SDS-PAGE (4-12 % Bis-Tris, silver staining) of pure racemase preparations (PL) purified from cultivation medium. Left and right lanes: protein standard SeeBlue[®] Plus2, Invitrogen.

4.1.3 Enzyme characterization

AArac2440 and AArac12996 (purified from medium as described in chapter 4.1.2 b) were characterized with respect to the temperature optimum, pH dependency, thermostability, substrate spectrum, and the influence of PLP. Relative activities were measured as described in *publication 4*.

Both enzymes show a maximum activity toward the basic amino acids L-lysine (100 % relative activity) and L-arginine, whereas the relative activities for L-Asn (AArac2440: 4.5 %; AArac12996: 1.9 %) and L-Thr (AArac2440: 0.5 %; AArac12996: 0.1 %) are comparatively low (Figure 9). The temperature optima and pH dependencies have been determined between 20 °C and 55 °C and pH 8 to pH 10.5, respectively (Figure 10). AArac2440 exhibits a maximum initial rate activity at 47.5 °C and at pH-values between 8.6 and 9.7. In contrast, AArac12996 shows maximum initial rate activity at 31 °C while having the same pH tolerance.

The thermostability of both enzymes was studied over a period of 7 days by incubating enzyme samples between 20 °C and 47 °C (Figure 11). The half life of AArac2440 dropped continuously from ca. 20 days, for samples stored at 20 °C, to ca. 3 days for samples stored at 47 °C. AArac12996 shows a quite different behavior. While samples stored at 20 °C and 30 °C exhibited an extraordinary stability (no activity loss over 7 days), incubation at higher temperatures resulted in a drastically decreased half life of the enzyme. Nevertheless, although the temperature screening (Figure 10) showed a rapid loss of initial activity for temperatures ≥ 31 °C, stability investigations for samples kept at 40 °C still exhibited a residual activity of about 16 % after 3 days when assayed at 30 °C. These results indicate a

reversible inactivation of AArac12996 at temperatures between 31 °C and 40 °C. At 47 °C AArac12996 was inactivated irreversibly and showed no residual activity after only 2 h of incubation.

The influence of additional PLP, which is covalently bound as a cofactor to the active center of both racemases, was investigated in the concentration range between 0 and 50 μ M. Within this range PLP had no influence on the enzyme activity.

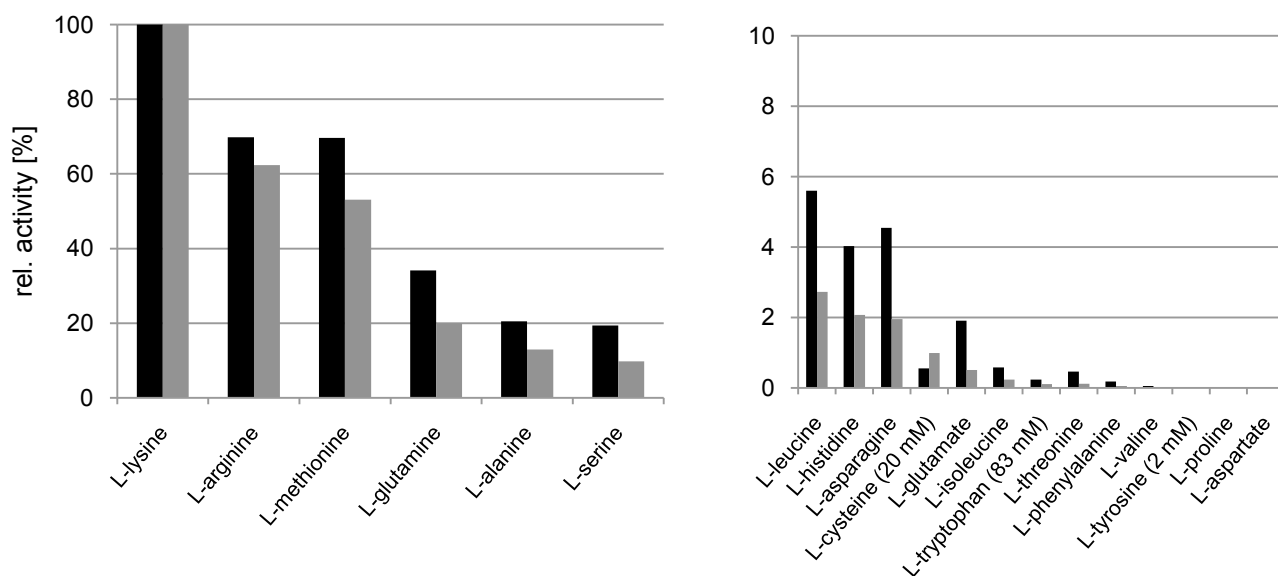


Figure 9: Substrate spectrum of AArac2440 (black bars) and AArac12996 (grey bars). Relative initial rate activities for all chiral proteinogenic AA (initial substrate concentration=190 mM (unless otherwise indicated), T=30 °C).

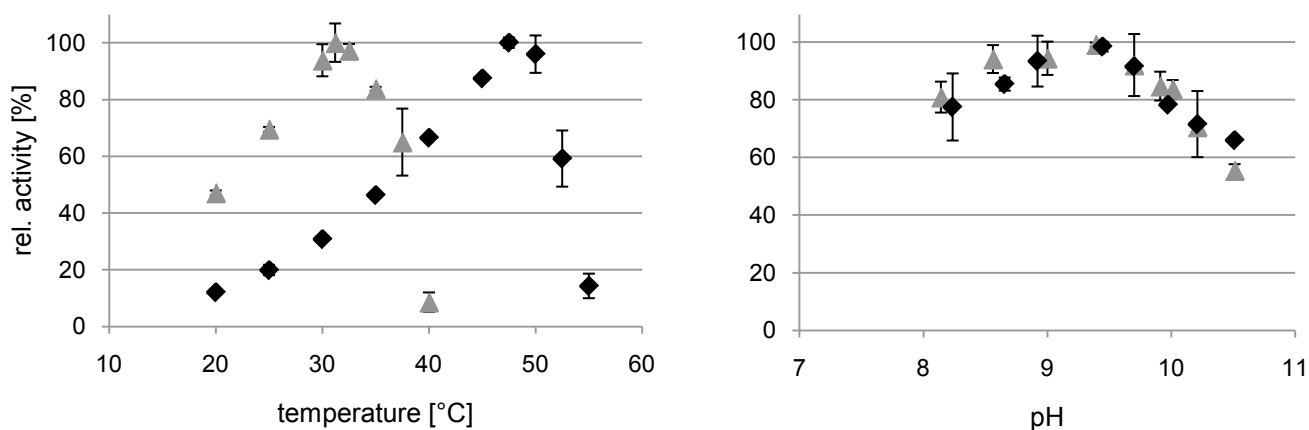


Figure 10: Temperature and pH dependency of AArac2440 (◆) and AArac12996 (▲). Relative initial rate activities were measured between 20 °C and 55 °C and between pH 8 and pH 10.5, respectively. Measurements were performed in duplicates (initial substrate concentration=190 mM L-Asn, T=30 °C, **Publication 4**, Figures 2 and 3).

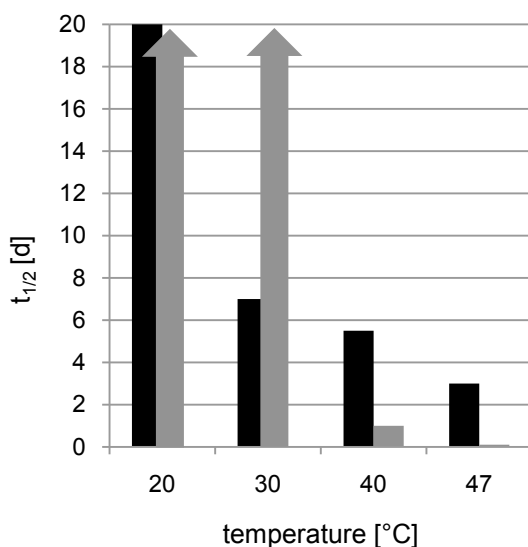


Figure 11: Temperature stability. Half lives of AArac2440 (black bars) and AArac12996 (grey bars) between 20 °C and 47 °C. Arrows indicate longer half lives than 20 days. Residual activities were determined at 30 °C using 190 mM L-Asn as substrate.

The kinetic parameters were determined for crude and purified lyophilisates of AArac2440 as well as for purified AArac12996 under reaction conditions according to their catalytic approach. The following substrate/reaction conditions have been investigated:

- AArac2440:
- 1 a-e) Crude lyophilisate (CL), D- and L-Met: 95 vol.% 100 mM KPi, 5 vol.% methanol, pH 7, T=20-40 °C with steps of 5 °C
 - 2 a-b) Crude lyophilisate (CL), D- and L-Met: 95 vol.% 100 mM KPi, 5 vol.% methanol, T=25°C, pH 6 and pH 8
 - 3 a-e) Pure lyophilisate (PL), D- and L-Asn: 100 vol.% H₂O, T=20-40 °C with steps of 5 °C
 - 4) Pure lyophilisate (PL), D- and L-Thr: 100 vol.% H₂O, T=30 °C
- AArac12996:
- 5) Pure lyophilisate (PL), D- and L-Asn: 100 vol.% H₂O, T=34 °C
 - 6) Pure lyophilisate (PL), D- and L- Thr: 100 vol.% H₂O, T=30 °C

Table 4 lists all determined K_m and V_{max} values for the racemization (isomerization) of D- and L-isomers according to the enzymes' catalytic applications. All kinetic parameters were determined by non-linear regression using *Origin 7.0*. Due to the limited substrate solubility, kinetic measurements were not possible at optimal substrate concentrations, where the maximum enzyme activity (V_{max}) is achieved. As a reason, non-linear regression calculations of the kinetic parameters resulted in quite broad error ranges for V_{max} and K_m values.

Table 4: Kinetic parameter of AArac2440 and AArac12996 determined under reaction conditions according to the enzymes' catalytic applications.

no.	enzyme preparation	substrate	solvent: ratio	temperature [°C]	pH	$K_m(D)$ [mM]	$V_{max}(D)$ [U/g]	$K_m(L)$ [mM]	$V_{max}(L)$ [U/g]
1a	AArac2440 (CL)	Met	Kpi (100 mM)/MeOH: 95/5	20	7	25 (± 13.0%)	1696 (± 3.1%)	31 (± 17.0%)	1889 (± 4.5%)
1b	AArac2440 (CL)	Met	Kpi (100 mM)/MeOH: 95/5	25	7	22 (± 11.5%)	1892 (± 2.6%)	23 (± 14.7%)	2150 (± 3.3%)
1c	AArac2440 (CL)	Met	Kpi (100 mM)/MeOH: 95/5	30	7	23 (± 10.6%)	2075 (± 2.4%)	30 (± 15.7%)	2296 (± 4.0%)
1d	AArac2440 (CL)	Met	Kpi (100 mM)/MeOH: 95/5	35	7	30 (± 8.9%)	2512 (± 3.9%)	39 (± 11.6%)	2833 (± 3.5%)
1e	AArac2440 (CL)	Met	Kpi (100 mM)/MeOH: 95/5	40	7	32 (± 8.4%)	2668 (± 2.3%)	35 (± 11.4%)	2847 (± 3.2%)
2a	AArac2440 (CL)	Met	Kpi (100 mM)/MeOH: 95/5	25	6	42 (± 14.6%)	1160 (± 4.5%)	30 (± 22.3%)	1174 (± 5.9%)
2b	AArac2440 (CL)	Met	Kpi (100 mM)/MeOH: 95/5	25	8	28 (± 4.5%)	3627 (± 1.1%)	20 (± 8.7%)	2951 (± 1.9%)
3a	AArac2440 (PL)	Asn	H ₂ O: 100	20	n.d.	18 (± 26.1%)	770 (± 4.8%)	30 (± 19.3%)	1626 (± 5.6%)
3b	AArac2440 (PL)	Asn	H ₂ O: 100	25	n.d.	50 (± 33.3%)	1299 (± 11.4%)	47 (± 19.6%)	2427 (± 6.3%)
3c	AArac2440 (PL)	Asn	H ₂ O: 100	30	n.d.	62 (± 8.9%)	1881 (± 3.1%)	76 (± 10.0%)	3930 (± 3.9%)
3d	AArac2440 (PL)	Asn	H ₂ O: 100	35	n.d.	66 (± 8.2%)	2585 (± 2.8%)	101 (± 17.5%)	5683 (± 7.1%)
3e	AArac2440 (PL)	Asn	H ₂ O: 100	40	n.d.	103 (± 8.8%)	4032 (± 3.3%)	n.d.	n.d.
4	AArac2440 (PL)	Thr	H ₂ O: 100	30	n.d.	134 (± 13.3%)	731 (± 6.7%)	120 (± 30.6%)	1558 (± 13.7%)
5	AArac12996 (PL)	Asn	H ₂ O: 100	34	n.d.	14 (± 22.8%)	4760 (± 4.2%)	29 (± 6.1%)	13960 (± 1.7%)
6	AArac12996 (PL)	Thr	H ₂ O: 100	30	n.d.	186 (± 6.4%)	1866 (± 3.7%)	93 (± 20.0%)	1865 (± 8.3%)

4.1.4 Structural homologies

As already mentioned in the introduction, AArac2440 and AArac12996 show major homologies of their AA and DNA sequences as well as of their quaternary structures. AA and DNA sequence alignments of AArac2440 and AArac12996 were done with *Clone Manager 9 Professional Edition* and resulted in a 94 % homology of the AA sequences and a 91 % homology of the DNA sequences (see Appendix sections IV and V). There are no 3D-crystal structures available for AArac2440 and AArac12996. Justified by a high sequence identity of ca. 73 % to the well-known alanine racemase from *Pseudomonas aeruginosa* (pdb ID: 1SFT), homology models of both enzymes were calculated using the internet tool *EasyPred3D* (Figure 12).

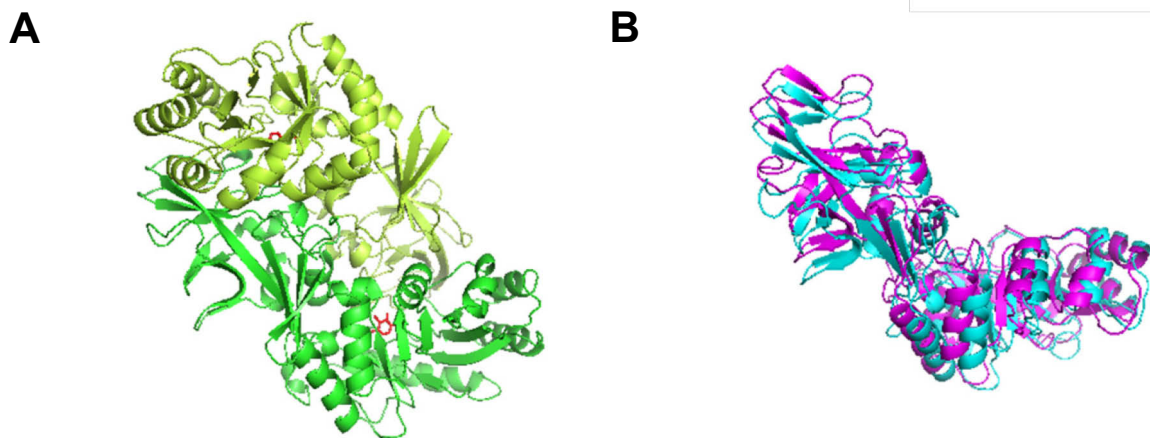


Figure 12: **A:** Structure of alanine racemase from *Pseudomonas aeruginosa* (pdb ID: 1SFT) with PLP bound covalently in each active center (red). **B:** Homology models of monomers of amino acid racemases AArac2440 (blue) and AArac12996 (purple) calculated with *EasyPred3D* (Lambert *et al.*, 2002).

Motivated by the unexpected enzyme secretion during cultivation (chapter 4.1.1), the full amino acid sequences of both enzymes were analyzed using *SignalP 3.0*. N-terminal signal peptides (probability of 1.000) and specific cleavage sites (probability of 0.92-0.93) between amino acids Ala24 and Ala25 were found in both cases. The sequences show the typical tripartite structure of signal peptides, consisting of a hydrophobic core region (h-region) flanked by a positively charged n-region and a polar c-region that contains the signal peptidase cleavage site (Ebbers *et al.*, 1997). *SignalP 3.0* uses virtual machines based on neural networks (NN) and Hidden Markov Models (HMM) for signal prediction (Nielsen *et al.*, 1998; Bendtsen *et al.*, 2004). For detailed information see Appendix section III.

4.1.5 Rational protein design of AArac2440

Both wildtype enzymes, AArac2440 and AArac12996, exhibit only low activities toward the isomerization of Thr (Figure 9). In order to improve the activity toward Thr the active site of AArac2440 was modified using site-directed mutagenesis.

To identify possible AA residues in the active center of AArac2440, which might hamper the optimal binding of Thr or a fast substrate release, the calculated homology model (Figure 12 B) was superimposed with the structure of the similar alanine racemase complexed with alanine phosphonate (substrate homologue, covalently bound to PLP in the active center, pdb ID: 1BD0). Thr was then modeled into the active site of AArac2440 in a congruent position like alanine phosphonate using *PYMOL*. From these studies a possible sterical hindrance for the binding of Thr by the side chain of Met349 was proposed (Figure 13 A). Therefore, Met349 was exchanged *in silico* by alanine and glycine, respectively. These models revealed a larger binding pocket for Thr (Figure 13 B and C).

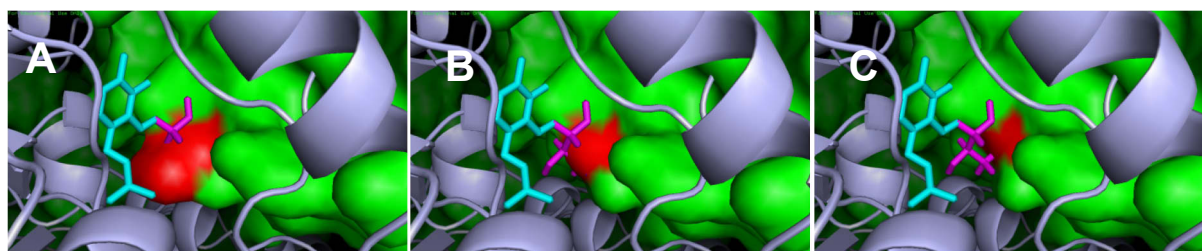


Figure 13: *In silico* modeling of the active center of AArac2440 with threonine/PLP-complex (purple/blue). **A:** Wildtype (Met349): Thr residue clashes into the side chain of Met349. **B:** Variant 1 (Met349Ala): reduced sterical hindrance of Thr residue by Ala349. **C:** Variant 2 (Met349Gly): no sterical hindrance of Thr residue by Gly349.

Based on these models, the variants were constructed using the *QuikChange*[®] method by Stratagene according to the instruction manual (Stratagene, 2004). Up- and down-primers were designed using the *QuikChange*[®] *Primer Design* program and synthesized by Eurofins MWG GmbH. The gene encoding AArac2440 was amplified by standard PCR in an Eppendorf thermocycler and cloned into the expression vector pBC SK+, which was then used as a template plasmid for the *QuikChange*[®] PCR. Competent *E. coli* XL1-blue cells were transformed with the mutation carrying plasmids by electroporation, incubated in LB-medium and transferred to LB-plates. Variants 1 (Met349Ala) and 2 (Met349Gly) formed homogeneous colonies, while the negative control did not show any growth. The correct point mutations of both variants were confirmed by AA sequencing (Agowa, Berlin):

Variant 1 (Met349Ala) → A1049G, T1050C, G1051G

Variant 2 (Met349Gly) → A1049G, T1050G, G1051G

Competent *E. coli* BL21(DE3) cells, used for overexpression of proteins cloned under the T7 expression system, were transformed with the mutation carrying plasmids. One colony of

each variant was grown in LB-medium and protein expression was induced with IPTG. Detailed information can be found in the appendix (section VI).

Activity measurements for the racemization of L-Asn and the epimerization of L-Thr were performed as described in *publication 4*. However, this approach was not successful as both variants were inactive and did not show any activity toward L-Asn or L-Thr. Thus, the exchange of Met349 led to complete inactivation of AArac2440.

4.2 Crystallization of amino acids

4.2.1 Conglomerates vs. racemic compounds

Amino acids differ in terms of their phase diagrams, as they can occur as conglomerates, racemic compounds or solid solutions (Jacques *et al.*, 1994). In case of conglomerate forming systems (ca. 10 % of all racemic substances), cost-efficient and quite simple PC holds great potential, whereas for racemic compound forming systems (ca. 90 % of all racemic substances) the application of PC is rather limited.

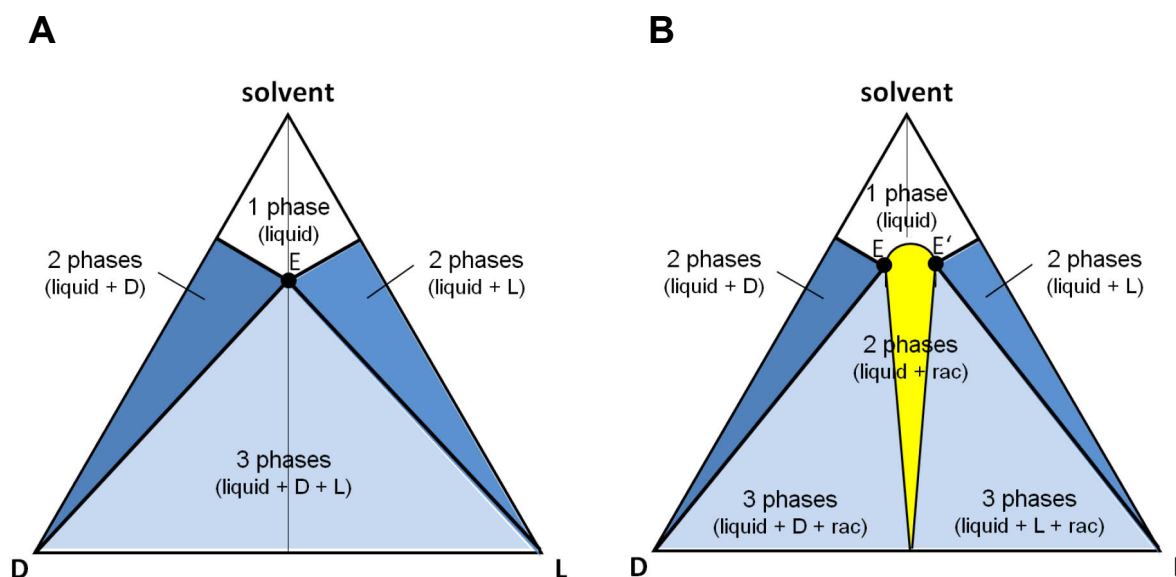


Figure 14: Examples for ternary phase diagrams of conglomerate forming systems (A) and racemic compound forming systems (B) showing different phase regions (D, L, rac: solid crystals of D-, L-isomers and racemate; E: eutectic point).

PC is only possible for systems being in the two-phase region of the respective ternary phase diagram, where liquid solution and solid crystals of one enantiomer are coexisting (Figure 14). For conglomerate forming systems this means PC of both enantiomers is possible starting from a racemic solution. When looking at the ternary phase diagram of systems forming racemic compounds, it becomes obvious that PC is more complex. In this case the positions of the eutectic points E and E' (solution compositions, where saturated solution and two

different solid phases coexist in equilibrium) within the diagram are important for the required enantiomeric starting composition of the liquid phase. If these points are close to the racemic composition, even poor enrichment of one enantiomer is sufficient to reach the two-phase region and to apply PC. However, systems with eutectic points far away from the racemic composition require highly enriched solutions for PC.

Considering the high costs of enantioseparation techniques that are employed for the enrichment of systems forming racemic compounds (such as advanced chromatographic methods like simulated moving bed chromatography (Bechtold *et al.*, 2006)), PC is only useful, if a low enantiomeric excess of the solution is sufficient (**publication 2**). In other cases the use of different enantioseparation methods, such as chromatography (alone or in combination with racemization of the undesired enantiomer; see **publication 3**, Fig. 3) as well as asymmetric biotransformations, may be more promising.

4.2.2 Preferential crystallization of asparagine

Asn is one of the two proteinogenic AA acids that form conglomerates and therefore was chosen as a model substrate for enzyme-assisted preferential crystallization. Due to the lack of reliable literature concerning crystallization properties of proteinogenic AA, solubility experiments with potential conglomerate forming AA were necessary beforehand. Besides Thr, whose crystallization properties have been investigated in detail by Elsner and Lorenz (Elsner *et al.*, 2005; Lorenz *et al.*, 2006; Elsner *et al.*, 2007; Bäckvall, 2008), two further proteinogenic AA were claimed to form conglomerates (Klussmann *et al.*, 2006). Klussmann and coworkers argued that arginine (Arg) exhibits a typical racemic composition (0 % *ee*) at the eutectic point; and Asn was described as conglomerate forming AA in “Enantiomers, Racemates, and Resolutions” (Jacques *et al.*, 1994), which is one of the few comprehensive textbooks covering enantioseparation of racemates by crystallization. A common and easy method to obtain first evidence about the expected crystallization type is to determine the solubilities of the racemate and the single enantiomers. Conglomerate forming systems ideally exhibit a relative solubility of two between the racemate [rac] and the enantiopure compound [ep] (double solubility rule (Meyerhoffer, 1904)). This solubility ratio α has been defined according to Equation 1.

$$\alpha = \frac{[\text{rac}]}{[\text{ep}]}$$

Equation 1

In order to evaluate crystallization properties of Arg and Asn in H₂O, the respective α -values were determined. Saturated solutions of racemic and enantiopure species of both AA were prepared at 30 °C and the concentrations of each enantiomer were determined by chiral HPLC

(column: Crownpak CR(+), 0.4x15 cm; mobile phase: HClO₄, pH 1, T=30 °C (for Arg) / T=0 °C (for Asn), 0.4 mL/min). The following solubility ratios α_{Arg} and α_{Asn} were determined:

Solubility of arginine (30 °C, H₂O):
 D-Arg: 1008 mM
 L-Arg: 1020 mM
 DL-Arg: 1208 mM
 $\rightarrow \alpha_{\text{Arg}} \approx 1.2$

Solubility of asparagine (30 °C, H₂O):
 D-Asn: 257 mM
 L-Asn: 256 mM
 DL-Asn: 512 mM
 $\rightarrow \alpha_{\text{Asn}} \approx 2.0$

Only Asn showed the typical solubility ratio $\alpha_{\text{Asn}} \approx 2$ and thus ideal behavior, *i.e.* the solubility of one enantiomer is not influenced by the presence of the other enantiomer. For more detailed information about the crystallization properties of Asn, the ternary phase diagram of Asn in H₂O was constructed at different temperatures. Therefore, solubilities of different mixtures of D- and L-Asn were determined at 25, 30, 35, 40 and 50 °C, with mass fractions of one enantiomer in the D-/L-mixture varying from 0.5 to 1. After saturation of the solution at distinct temperatures for at least 20 h, solid Asn was removed by filtration and the solution composition was determined *via* chiral HPLC. The resulting ternary phase diagram shows the typical structure of conglomerate forming systems with a racemic eutectic composition (Figure 15).

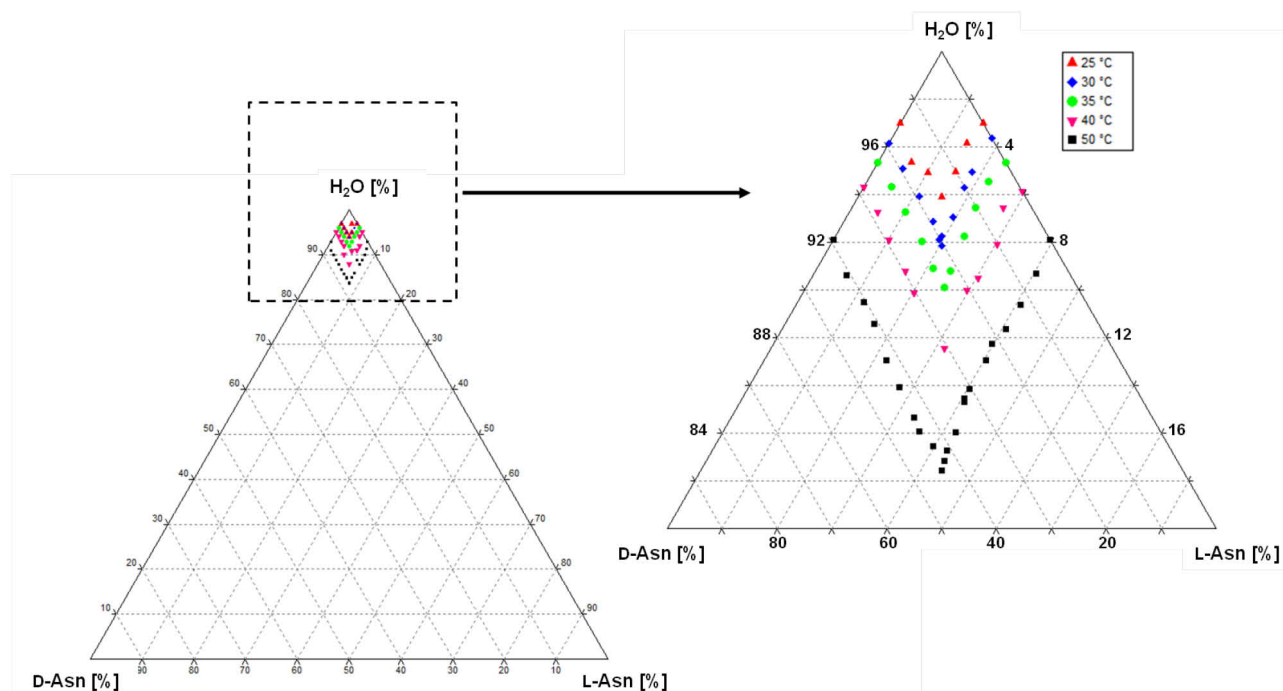


Figure 15: Ternary phase diagram of DL-Asn in H₂O at 25, 30, 35, 40 and 50 °C with typical racemic composition at eutectic point.

4.2.3 Crystallization of *allo*-threonine from diastereomeric solutions

Both, Thr (Elsner *et al.*, 2005) and *allo*-Thr belong to the group of conglomerate forming systems (Miyazaki *et al.*, 1994). Since crystallization was only performed from diastereomeric solutions, no further investigations of the preferential crystallization behavior or the construction of a ternary phase diagram were performed. Simple crystallization of *allo*-Thr from diastereomeric solutions consisting of *allo*-Thr and Thr is possible due to the low solubility limit of *allo*-Thr compared to Thr (Figure 16).

The crystallization of *allo*-Thr from diastereomeric solutions (consisting of 50 % *allo*-Thr and 50 % Thr) was investigated, in order to determine the reaction parameters for the planned *allo*-Thr production processes (chapter 4.4). Thereby, the main focus was laid on the crystallization yield and purity as a function of pH, while the temperature was fixed. To reduce the solubility of *allo*-Thr (Sapoundjiev *et al.*, 2006) for better crystallization yields, additional crystallization experiments were performed, where ethanol was added in different concentrations between 0 and 20 vol.%. To investigate the influence of the pH on the crystallization of *allo*-Thr, 1 mL of water was saturated with D-*allo*-Thr and L-Thr at 40 °C and the pH was adjusted with diluted NaOH or HCl. The solubility of both isomers (determined by HPLC) increased with pH whereas their ratio in the solution remained almost constant. Crystallization was performed in 500 µL samples by subcooling of the saturated solutions to 34 °C under constant shaking at 1400 rpm for 20 h. The precipitated crystals were separated from the solution by filtration, washed with 50 µL ice cold water, and re-suspended in water for subsequent HPLC analysis. A good diastereomeric excess (*de*) of the produced crystals could be achieved at all pH-values (Table 5).

Table 5: Solubility of D-*allo*-Thr and L-Thr at 40 °C and diastereomeric excess (de_{allo}) of produced crystals.

pH	D- <i>allo</i> -Thr [mM]	L-Thr [mM]	ratio of D- <i>allo</i> -Thr in solution	de_{allo} of crystals
5.5	295.4	350.2	45.8 %	95.4 %
6	286.4	341.4	45.6 %	93.3 %
7	289.1	336.9	46.2 %	97.0 %
8	331.9	391.0	45.9 %	97.0 %
8.8	444.7	579.3	43.4 %	87.4 %

The solubilities of D-*allo*-Thr and L-Thr were investigated at pH 8.5, which was chosen with respect to the pH-optimum of AArac12996 (Figure 10). Therefore, saturated solutions of D-*allo*-Thr and L-Thr were prepared between 20 °C and 40 °C and analyzed by HPLC. As can be seen in Figure 16, the solubility of Thr is significantly higher compared to the solubility of *allo*-Thr. Due to identical physical properties of enantiomeric compounds the respective counter-enantiomers L-*allo*-Thr and D-Thr have the same solubility.

An increase of the ethanol concentration from 0 to 20 vol.% in saturated *allo*-Thr/Thr solutions, led to a drastic decrease of solubility of ca. 40 %, which may be beneficial for better crystallization yields. However, de_{allo} dropped to ca. 40 % and thus crystallization of pure *allo*-Thr was not possible with ethanol as cosolvent.

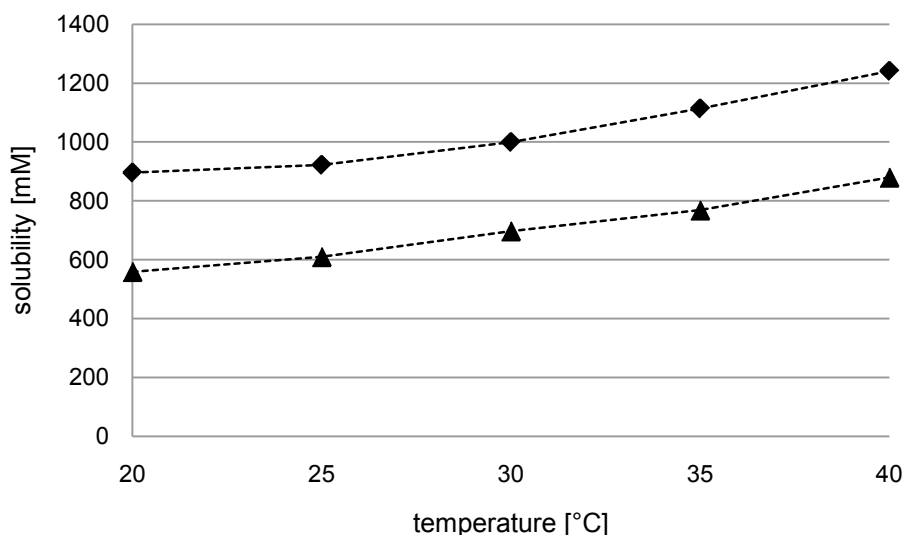


Figure 16: Solubility of L-Thr (◆) and D-*allo*-Thr (▲) in H₂O (pH-value was adjusted to pH 8.5) between 20 °C and 40 °C. The given data represent the mean values of four individual solubility measurements at each temperature with standard deviations <1 %.

4.3 Enzyme-assisted preferential crystallization of asparagine

In contrast to simple preferential crystallization (PC) as described in chapter 4.2.2, the combination of PC with a racemization step results in a concurrent relative increase of the desired enantiomer and a decrease of the undesired one in the liquid phase. As long as racemization is faster than crystallization the composition of the liquid phase moves directly toward the eutectic point associated with the chosen crystallization temperature. Thereby the driving force for crystallization of the desired enantiomer is constantly increased while the crystallization of the counter-enantiomer is suppressed. The “recycling” of the undesired enantiomer by racemization allows overcoming the usual yield limitation of 50 % for classical resolution methods (chapter 1.3.1). This enzyme-assisted PC is a variation of the classical dynamic kinetic resolution (DKR), in which the asymmetric transformation of one enantiomer is replaced by PC, and *in situ* racemization is performed using an amino acid racemase from *Pseudomonas putida* (Figure 17).

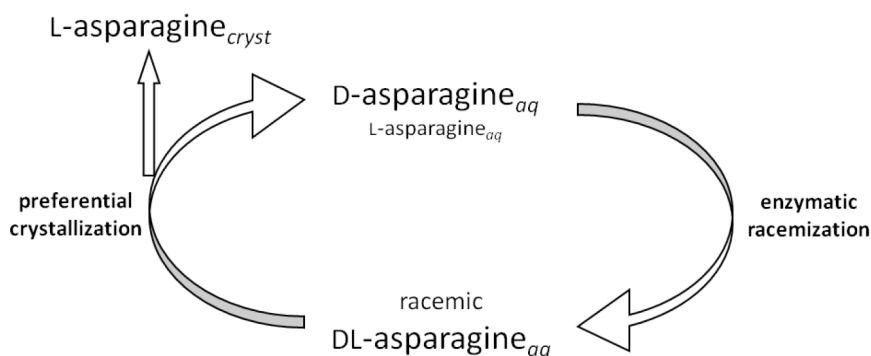


Figure 17: Principle of enzyme-assisted preferential crystallization at the example of L-Asn from a supersaturated racemic solution. While L-Asn is removed from the system by crystallization, the resulting excess of D-Asn in solution (*aq*) is racemized enzymatically.

Enzymatic racemization instead of chemically (acid/base) or temperature induced racemization, together with self-contained crystallization from a supersaturated solution without solvent evaporation, make this process an environmentally friendly approach and led to a significant increase of crystallized L-Asn. **Publication 3** summarizes the experiments which have been performed for the crystallization of L-Asn (batch mode) and results in a first experimental proof of enzyme-assisted PC as a new process concept.

4.3.1 Reactor setups

Enzyme-assisted PC of L-Asn has been studied in a batch and in a semi-continuously operated reactor, respectively:

a) Batch

The reactor setup consisted of a tempered crystallization vessel with a polarimeter-bypass, in which the excess of the counter-enantiomer was monitored online in the crystallization solution (Figure 18). The crystallization vessel was equipped with a glass frit (pore size of 16-40 μm) for crystal retention at its outlet and with an overhead mixer for homogeneous mixing of the crystals in solution. The temperature of the crystallizer was controlled by a water filled thermostat. The crystallization solution was pumped through a polarimetric cell and back into the crystallizer using a peristaltic pump. To prevent blocking of the tubings by crystal nucleation the complete system was placed in an incubator and tempered to the solution saturation temperature (T_{sat}). Detailed reactor parameters are described in **publication 3**. The crystallization process stopped when the concentration of Asn has reached the saturation concentration at the crystallization temperature (T_{cryst}) and the solution was no longer supersaturated.

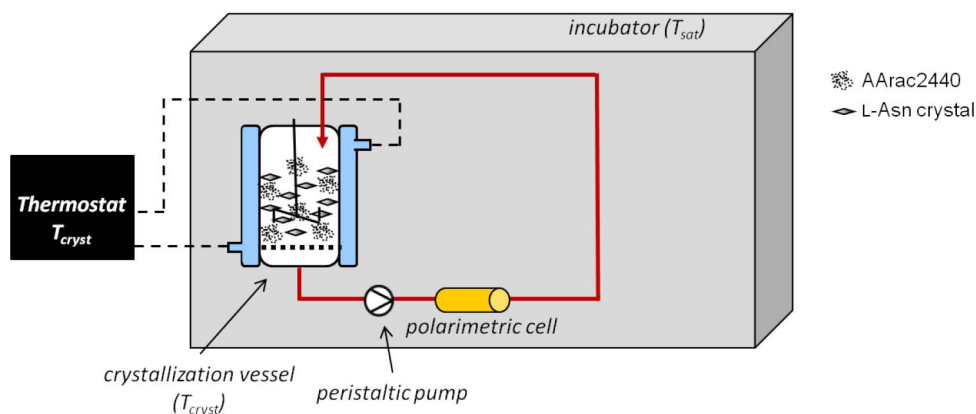


Figure 18: Reactor setup for enzyme-assisted batch crystallization of L-Asn. The crystallization vessel was cooled down to the crystallization temperature ($T_{cryst}=32\text{ }^{\circ}\text{C}$) for solution supersaturation, while the remaining reactor parts are tempered to a higher saturation temperature ($T_{sat}=35\text{ }^{\circ}\text{C}$). The formation of an enantiomeric excess in solution was monitored online with a polarimeter.

b) *Semi-continuous*

In order to increase the possible crystal yield of enzyme-assisted PC, it is necessary to feed racemic Asn to the system. Therefore, three requirements must be considered:

- 1) No substrate feed in form of solid DL-Asn crystals is possible, since they would act as seed crystals and interrupt PC of L-Asn.
- 2) No substrate feed in form of an aqueous DL-Asn solution is possible, since this would increase the overall reaction volume making water removal necessary.
- 3) To maintain a constant concentration of the solution, the applied DL-Asn feed must compensate the L-Asn crystallization velocity.

Given requirements were met by a stainless steel filter module integrated in the polarimeter bypass that contained a racemic Asn crystal stock (Figure 19). By pumping the solution through the filter module, dynamic re-saturation with racemic Asn at T_{sat} was achieved.

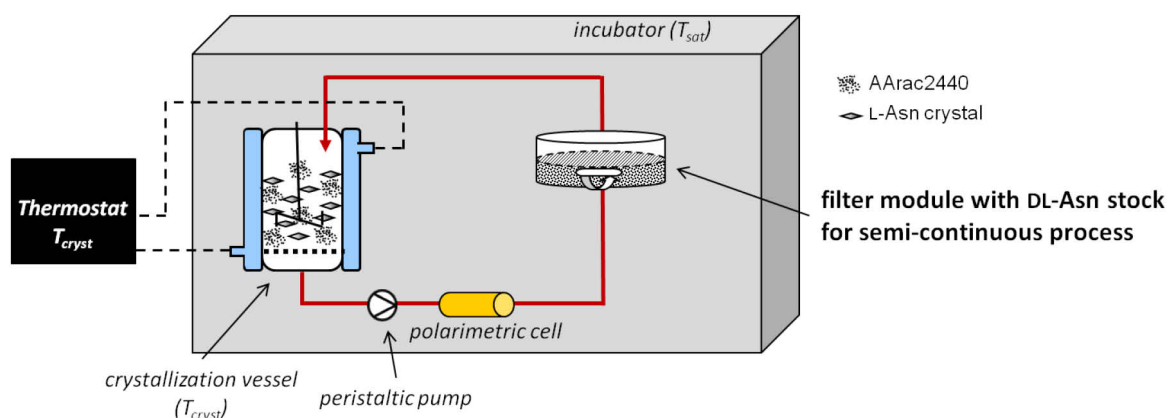


Figure 19: Reactor setup for enzyme-assisted semi-continuous crystallization of L-Asn. A racemic Asn feed is supplied by an additional integrated filter module containing a racemic Asn stock.

4.3.2 Process performance

a) Batch

To demonstrate the superior properties of enzyme-assisted PC in terms of yield increase, 20 mL of a supersaturated racemic Asn solution ($\Delta T = -3^\circ\text{C}$) were seeded with $m_{\text{seed}} = 5$ mg of enantiopure L-asparagine monohydrate (L-Asn \cdot H $_2$ O) crystals as described in **publication 3** (batch mode). *In situ* racemization of the liquid phase was catalyzed by purified AArac2440. The influence of the enzyme concentration on the *ee* of crystallized L-Asn was investigated by increasing the concentration of AArac2440 from 0 to 1 mg/mL. PC alone (without AArac2440) yielded a maximum of 31 mg L-Asn \cdot H $_2$ O ($\geq 99.5\%$ *ee*) after the process was interrupted before the counter-enantiomer started to crystallize. In contrast, the addition of 1 mg/mL AArac2440 led to a ca. six fold yield increase (198 mg L-Asn \cdot H $_2$ O). However, the *ee* dropped to about 92 %. Furthermore, it could be shown that the product *ee* increases with the concentration of AArac2440 (Figure 20). Fast racemization velocities kept the composition of the solution closer to racemic (compared to slow racemization), and thus suppressed D-Asn crystallization more efficiently. As an example, Figure 21 shows the *ee* of the crystallization solution during PC without racemization and enzyme-assisted PC with 0.5 mg/mL AArac2440. The crystals of L-Asn, that were grown on seed crystals, can be distinguished clearly from the fine crystals of D- and L-Asn, which were formed by secondary nucleation (Figure 22).

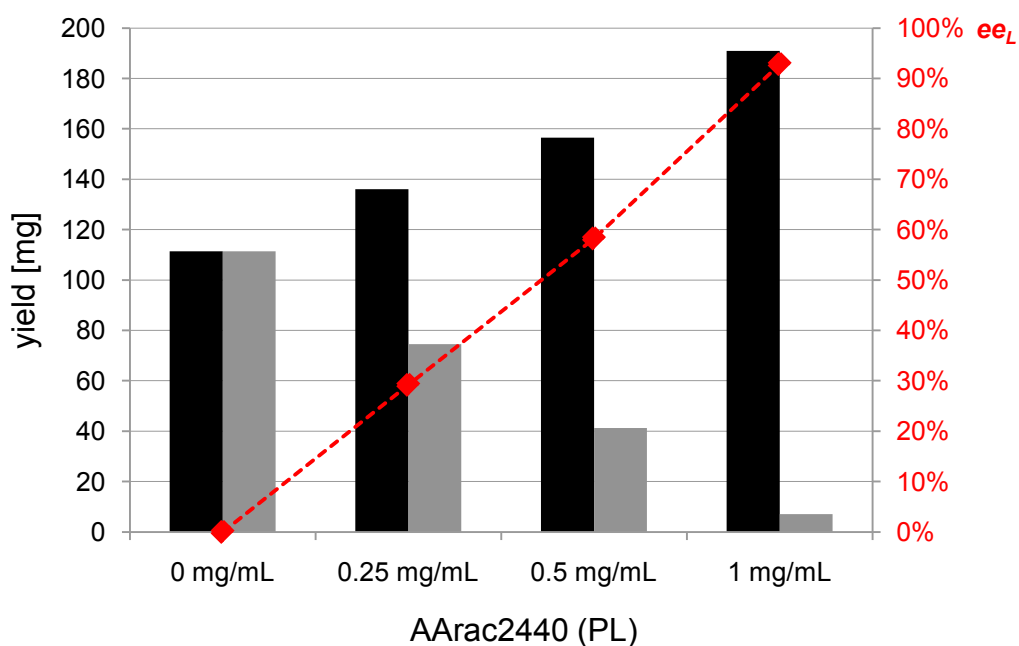


Figure 20: Product yields (black bars: L-Asn \cdot H $_2$ O, grey bars: D-Asn \cdot H $_2$ O) and *ee*_L (♦) of enzyme-assisted PC with AArac2440, applied in different concentrations from 0 to 1 mg/mL (batch mode). The product *ee*_L reached ca. 92 % when 1 mg/mL AArac2440 was applied. Process parameters: $T_{\text{sat}} = 35^\circ\text{C}$, $T_{\text{crist}} = 32^\circ\text{C}$, $V = 20$ mL, $m_{\text{seed}} = 5$ mg.

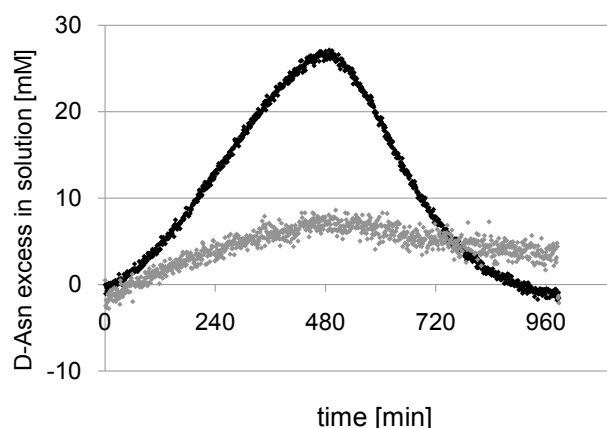


Figure 21: Monitoring of excess D-Asn in the crystallization solution during PC without racemization (black) and enzyme-assisted PC with 0.5 mg/mL AArac2440 (grey). Data was determined online by optical rotation measurement.



Figure 22: Product crystals of enzyme-assisted PC with 1 mg/mL AArac2440. Grown seed crystals of L-Asn can be distinguished clearly from fine secondary crystals of D- and L-Asn (scale in cm).

b) *Semi-continuous*

For semi-continuous enzyme-assisted PC, a filter module with a feed-stock of racemic Asn was implemented in the reactor setup (chapter 4.3.1 b). The concentration decrease of Asn in the solution, caused by crystallization of L-Asn, was compensated by dynamic re-saturation in the filter module. Thus, the absolute product yield was increased by the amount of fed Asn up to ca. 700 mg. Similar to the results presented for the batch process, the ee_L of the produced crystals increased with the amount of applied AArac2440.

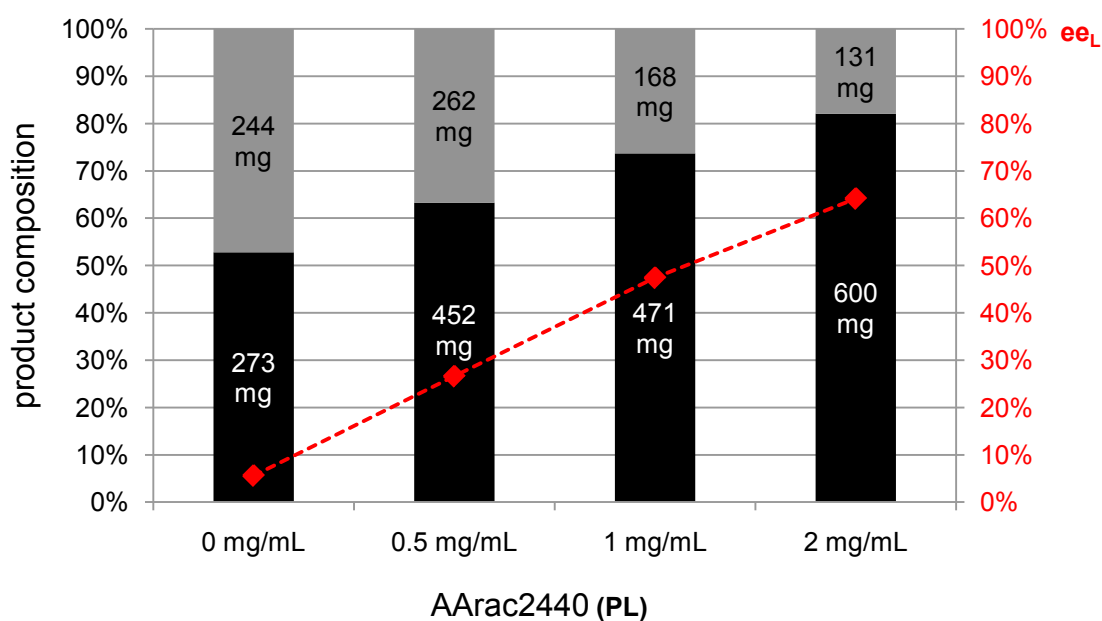


Figure 23: Product compositions and yields (black bars: L-Asn*H₂O, grey bars: D-Asn*H₂O) and ee_L (♦) obtained by semi-continuous enzyme-assisted PC in the absence and presence of AArac2440 (0.5 to 2 mg/mL). Product ee_L did not exceed 64 % when 2 mg/mL AArac2440 was applied. Process parameters: $m_{\text{feed}}=500$ mg DL-Asn, $T_{\text{sat}}=35$ °C, $T_{\text{cryst}}=32$ °C, $V=20$ mL, $m_{\text{seed}}=5$ mg.

However, the maximum ee_L that was reached during semi-continuous enzyme-assisted PC using 2 mg/mL AArac2440 did not exceed 64 % (Figure 23). Hence, no product purities comparable to the ones reached during batch crystallization of L-Asn could be achieved.

4.3.3 Benefits and limits

Enzyme-assisted PC has the potential of overcoming yield limitations of classical resolution processes by “recycling” the undesired enantiomer, so that a theoretical yield of 100 % becomes possible. However, in the present example the possible yield is limited by the relatively small degree of supersaturation of the Asn solution during PC, which determines the maximum possible yield (Equation 2):

$$m_{\text{product}} = (c_{\text{sat}} - c_{\text{cryst}}) \cdot V$$

Equation 2

with m_{product} being the maximum possible yield, V being the reaction volume, and $c_{\text{sat/cryst}}$ being the solubility limits of Asn at saturation and crystallization temperatures, respectively. Consequently, the yield of the process can only be increased by a continuous feed of the racemic substrate, which theoretically could yield 100 % enantiopure product (in relation to racemic feed). Promising results using this approach were demonstrated by semi-continuous enzyme-assisted PC, where the product yield could be increased by the amount of the racemic feed.

To evaluate the efficiency of the biocatalyst, the residual enzyme activity of applied AArac2440 was determined after enzyme-assisted PC. Four independent experiments revealed no loss of activity after a process time of 20 h. Easy enzyme recovery by ultrafiltration (membrane cutoff: 10 kDa) and lyophilization additionally contribute to an attractive new process for the chiral resolution of AA. However, further optimization of the reactor setup as well as of the process parameters (*e.g.* degree of supersaturation, type and velocity of stirring, reactor volume, and product recovery) are necessary to achieve satisfying results in terms of optical purity.

In contrast to DKR or deracemization processes by stereoselective biotransformations (Turner, 2004), the production of both isomers with only one racemase is possible. This is a considerable advantage, since no adaption of the enzyme’s stereoselectivity or the use of another enzyme is required for the production of the second enantiomer. In fact, only the chirality of the used seed crystals determines the final product chirality.

4.4 Production of chiral *allo*-threonine

As was already mentioned in the introduction, various chemical multi-step reactions have been described for the production of racemic and chiral *allo*-Thr. Their complexity and usually low yields render these processes very cost-intensive, whereas enzymatic approaches are rather rare (Pons *et al.*, 1990; Beaulieu, 1991; Blaskovich *et al.*, 1993; Lloyd-Williams *et al.*, 1997; Cardillo *et al.*, 1998).

In the course of this project, valuable chiral L- and D-*allo*-Thr was produced by enzymatic isomerization of the cheap starting material Thr with AArac12996 (PL) in combination with simple product crystallization from aqueous solutions. AArac12996 was preferred for the application as a process enzyme, since it exhibits an excellent stability at 30 °C (chapter 4.1.3).

Two different process strategies for the production of chiral *allo*-Thr were investigated, which will be discussed in chapter 4.4.2.

4.4.1 Identification of threonine isomers

Enzymatic isomerization (epimerization) of diastereomeric Thr by amino acid racemases does not yield the respective counter-enantiomers, as it is the case during isomerization of AA with only one chiral center. Since only the stereoconformation of the α -amino group is affected by the isomerization reaction while the β -hydroxy group remains unchanged, Thr is interconverted to *allo*-Thr (**publication 4**, Figure 1).

The identity of the reaction products of D- and L-Thr was verified by chiral HPLC and ¹H-NMR spectroscopy in D₂O. Chiral HPLC was able to separate three peaks, which could be assigned to D-Thr/D-*allo*-Thr, L-*allo*-Thr and L-Thr (Figure 24). Since it was not possible to distinguish D-Thr and D-*allo*-Thr by HPLC, only the ratio a between D- and L-isomers could be determined.

$$a = \frac{[\text{D-Thr}] + [\text{D-}i\text{allo-Thr}]}{[\text{L-Thr}] + [\text{L-}i\text{allo-Thr}]}$$

Equation 3

Due to the different chemical environments in diastereomeric molecules, epimers can be distinguished from each other by ¹H-NMR spectroscopy, while enantiomers show the same peak pattern (Figure 25). The ratio b between Thr and *allo*-Thr could be determined from the peak areas by Equation 4.

$$b = \frac{[D - \text{Thr}] + [L - \text{Thr}]}{[D - \text{allo} - \text{Thr}] + [L - \text{allo} - \text{Thr}]}$$

Equation 4

The absolute concentrations [D-Thr] and [D-*allo*-Thr] could then be calculated from Equation 3 and Equation 4. [L-Thr] and [L-*allo*-Thr] can be determined in an equivalent way.

$$[D - \text{allo} - \text{Thr}] = \frac{[L - \text{Thr}](a + 1) + [L - \text{allo} - \text{Thr}](a - b)}{b + 1}$$

Equation 5

$$[D - \text{Thr}] = a([L - \text{Thr}] + [L - \text{allo} - \text{Thr}]) - [D - \text{allo} - \text{Thr}]$$

Equation 6

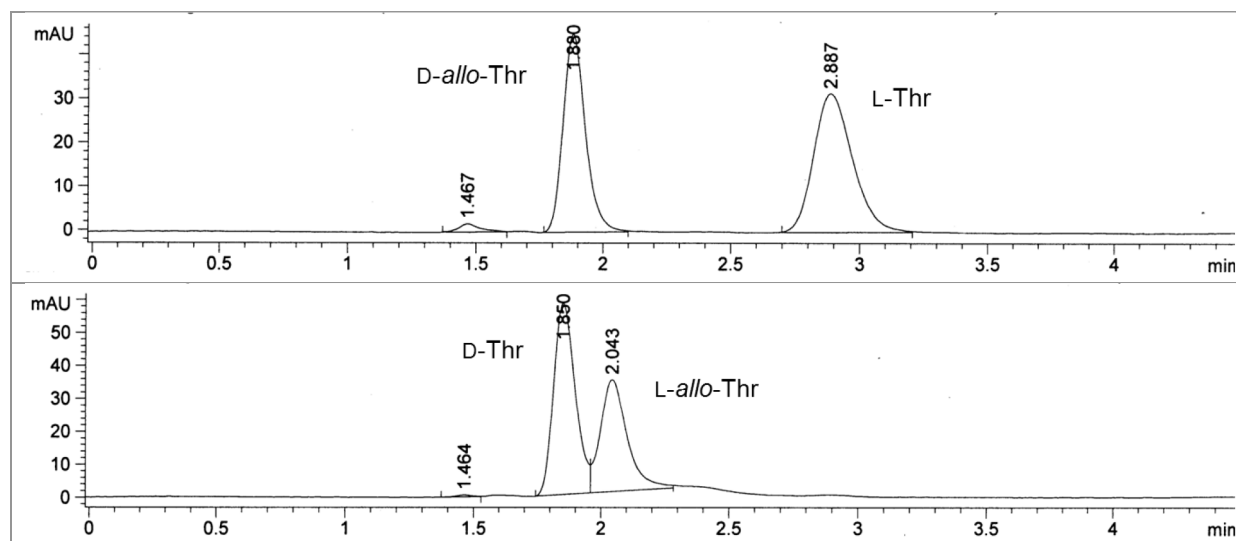


Figure 24: HPLC chromatograms of threonine isomers (column: Crownpak CR(+), mobile phase: HClO_4 (pH1), flow: 0.8 mL/min, $T=5^\circ\text{C}$). Retention times t_r : $t_r(\text{D-Thr})=1.85$ min, $t_r(\text{D-*allo*-Thr})=1.88$ min, $t_r(\text{L-*allo*-Thr})=2.04$ min and $t_r(\text{L-Thr})=2.89$ min.

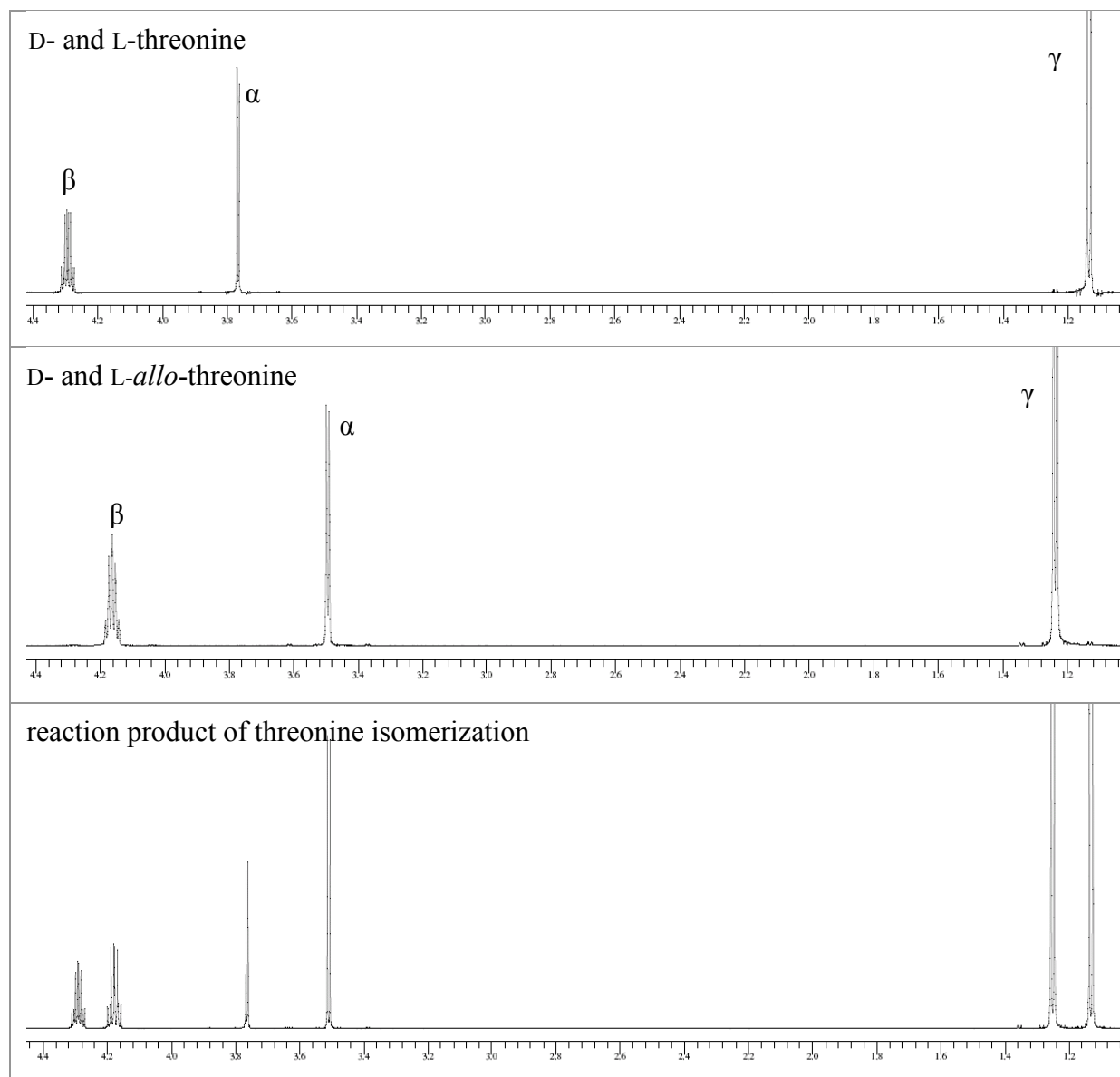


Figure 25: ^1H -NMR-spectra (Bruker, Avance DR X 600, 600 MHz) of Thr (top), *allo*-Thr (middle) and the reaction product of Thr isomerization (bottom) in D_2O showing peaks for α -, β - and γ -protons (Thr: 600 MHz, ppm: δ = 1.23-1.24 (d, 3H, J =6.42, CH_3), 3.49-3.50 (d, 1H, J =4.91, CH), 4.14-4.18 (m, 1H, CH); *allo*-Thr: 600 MHz, ppm: δ = 1.14-1.15 (d, 3H, J =6.42, CH_3), 3.77-3.78 (d, 1H, J =3.77, CH), 4.28-4.32 (m, 1H, CH)).

4.4.2 Process modes

Both enantiomers of *allo*-Thr have been produced by enzymatic isomerization of Thr and simultaneous crystallization. For a better understanding, this process may be separated into three individual physical and biocatalytic reaction steps, which all take place simultaneously in one reaction vessel and result in a dynamic interaction (Figure 26):

- “removal” of Thr from the saturated solution by isomerization to *allo*-Thr
- solution of excess (solid) D- or L-Thr
- crystallization of accumulating D- or L-*allo*-Thr upon exceeding the solubility limit

The dynamic interaction of these three steps yields a constant solution composition of about 42 % D- or L-*allo*-Thr and 58 % L- or D-Thr, respectively.

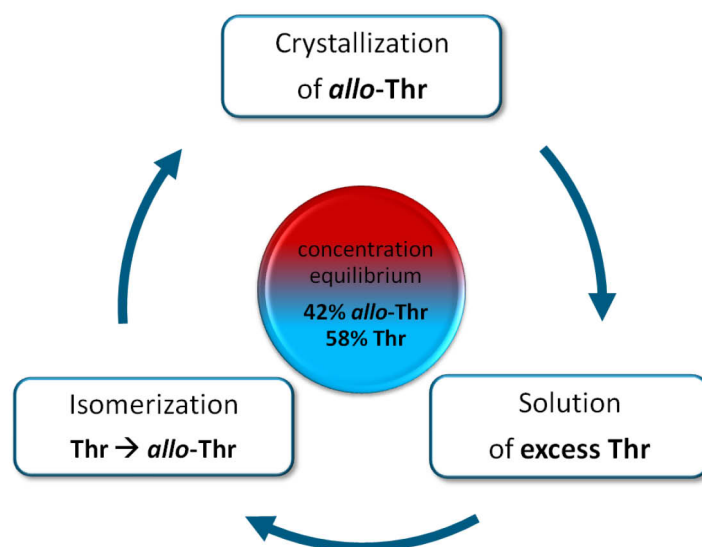


Figure 26: Production of chiral *allo*-Thr by enzymatic isomerization and crystallization. The dynamic process consists of three steps: isomerization (Thr \rightarrow *allo*-Thr), crystallization (*allo*-Thr) and solution of excess Thr.

In contrast to enzyme-assisted PC of Asn, where the reaction process could be monitored polarimetrically, here the solution composition as well as the optical purity of the crystals were determined by chiral HPLC and $^1\text{H-NMR}$ (chapter 4.4.1).

The production of D- and L-*allo*-Thr was investigated in a repetitive batch and in a continuously operated reactor.

a) Repetitive batch production in one single reaction vessel

Both enantiomers of *allo*-Thr were produced separately starting from either D- or L-Thr as a substrate. Enzymatic isomerization of Thr to the respective *allo*-Thr enantiomer using AArac12996 was performed in a tempered 30 mL reaction vessel as described in **publication 4**. Therefore, the reaction solution was saturated with the respective chiral Thr until a sediment was formed (Figure 27, I). Crystallization of the accumulating enantiomer of *allo*-Thr occurred in the same reaction vessel and started upon exceeding its solubility limit, which is lower compared to the one of Thr in water (Figure 16). As a result, an equilibrium concentration of ca. 42 % *allo*-Thr and 58 % Thr was formed in the solution (Figure 27, II). Upon complete solution of the excess Thr, the described dynamic process was interrupted and only *allo*-Thr remained in crystalline form (Figure 27, III). The crystals were separated by filtration and dried at 60 °C. By the addition of fresh Thr the next batch was started. Steps II

and III were repeated for a repetitive batch crystallization. Figure 27 depicts a repetitive batch process for the production of D-*allo*-Thr starting from a saturated L-Thr solution.

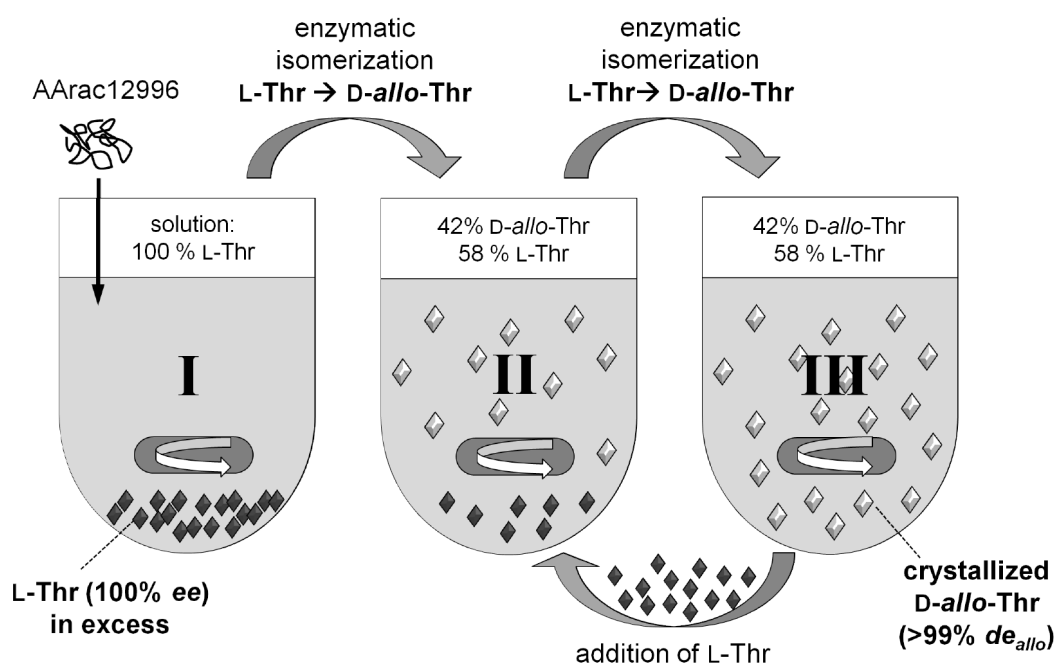


Figure 27: Repetitive batch crystallization of D-*allo*-Thr in one single reaction vessel. **I:** AArac12996 is added to a saturated L-Thr solution (starting condition) **II:** dynamic process of crystallization (D-*allo*-Thr), solution (L-Thr) and isomerization (L-Thr → D-*allo*-Thr) **III:** addition of fresh L-Thr when excess has depleted. Steps II and III are repeated for repetitive batch crystallization.

Repetitive batch processes (20 mL scale) were performed for the production of D- and L-*allo*-Thr, respectively. The process data and yields for both enantiomers are summarized in **publication 4**. The production of D-*allo*-Thr was performed over 55 days and consisted of 12 batches with yields of 1.6 to 4.4 g D-*allo*-Thr per batch and a de_{allo} between 96.9 and 100 %. A space time yield (STY) of 28 g/(L·d) and a final yield of 30.8 g D-*allo*-Thr ($de_{allo} > 99.2\%$) were achieved. The production of L-*allo*-Thr was performed over 56 days and consisted of 12 batches with yields of 1.5 to 4.0 g L-*allo*-Thr per batch and a de_{allo} between 94.6 and 100 %. A STY of 28.8 g/(L·d) and a final yield of 32.2 g L-*allo*-Thr ($de_{allo} > 98.4\%$) were obtained using a total amount of 20 mg AArac12996. The enzyme showed a remarkable high stability ($t_{1/2}=32$ d) under process conditions yielding 2.56 g D-*allo*-Thr and 1.62 g L-*allo*-Thr per mg AArac12996, respectively.

b) Continuous production with separate crystallization vessel

Another process concept was investigated where crystallization of *allo*-Thr and solution of excess Thr were performed in two separate reaction vessels. Thereby, a continuous product separation should be enabled. Figure 28 depicts the reactor setup, which consisted of two tempered 150 mL reaction vessels (25 °C and 30 °C, connected by silicon tubings), each

having two inner glass circlets. These circlets break the stirring turbulences and prevent the crystals from being flushed out of the vessel. Both vessels were separated by a third small vessel (volume of ca. 20 mL), that was heated to 40 °C and served as a solution trap for flushed crystals. The reaction solution was pumped from vessel 1 (solution of Thr) through vessel 2 (solution of small, flushed crystals) into vessel 3 (crystallization of *allo*-Thr), from where it was led back to vessel 1.

For a continuous product separation, crystallization of D- or L-*allo*-Thr may only occur in reaction vessel 3. Therefore, the *allo*-Thr concentration must be below the solubility limit at T_{sat} (vessel 1). This can only be provided by a sufficiently low temperature in vessel 3 (T_{cryst}) leading to fast crystallization of *allo*-Thr.

The described process was performed for a continuous D-*allo*-Thr production, where T_{sat} was 30 °C and T_{cryst} was varied between 20 °C and 30 °C. For isomerization of Thr, enzyme concentrations between 0.1 mg/mL and 1 mg/mL were applied. Table 6 summarizes the diastereomeric excesses and yields of D-*allo*-Thr in both reaction vessels at different crystallization temperatures using 0.35 mg/mL AArac12996. As expected, the amount of crystallized D-*allo*-Thr in vessel 3 increased by cooling. However, at all investigated temperatures even more D-*allo*-Thr precipitated in vessel 1, and thus making a continuous product separation from vessel 3 impossible. Since very good yields and purities could be achieved during repetitive batch crystallizations of *allo*-Thr (chapter 4.4.2 a), the continuous process was not further optimized.

Table 6: Summary of D-*allo*-Thr production with continuous product separation at different crystallization temperatures. $T_{\text{sat}}=30\text{ °C}$, AArac12996: 0.35 mg/mL.

T_{cryst} [°C]	reaction time [d]	vessel 3		vessel 1	
		yield (D- <i>allo</i> -Thr) [g]	de_{allo} [%]	yield (D- <i>allo</i> -Thr) [g]	de_{allo} [%]
20	2	3.18	86.8	8.41	15.0
25	3	2.56	99.4	11.07	99.4
30	3	0.13	90.2	19.44	55.8

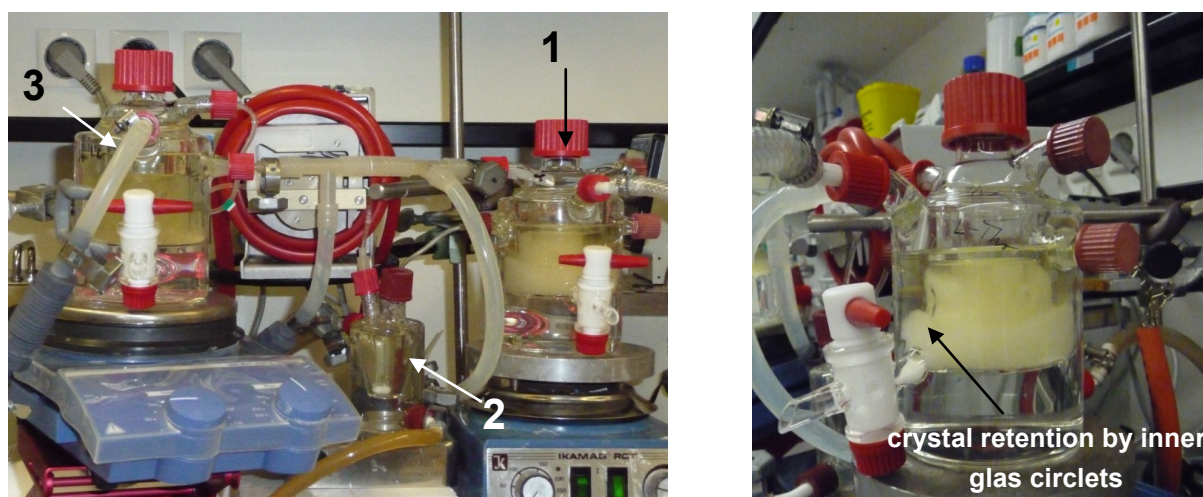
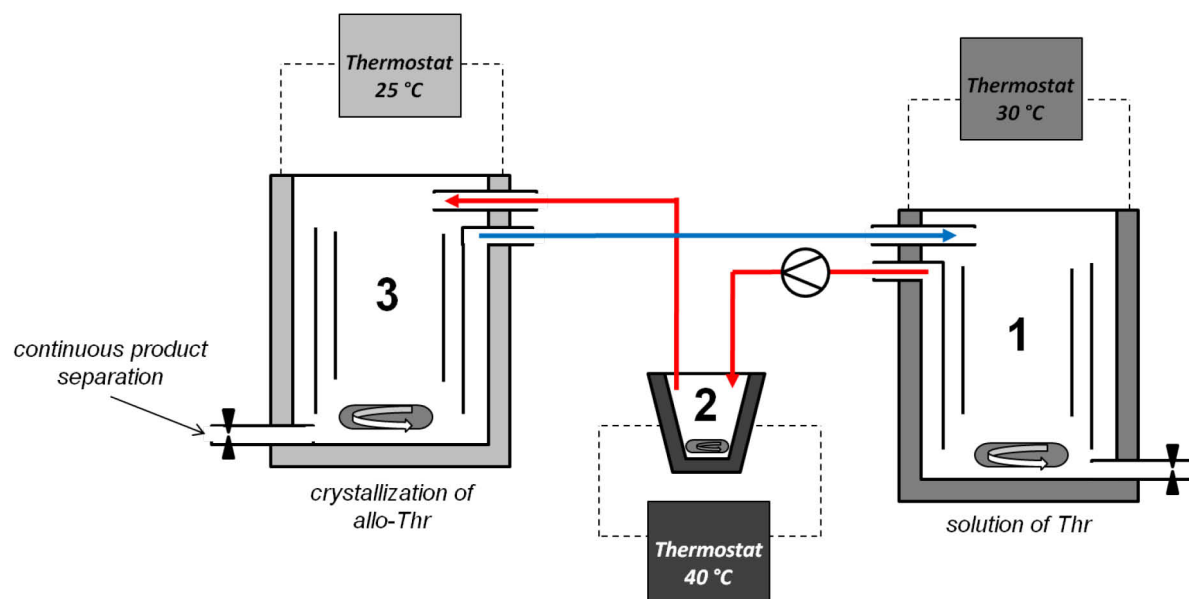


Figure 28: Reactor setup for the continuous production of *allo*-Thr by enzymatic isomerization of Thr and crystallization of *allo*-Thr in separated reaction vessels. **Top and bottom (left):** Scheme and photo of reactor setup. 1) solution of excess Thr, 30 °C, 2) crystal trap, 40 °C, 3) crystallization of *allo*-Thr, 25 °C. The reaction solution was adjusted to pH 8.5 (using NaOH) and pumped with a peristaltic pump (10 mL/min) from vessel 1 (solution of Thr) through vessel 2 (solution of small, flushed crystals) into vessel 3 (crystallization of *allo*-Thr), from where it was led back to vessel 1. For enzymatic Thr isomerization, 0.35 mg/mL AArac12996 were added to the solution. All three vessels were stirred with magnetic bars. **Bottom (right):** tempered reaction vessel with inner glass circlets for crystal retention. A distinct border between turbulent (cloudy solution) and non-turbulent area (clear solution) is detectable.

4.4.3 Benefits and limits of the new *allo*-threonine process

As already stated in the introduction, the use of *allo*-Thr for large-scale syntheses is hampered by the high costs of the currently applied chemical multi-step syntheses, which require careful purification of each reaction step. Besides, there are also biocatalytic syntheses described in the literature. Kataoka (Kataoka *et al.*, 1998) reported a stereoselective C-C bond formation between glycine and acetaldehyde using *L*-*allo*-Thr aldolase from *Aeromonas jandaei* DK-3. The same reaction is catalyzed by the serine hydroxymethyltransferase GlyA from *E. coli* (Makart *et al.*, 2007). Lim (Lim *et al.*, 1993) reported on an amino acid racemase from

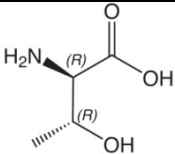
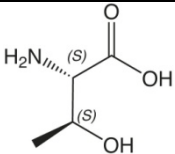
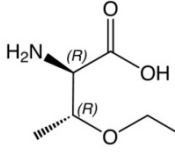
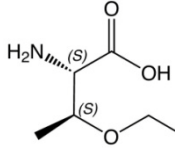
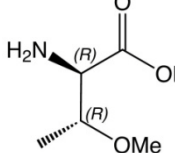
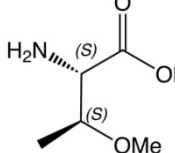
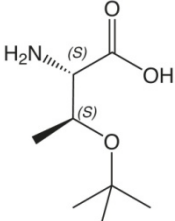
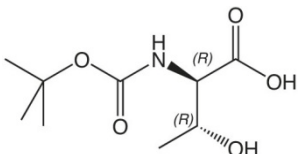
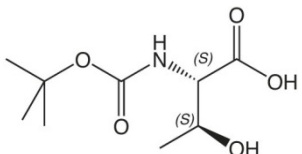
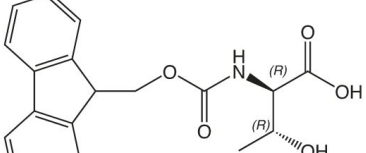
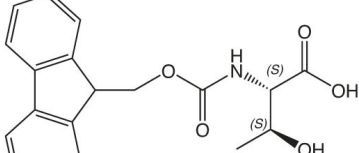
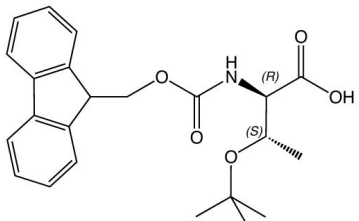
Pseudomonas putida ATCC 17642 with a threonine- α -epimerase activity (EC 5.1.1.6), which is the only reference of an enzymatic isomerization of Thr in the literature. γ -halogenated derivatives of Thr were synthesized using L- and D-threonine aldolases from *Pseudomonas putida* starting from glycine and the corresponding halogenated aldehydes yielding a *de* up to 97 % (Steinreiber *et al.*, 2007). Nevertheless, chemical methods clearly outnumber the described enzymatic approaches. For example Blaskovich (Blaskovich *et al.*, 1993) described an 8-step synthesis of D- and L-*allo*-Thr starting from the respective *cis*-isomers with a total yield of 38 %.

The repetitive batch process, which has been developed in this thesis, offers an extraordinary simple method for the production of optically pure *allo*-Thr using the same amino acid racemase for both enantiomers. Compared to chemical synthesis methods for *allo*-Thr this process consists of only one enzyme catalyzed reaction (isomerization of bulk Thr) and simultaneous crystallization of *allo*-Thr in one single reaction vessel. The process is carried out at moderate temperatures in water and avoids any toxic or harmful compounds, thus being environmentally friendly. The product recovery is performed by simple filtration and subsequent crystal drying, which makes downstream processing very comfortable. In contrast to other biocatalytic production and separation methods for *allo*-Thr (Makart *et al.*, 2008), very high product purities with *de_{allo}* > 99% can be achieved. The excellent stability of the biocatalyst AArac12996 in the process easily allows for several batches with the same enzyme sample, and thus makes complete conversion of the substrate possible. As demonstrated in chapter 4.4.2, a repetitive batch mode is advantageous over a continuous process due to the simple and robust process control.

4.4.4 Added value by threonine isomerization

Valuable chiral *allo*-Thr can be produced by the described simple process from low-priced Thr. In case of D-*allo*-Thr, cheap bulk L-Thr (ca. 1 €/g, catalogue price VWR 2010), which is mainly produced by fermentation with optimized strains of *Escherichia coli* and *Serratia marcescens* (Hermann, 2003; Leuchtenberger *et al.*, 2005), is the starting material. The high enzyme stability, as well as low maintenance of the running repetitive batch process, result in a profitable added value. Easy purification of AArac12996 from the culture medium yielded ca. 160 mg purified enzyme preparation per liter cultivation medium (chapter 4.1.2). The enzyme consumption during D-*allo*-Thr production was ca. 0.39 mg/g_{D-*allo*-Thr} (**publication 4**). Therefore, one batch of AArac12996 (160 mg) purified from 1 liter cultivation medium is sufficient for the production of ca. 410 g D-*allo*-Thr with a market value of more than 150000 € (catalogue price Jan. 2011, IRIS Biotech GmbH, Germany). Besides D- and L-*allo*-Thr, there are several derivatives commercially available (Table 7) ranging between 110 and 575 €/g.

Table 7: Commercially available derivatives of *allo*-Thr (catalogue prices Jan. 2011, IRIS Biotech GmbH, Germany).

Derivative	D-enantiomer	L-enantiomer
D/L- <i>allo</i> -Thr	 390 €/g	 225 €/g
D/L- <i>allo</i> -Thr(Et)-OH	 575 €/g	 550 €/g
D/L- <i>allo</i> -Thr(Me)-OH	 575 €/g	 550 €/g
L- <i>allo</i> -Thr(tBu)-OH		 250 €/g
Boc-D/L- <i>allo</i> -Thr-OH*DCHA	 250 €/g	 200 €/g
Fmoc-D/L- <i>allo</i> -Thr-OH	 110 €/g	 200 €/g
Fmoc-L- <i>allo</i> -Thr(tBu)-OH		 200 €/g

CHAPTER 5

CONCLUSIONS

5 Conclusions

Two different approaches for enzyme-assisted crystallization of chiral amino acids have been investigated in this thesis. Both approaches use purified amino acid racemases from *Pseudomonas putida*, which have been characterized in detail. While in approach 1 the racemase is applied for racemization of the proteinogenic amino acid Asn, approach 2 uses the enzyme for the isomerization of Thr to *allo*-Thr.

Approach 1: Enzyme-assisted preferential crystallization of L-Asn from a racemic solution

A new method, based on the combination of enzymatic racemization and preferential crystallization of single enantiomers from racemic solutions, was investigated. The ternary system DL-Asn in water was found to form conglomerates upon crystallization from racemic solutions and thus to allow enantioseparation by preferential crystallization. Purified AArac2440 was used for *in situ* racemization of the crystallization solution, thus keeping the solution *ee* close to racemic and thereby prolonging preferential crystallization. This process is the first successful demonstration of enzyme-assisted preferential crystallization. However, further optimization of the reactor setup as well as of the process parameters (*e.g.* degree of supersaturation, type and velocity of stirring, reactor volume, and product recovery) are necessary to achieve satisfying results in terms of optical product purity.

Approach 2: Enzymatic production of chiral *allo*-Thr by isomerization of Thr and crystallization

Valuable chiral D- and L-*allo*-Thr were produced by isomerization of the respective Thr enantiomers with AArac12996 and simultaneous crystallization from aqueous solutions. The repetitive batch process, which integrates isomerization and crystallization in one single reaction vessel, was superior to a continuous process with two separate isomerization and crystallization vessels. Both enantiomers of the produced *allo*-Thr were obtained with very good diastereomeric excess ($de_{allo} > 98\%$). The high stability of AArac12996 under process conditions ($t_{1/2} = 32$ d) as well as low process maintenance effort, offer a simple and economically interesting method for the production of high-priced *allo*-Thr for synthetic applications in the pharmaceutical industry.

To expand the general scope of application of the presented processes, enzymatic racemization, which is the process' bottleneck, must be the focus of intensive research. By the use of improved catalysts the possible substrate spectrum might not be limited to natural amino acids but also non-proteinogenic amino acids or even other substance groups may become available. Especially modern evolutionary methods or rational protein design for altered substrate spectra of wild type racemases (Kino *et al.*, 2007) might lead to new production processes for chiral compounds.

CHAPTER 6

REFERENCES

6 References

- Alexander, F. W., Sandmeier, E., Mehta, P. K., Christen, P.,** Evolutionary relationships among pyridoxal-5'-phosphate-dependent enzymes - Regio-specific alpha-family, beta-family, and gamma-family. *Eur. J. Biochem.* (1994) 219: 953-960.
- Archer, I. V., Arnold, A. A., Carr, R., Fotheringham, I. G., Speight, R. E., Taylor, P. P.,** Chemo-enzymatic synthesis of unnatural amino acids in *Asymmetric synthesis and application of alpha-amino acids*. Soloshonok, V. A., Izawa, K. (2009) Washington D. C, American Chemical Society. 1009: 322-336.
- Bäckvall, J.-E.,** Asymmetric catalysis via dynamic kinetic resolution in 359 *Asymmetric synthesis - The essentials*. Christmann, M., Bräse, S. (2008) Weinheim, Wiley-VCH: 169-178.
- Beaulieu, P. L.,** Diastereospecific synthesis of D- and L-*allo*-threonines and trichlorinated derivatives suitable for the preparation of tritium labelled material. *Tetrahedron Lett.* (1991) 32: 1031-1034.
- Bechtold, M., Heinemann, M., Panke, S.,** Suitability of teicoplanin-aglycone bonded stationary phase for simulated moving bed enantioseparation of racemic amino acids employing composition-constrained eluents. *J. Chromatogr. A* (2006) 1113: 167-176.
- Bendtsen, J. D., Nielsen, H., von Heijne, G., Brunak, S.,** Improved prediction of signal peptides: SignalP 3.0. *J. Mol. Biol.* (2004) 340: 783-795.
- Bercovici, D., Fuller, M. F.,** Industrial amino acids in nonruminant animal nutrition in 372 *Biotechnology in Animal Feeds and Animal Feeding*. Wallace, R. J., Chesson, A. (1995) Weinheim, VCH Press: 93-113.
- Blaskovich, M. A., Lajoie, G. A.,** Stereoselective synthesis of *allo*-threonine and beta-2^H-*allo*-threonine from threonine. *Tetrahedron Lett.* (1993) 34: 3837-3840.
- Bommarius, A. S., Schwarm, M., Drauz, K.,** Biocatalysis to amino acid-based chiral pharmaceuticals - examples and perspectives *J. Mol. Catal. B: Enzym.* (1998) 5: 1-11.
- Breslow, R., Cheng, z.-L.,** On the origin of terrestrial homochirality for nucleosides and amino acids. *Proc. Natl. Acad. Sci. U. S. A. (PNAS)* (2009) 106: 9144-9146.
- Brown, K.,** BIO024B, Amino acids: Highlighting synthesis applications; available online: <http://www.Bccresearch.Com/report/bio024b.html>." (2005).
- Buchholz, K., Poulsen, P. B.,** *Applied Biocatalysis*. (2000) Amsterdam, Harwood Academic Publishers.
- Buchner, E.,** Alkoholische Gärung ohne Hefezellen (Vorläufige Mitteilung). *Ber. Dtsch. Chem. Ges.* (1897) 30: 117-124.
- Burke, J., Terrence R., Knight, M., Chandrasekhar, B.,** Solid phase synthesis of viscosin, a cyclic depsipeptide with antibacterial and antiviral properties. *Tetrahedron Lett.* (1989) 30: 519-522.
- Cardillo, G., Gentilucci, L., Tolomelli, A., Tomasini, C.,** Formation of aziridine-2-amides through 5-Halo-6-methylperhydropyrimidin-4-ones. A route to enantiopure L- and D-threonine and *allo*-threonine. *J. Org. Chem.* (1998) 63: 3458-3462.

- Chassagnole, C., Rais, B., Quentin, E., Fell, D. A., Mazat, J. P.**, An integrated study of threonine-pathway enzyme kinetics in *Escherichia coli*. *Biochem. J.* (2001) 356: 415-423.
- CLIB2021**, CLIB 2021: Cluster Industrielle Biotechnologie: http://www.bmbf.de/pub/clib2021_nrw.pdf (2007).
- Collet, A.**, Separation and purification of enantiomers by crystallisation methods. *Enantiomer* (1999) 4: 157-172.
- Drauz, K.**, Chiral amino acids: A versatile tool in the synthesis of pharmaceuticals and fine chemicals. *Chimia* (1997) 51: 310-314.
- Driessen, A. J. M., Fekkes, P., van der Wolk, J. P. W.**, The Sec system. *Curr. Opin. Microbiol.* (1998) 1: 216-222.
- Ebbers, E. J., Ariaans, G. J. A., Houbiers, J. P. M., Bruggink, A., Zwanenburg, B.**, Controlled racemization of optically active organic compounds: Prospects for asymmetric transformation. *Tetrahedron* (1997) 53: 9417-9476.
- Eggeling, L., Pfefferle, W., Sahm, H.**, Amino acids in 362 *Biotechnology*. Ratledge, C., Kristiansen, B. (2006) Cambridge, Cambridge University Press: 335-357.
- Eliel, E. L., Wilen, S. H., Doyle, M. P.**, *Basic Organic Stereochemistry*. (2001) New York, Wiley.
- Eliot, A. C., Kirsch, J. F.**, Pyridoxal phosphate enzymes: Mechanistic, structural, and evolutionary considerations. *Annu. Rev. Biochem.* (2004) 73: 383-415.
- Elsner, M. P., Menendez, D. F., Muslera, E. A., Seidel-Morgenstern, A.**, Experimental study and simplified mathematical description of preferential crystallization. *Chirality* (2005) 17: 183-195.
- Elsner, M. P., Ziomek, G., Seidel-Morgenstern, A.**, Simultaneous preferential crystallization in a coupled, batch operation mode - Part 1: Theoretical analysis and optimization. *Chem. Eng. Sci.* (2007) 62: 4760-4769.
- Enright, A., Alexandre, F. R., Roff, G., Fotheringham, I. G., Dawson, M. J., Turner, N. J.**, Stereoinversion of beta- and gamma-substituted alpha-amino acids using a chemo-enzymatic oxidation-reduction procedure. *Chem. Commun.* (2003) 2636-2637.
- FDA**, FDA'S policy statement for the development of new stereoisomeric drugs. *Chirality* (1992) 4: 338-340.
- Festel, G., Knoll, J., Gotz, H., Zinke, H.**, Der Einfluss der Biotechnologie auf Produktionsverfahren in der Chemieindustrie. *Chem. Ing. Tech.* (2004) 76: 307-312.
- Fischer, E.**, Einfluss der Conformation auf die Wirkung der Enzyme. *Chem. Ber.* (1894) 27: 2985-2993.
- Flippin, L. A., Jalali-Araghi, K., Brown, P. A., Burmeister, H. R., Vesonder, R. F.**, Structure of the fatty acid component of an antibiotic cyclodepsipeptide complex from the genus fusarium. *J. Org. Chem.* (1989) 54: 3006-3007.
- Fogassy, E., Nógrádi, M., Kozma, D., Egri, G., Palovics, E., Kiss, V.**, Optical resolution methods. *Org. Biomol. Chem.* (2006) 4: 3011-3030.
- Francotte, E. R.**, Enantioselective chromatography as a powerful alternative for the preparation of drug enantiomers. *J. Chromatogr. A* (2001) 906: 379-397.

- Frey, P., Hegeman, A. D.,** *Enzymatic reaction mechanisms*. (2006) Oxford, Oxford University Press Inc.
- Goldberg, K., Schroer, K., Lütz, S., Liese, A.,** Biocatalytic ketone reduction - a powerful tool for the production of chiral alcohols - part I: processes with isolated enzymes. *Appl. Microbiol. Biotechnol.* (2007) 76: 237-248.
- Grishin, N. V., Phillips, M. A., Goldsmith, E. J.,** Modeling of the spatial structure of eukaryotic ornithine decarboxylases. *Protein Sci.* (1995) 4: 1291-1304.
- Gröger, H., Dietz, F. R.,** Biocatalytic synthesis of natural and non-natural alpha-amino acids in 334 *Wiley Encyclopedia of Chemical Biology* (2009), John Wiley & Sons: 191-204.
- Hermann, T.,** Industrial production of amino acids by coryneform bacteria. *J. Biotechnol.* (2003) 104: 155-172.
- Hoffritz, J.,** Faible für Vampire; Vom Pionier zum Resteverwerter: Die Biotech-Branche lebt von alten Patenten der Pharmakonzerne - mit wechselndem Erfolg in *Die Zeit (Wirtschaft)* (2007) 9th of Nov. 2007.
- Ikeda, H., Yonetani, Y., Hashimoto, S.-i., Yagasaki, M., Soda, K.,** Amino acid racemase having low substrate specificity and process for producing racemic amino acid (2003) Japan, WO 03/074690 A1.
- Ishiwata, K. I., Fukuhara, N., Shimada, M., Makiguchi, N., Soda, K.,** Enzymatic production of L-tryptophan from DL-serine and indole by a coupled reaction of tryptophan synthase and amino-acid racemase. *Biotechnol. Appl. Biochem.* (1990) 12: 141-149.
- Jacques, J., Collet, A., Wilen, S. H.,** *Enantiomers, Racemates, and Resolutions*. (1994) Malabar (USA), Krieger.
- Kataoka, M., Wada, M., Ikemi, M., Morikawa, T., Miyoshi, T., Shimizu, S.,** Novel threonine aldolases and their application to stereospecific synthesis of beta-hydroxy-alpha-amino acids. *Ann. N. Y. Acad. Sci.* (1998) 864: 318-322.
- Kino, K., Sato, M., Yoneyama, M., Kirimura, K.,** Synthesis of DL-tryptophan by modified broad specificity amino acid racemase from *Pseudomonas putida* IFO 12996. *Appl. Microbiol. Biotechnol.* (2007) 73: 1299-1309.
- Klussmann, M., Iwamura, H., Mathew, S. P., Wells, D. H., Pandya, U., Armstrong, A., Blackmond, D. G.,** Thermodynamic control of asymmetric amplification in amino acid catalysis. *Nature* (2006) 441: 621-623.
- Kühne, W.,** Über das Verhalten verschiedener organisierter und sog. ungeformter Fermente in 351 *Verhandlungen des naturhistorisch-medizinischen Vereins zu Heidelberg* (1877), Nabu Press. 1: 190-193.
- Lambert, C., Leonard, N., De Bolle, X., Depiereux, E.,** ESyPred3D: Prediction of proteins 3D structures. *Bioinformatics* (2002) 18: 1250-1256.
- Lee, T., Lin, Y. K.,** The origin of life and the crystallization of aspartic acid in water. *Cryst. Growth Des.* (2010) 10: 1652-1660.
- Leonhartsberger, S., Mucke, M.,** Therapeutic proteins due *E. coli* secretion technology. *Nachr. Chem.* (2009) 57: 1012-1014.
- Leuchtenberger, W., Huthmacher, K., Drauz, K.,** Biotechnological production of amino acids and derivatives: current status and prospects. *Appl. Microbiol. Biotechnol.* (2005) 69: 1-8.

- Lim, Y.-H., Yokoigawa, K., Esaki, N., Soda, K.**, A new amino acid racemase with threonine alpha-epimerase activity from *Pseudomonas putida*: Purification and characterization. *J. Bacteriol.* (1993) 175: 4213-4217.
- Lloyd-Williams, P., Carulla, N., Giralt, E.**, Simple methods for the preparation of protected derivatives of D-*allo*- and L-*allo*-threonine. *Tetrahedron Lett.* (1997) 38: 299-302.
- Lorenz, H., Perlberg, A., Sapoundjiev, D., Elsner, M. P., Seidel-Morgenstern, A.**, Crystallization of enantiomers. *Chem. Eng. Process.* (2006) 45: 863-873.
- Lorenz, H., Capla, F., Polenske, D., Elsner, M. P., Seidel-Morgenstern, A.**, Crystallization based separation of enantiomers. *J. UCTM* (2007) 42: 5-16.
- Makart, S., Bechtold, M., Panke, S.**, Towards preparative asymmetric synthesis of beta-hydroxy-alpha-amino acids: L-*allo*-threonine formation from glycine and acetaldehyde using recombinant GlyA. *J. Biotechnol.* (2007) 130: 402-410.
- Makart, S., Bechthold, M., Panke, S.**, Separation of amino acids by simulated moving bed under solvent constrained conditions for the integration of continuous chromatography and biotransformation. *Chem. Eng. Sci.* (2008) 63: 5347-5355.
- Matsui, D., Oikawa, T., Arakawa, N., Osumi, S., Lausberg, F., Stähler, N., Freudl, R., Eggeling, L.**, A periplasmic, pyridoxal-5'-phosphate-dependent amino acid racemase in *Pseudomonas taetrolens*. *Appl. Microbiol. Biotechnol.* (2009) 83: 1045-1054.
- May, O., Verseck, S., Bommarius, A., Drauz, K.**, Development of dynamic kinetic resolution processes for biocatalytic production of natural and nonnatural L-amino acids. *Org. Process Res. Dev.* (2002) 6: 452-457.
- Meyerhoffer, W.**, Stereochemical notices. *Ber. Dtsch. Chem. Ges.* (1904) 37: 2604-2610.
- Miyazaki, H., Morita, H., Shiraiwa, T., Kurokawa, H.**, Optical resolution by preferential crystallization and replacing crystallization of DL-*allo*threonine. *Bull. Chem. Soc. Jpn.* (1994) 67: 1899-1903.
- Muecke, M., Leonhartsberger, S.**, Increasing production process efficiency. *Genetic Engineering & Biotechnology News* (2009) 29: 56-57.
- Nielsen, H., Krogh, A.**, Prediction of signal peptides and signal anchors by a hidden Markov model. *Proc. 6th int. conf. ISMB* (1998) 6: 122-130.
- Pasteur, L.**, *Researches on the molecular asymmetry of natural organic products*. Alembic Club Reprints (1897) Edinburgh, Livingstone.
- Patel, R. N.**, Biocatalysis: Synthesis of chiral intermediates for drugs. *Curr. Opin. Drug Discovery Dev.* (2006) 9: 741-764.
- Patel, R. N.**, Chemo-enzymatic synthesis of pharmaceutical intermediates. *Expert. Opin. Drug Discov.* (2008) 3: 187-245.
- Payen, A., Persoz, J.-F.**, Memoir on diastase, the principal products of its reactions and their applications to the industrial arts in 337 *Annales de Chimie et de Physique, 2nd series* (1833) Paris. 53: 73-92.
- Pons, D., Savignac, M., Genet, J.-P.**, Efficient syntheses of enantiomerically pure L and D-*allo*threonines and (S) and (R) isoserines. *Tetrahedron Lett.* (1990) 31: 5023-5026.
- QIAGEN**, QIAquick® PCR Purification Kit - Instruction Manual. (2002)

-
- Ran, N. Q., Zhao, L. S., Chen, Z. M., Tao, J. H.**, Recent applications of biocatalysis in developing green chemistry for chemical synthesis at the industrial scale. *Green Chem.* (2008) 10: 361-372.
- Reynolds, K., Martin, J., Shen, S.-J., Esaki, N., Soda, K., Floss, H. G.**, Mechanistic studies of two amino acid racemases of broad substrate specificity from *Pseudomonas striata* and *Aeromonas caviae*. *J. Basic Microbiol.* (1991) 31: 177-188.
- Rodrigo, A. A., Lorenz, H., Seidel-Morgenstern, A.**, Online monitoring of preferential crystallization of enantiomers. *Chirality* (2004) 16: 499-508.
- Sapoundjiev, D., Lorenz, H., Seidel-Morgenstern, A.**, Solubility of chiral threonine species in water/ethanol mixtures. *J. Chem. Eng. Data* (2006) 51: 1562-1566.
- Schmid, A., Dordick, J. S., Hauer, B., Kiener, A., Wubbolts, M., Witholt, B.**, Industrial biocatalysis today and tomorrow. *Nature* (2001) 409: 258-268.
- Schneider, G., Kack, H., Lindqvist, Y.**, The manifold of vitamin B-6 dependent enzymes. *Structure* (2000) 8: R1-R6.
- Schnell, B., Faber, K., Kroutil, W.**, Enzymatic racemisation and its application to synthetic biotransformations. *Adv. Synth. Catal.* (2003) 345: 653-666.
- Schoemaker, H. E., Mink, D., Wubbolts, M. G.**, Dispelling the myths - Biocatalysis in industrial synthesis. *Science* (2003) 299: 1694-1697.
- Schulze, B., Wubbolts, M. G.**, Biocatalysis for industrial production of fine chemicals. *Curr. Opin. Biotechnol.* (1999) 10: 609-615.
- Sheldon, R. A.**, Consider the environmental quotient. *Chem. Tech.* (1994) 38-47.
- Soloshonok, V. A., Izawa, K.**, Eds. Asymmetric synthesis and application of alpha-amino acids, ACS Symposium Series 1009 (2009) Washington, American Chemical Society.
- Stecher, H., Faber, K.**, Biocatalytic deracemization techniques: Dynamic resolutions and stereoinversions. *Synthesis* (1997) 1-16.
- Steinreiber, J., Fesko, K., Mayer, C., Reisinger, C., Schürmann, M., Griengl, H.**, Synthesis of gamma-halogenated and long-chain beta-hydroxy-alpha-amino acids and 2-amino-1,3-diols using threonine aldolases. *Tetrahedron* (2007) 63: 8088-8093.
- Straathof, A. J. J., Panke, S., Schmid, A.**, The production of fine chemicals by biotransformations. *Curr. Opin. Biotechnol.* (2002) 13: 548-556.
- Stratagene**, QuikChange® Site-Directed Mutagenesis Kit - Instruction Manual. (2004)
- Stryer, L.**, *Biochemie*. (2007) Heidelberg, Spektrum Akademischer Verlag.
- Sturmer, R., Breuer, M.**, Enzymes as catalysts - Chemistry and biology hand in hand. *Chem. unserer Zeit* (2006) 40: 104-111.
- Sumner, J. B., Myrbäck, K.**, *The Enzymes Vol. 1*. (1950) New York, Academic Press.
- Suominen, I., Karp, M., Lahde, M., Kopio, A., Glumoff, T., Meyer, P., Mantsala, P.**, Extracellular production of cloned alpha-amylase by *Escherichia coli*. *Gene* (1987) 61: 165-176.
- Tauber, H.**, *The Chemistry and Technology of Enzymes*. (1949) New York, Wiley.
- Thayer, A. M.**, Enzymes at work. *Chem. Eng. News* (2006) 84: 15-25.
- Turner, M. K.**, Perspectives in biotransformations in 340 *Biotechnology: Biotransformations I*. Kelly, D. R. (1998) Weinheim, Wiley VCH. 8a: 5-23.

-
- Turner, N. J.**, Enzyme catalysed deracemisation and dynamic kinetic resolution reactions. *Curr. Opin. Chem. Biol.* (2004) 8: 114-119.
- Walsh, J. J.**, *Louis Pasteur*. Catholic Encyclopedia (1913) New York, Robert Appleton Company.
- Watson, J. D., Crick, F. H. C.**, Molecular structure of nucleic acids - a structure for deoxyribose nucleic acid. *Nature* (1953) 171: 737-738.
- Wipf, P., Miller, C. P.**, Stereospecific synthesis of peptide analogs with *allo*-threonine and *D-allo*-threonine residues. *J. Org. Chem.* (1993) 58: 1575-1578.
- Woodley, J. M.**, New opportunities for biocatalysis: making pharmaceutical processes greener. *Trends Biotechnol.* (2008) 26: 321-327.
- Würges, K., Pfromm, P. H., Rezac, M. E., Czermak, P.**, Activation of subtilisin Carlsberg in hexane by lyophilization in the presence of fumed silica. *J. Mol. Catal. B: Enzym.* (2005) 34: 18-24.
- Yoshimura, T., Esaki, N.**, Amino acid racemases: Functions and mechanisms. *J. Biosci. Bioeng.* (2003) 96: 103-109.
- Yoshimura, T., Mihara, H., Ohshima, T., Tanizawa, K.**, Kenji Soda - researching enzymes with the spirit of an alpinist. *J. Biochem.* (2010) 148: 371-379.
- Yuryev, R., Liese, A.**, Biocatalysis: The outcast. *ChemCatChem* (2010) 2: 103-107.

APPENDIX

APPENDIX**I DNA sequences****AArac2440**

1 ATGCCCTTTCGCCGTACCCTTCTGGCTGCATCCCTGGCACTTCTGATCACCGGACAGGCC
61 CCCCTGTATGCGGCACCACCGTTGTTCGATGGACAACGGCACCAACACCCTGACCGTGCAA
121 AACAGCAATGCCTGGGTCGAAGTCAGCGCCAGCGCCCTGCAGCACAACATCCGCACGCTG
181 CAGGCCGAGCTGGCCGGCAAGTCCAAGCTGTGCGCCGTGCTCAAGGCCGATGCCTATGGC
241 CACGGTATCGGCCTGGTAATGCCATCGATCATCGCCCAAGGCGTGCCCTGCGTGGCGGTG
301 GCCAGCAACGAGGAGGCCCGCGTGGTCCGCGCCAGTGGCTTACCAGGGCAACTGGTGCGG
361 GTACGCCTGGCCAGCCTCAGCGAGCTGGAAGATGGCTTGCAGTACGACATGGAAGAGCTG
421 GTGGGCAGCGCGGAATTTGCCCGCCAGGCCGATGCCATCGCCGCGCGCCATGGCAAGACC
481 TTGCGCATTACATGGCGCTCAACTCCAGCGGCATGAGCCGCAACGGGGTGGAGATGGCC
541 ACCTGGTCCGGCCGGTGGCAAGCGCTGCAGATCACCAGACCAGAAGCACCTCAAGCTGGTC
601 GCGCTGATGACCCACTTCGCCGTGGAAGACAAGGACGATGTACGCAAGGGCCTGGCGGCA
661 TTCAACGAGCAGACCGACTGGTTGATCAAGCACGCCAGGCTGGACCCGAGCAAGCTCACC
721 CTGCACGCCGCCAACTCGTTCGCTACGCTGGAAGTGCCGGAAGCGCGCCTGGACATGGTA
781 CGAACGGGTGGCGCGCTGTTCCGGCGACACCGTGCCGGCGCGCACCGAGTACAAACGTGCG
841 ATGCAGTTCAAATCGCACGTGGCGGCGGTGCACAGCTATCCGGCCGGCAACACCGTGGGC
901 TATGACCGCACCTTACCCTGGCCCGTGATTCGCGGCTGGCCAACTTACGGTTCGGGTAC
961 TCCGATGGCTACCGCCGGGTATTACCAACAAGGGCCATGTGCTGATCAACGGCCACCGT
1021 GTGCCGGTTCGTGGGCAAGGTGTCGATGAACACGCTGATGGTTCGATGTCACCGACTTCCCT
1081 GATGTGAAGGGGGGTAACGAAGTGGTGTCTGTTCCGGCAAGCAGGCCGGGGGCGAAATCACC
1141 CAGGCCGAGATGGAAGAAATCAACGGCGCGTTCGCTCGCCGATTTGTACACCGTATGGGGC
1201 AATTCCAACCCGAAGATACTCGTTCGACTGA

AArac12996

1 ATGCAATTTAGCCGTACCCTCCTGGCTGCATCCCTCGCTCTGCTGATCACTGGCCAGGCC
61 CCGCTGTACGCCGACCGCCCCTGTTCGATGGACAACGGCACCAACCGCCCTGACCGCGCAG
121 AACAGCAACGCCTGGGTCGAAATCAGTGCCGCGCACTGCAACACAACATCCGTACCTTG
181 CAGGCCGAGTTGGGCGGCAAGTCCAAGCTGTGCGCCGTGCTCAAGGCCGACGCCTATGGC
241 CACGGTATCGGCCTGGTATGCCGTGATCATCGCCAGGGCGTGCCCTGCGTGGCGGTG
301 GCCAGCAACGAGGAGGCACGCGTGGTCCGCGCCAGTGGCTTACCAGGGCAACTGGTTCGG
361 GTACGCCTGGCCAGCCTCGGCGAAGTGGAAGATGCCTTGCAGTACGACATGGAAGAGCTG
421 GTTGGCAGCGCCGAGTTCGCCCGCCAGCTCGATGCCATCGCCGAACGCCACGGCAAGACC
481 CTGCGCATTACATGGCGCTCAATTCCAGCGGCATGAGCCGCAACGGCGTGGAAATGACC
541 ACCTGGTCCGGCCGGGGTGAAGCGCTGCAGATCACTGACCAGAAGCACCTCCAGCTGGTC
601 GCGCTGATGACTCACTTCGCCGTGGAAGACAAGGACGATGTGCGCAAAGGCCTGGCAGCG
661 TTCAACGAACAGACCGACTGGCTGATCAAGCACGCGAAGCTTGATCGCAGCAAGCTCACC
721 CTGCATGCCGCCAACTCCTTCGCTACGCTGGAAGTGCCGGAAGCGCACCTGGACATGGTG
781 CGTACCGGTGGCGCGCTGTTCCGGCGACACCGTGCCGACGCGCACCGAATACCAACGTGTC
841 ATGCAGTTCAAAGTCGCACGTGGCGGCGGTGCACAGCTACCCGGCAGGCAACACCGTTCGGC
901 TACGACCGCACCTTACCCTGGCGCGTGATTCGCGCCTGGCCAACTTACCCTGGGTTAC
961 TCCGATGGCTACCGCCGGGTGTTACCAACAAGGGCCATGTGCTGATCAACGGCCACCGA
1021 GTGCCAGTGGTGGGCAAGGTGTCGATGAACACCTTATGGTTCGATGTCACCGATTTCCCC
1081 GATGTGAAGGGGGGCAACGAAGTGGTGTCTGTTCCGGCAAACAGGCCGGGAGGGAGATCACC
1141 CAGGCCGAGATAGAAGAAATCAACGGCGCGTTCGCTCGCCGACCTTACACCGTATGGGGC
1201 AGTTCCAACCCGAAGATTCTCGTTCGACTGA

II AA sequences

AArac2440

1 MPFRRTLLAASLALLITGQAPLYAAPPLSMDNGTNTLTVQNSNAWVEVSASALQHNIRTL
61 QAELAGKSKLCAVLKADAYGHGIGLVMPHSIIAQGVPCVAVASNEEARVVRASGFTGQLVR
121 VRLASLSELEDGLQYDMEELVGSAEFARQADAIAARHGKTLRIHMALNSSGMSRNGVEMA
181 TWSGRGEALQITDQKHLKLVALMTHFAVEDKDDVRKGLAAFNEQTDWLIK HARLDRSKLT
241 LHAANSFATLEVPEARLDMVRTGGALFGDTPARTEYKRAMQFKSHVAAVHSYPAGNTVG
301 YDRTFTLARDSRLANITVGYS DGYRRVFTNKGHV LINGHRVPVVGK VSMNTLMVDVDFP
361 DVKGGNEVV LFGKQAGGEITQAEMEEINGALLADLYTVWGN SNP KILVD

AArac12996

1 MQFSRRTLLAASLALLITGQAPLYAAPPLSMDNGTTALTAQNSNAWVEISA
51 GALQHNIRTLQAELGGKSKLCAVLKADAYGHGIGLVMPHSIIAQGVPCVAV
101 ASNEEARVVRASGFTGQLVRVRLASLGEVEDALQYDMEELVGSAEFARQL
151 DAIAERHGKTLRIHMALNSSGMSRNGVEMTTWSGRGEALQITDQKHLQLV
201 ALMTHFAVEDKDDVRKGLAAFNEQTDWLIK HAKLDRSKLTLHAANSFATL
251 EVPEAHLDMVRTGGALFGDTPTRTEYQRVMQFKSHVAAVHSYPAGNTVG
301 YDRTFTLARDSRLANITVGYS DGYRRVFTNKGHV LINGHRVPVVGK VSMN
351 TLMVDVDFPDVKGGNEVV LFGKQAGREITQAEIEEINGALLADLYTVWG
401 SSNP KILVD

N-terminal signal peptides are highlighted in red.

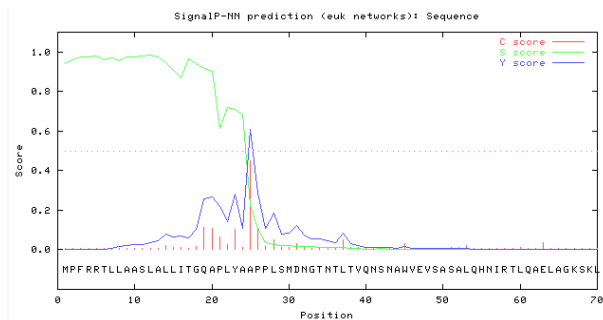
III N-terminal signal sequences

The full amino acid sequences of AArac2440 and AArac12996 were analyzed by *SignalP 3.0* and N-terminal signal peptides were found with a probability of 1.000. Specific cleavage sites were found between Ala24 and Ala25 with a probability of 0.930 and 0.923, respectively.

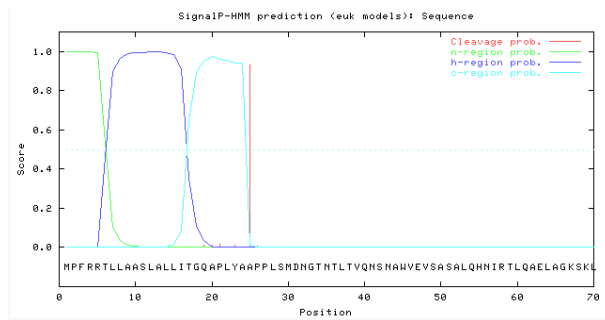
SignalP 3.0 uses virtual machines based on neural networks (NN) and Hidden Markov Models (HMM) for signal prediction (Nielsen *et al.*, 1998; Bendtsen *et al.*, 2004).

AArac2440:

NN result:

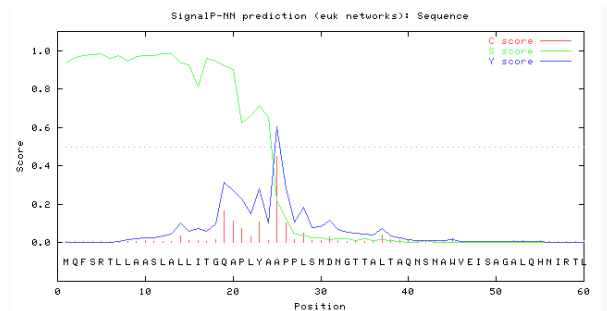
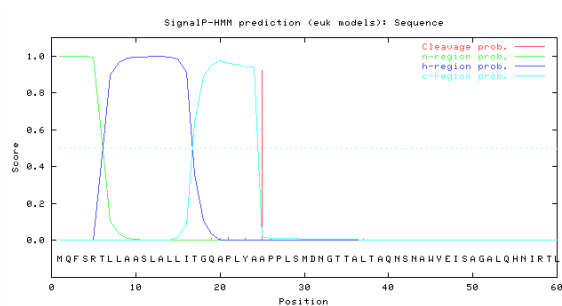


HMM result:



Measure	Position	Value	Cutoff	signal peptide?
max. C	25	0.451	0.32	YES
max. Y	25	0.611	0.33	YES
max. S	12	0.984	0.87	YES
mean S	1-24	0.908	0.48	YES
D	1-24	0.759	0.43	YES

Prediction	Signal peptide
Signal peptide probability:	1.000
Signal anchor probability:	0.000
Max cleavage site probability:	0.930 between pos. 24 and 25

AArac12996:*NN result:**HMM result:*

Measure	Position	Value	Cutoff	signal peptide?
max. C	25	0.451	0.32	YES
max. Y	25	0.605	0.33	YES
max. S	12	0.985	0.87	YES
mean S	1-24	0.902	0.48	YES
D	1-24	0.754	0.43	YES

Prediction	Signal peptide
Signal peptide probability:	1.000
Signal anchor probability:	0.000
Max cleavage site probability:	0.923 between pos. 24 and 25

IV Alignment of amino acid sequences of AArac2440 and AArac12996

■ Homology Block: Percent Matches 94 Score 741 Length 405

Sequence View: Difference Format, Color behind non-matches

AArac2440	5	rtllaaslaallitgqaplyaaapplmsdngtntltvqnsnawvevsasalqhnirtlqaelagksklcavlkadayghgiglvmpsiiaqgvpcvasneearvvrasgftgqlvrvr lasiseledglqydmeelvgsa
AArac12996	5ta.a.....i..g.....g.....g.v.a.....
AArac2440	145	efarqadaiaarhgktlr ihmalmnssgmsrngvematswgrgealqitdqkhlkllvalmthfavedkddvrkglaaafneqtdwlikharldrskltlhaansfat levpearldmwrtggalfgdtvparteykramqfk
AArac12996	145l...e.....t.....g.....k.....h.....t...g.v....
AArac2440	285	shvaavhsypagntvgydrftflardsrlanitvgysdgyrvftnkghvlinghrvpvgkvsmntlmvdvtdfpdvkggnevvlfgkqaggeitqaemeeingalladlytvwgnspkilvd
AArac12996	285r.....i.....s.....

V Alignment of DNA sequences of AArac2440 and AArac12996

■ Homology Block: Percent Matches 91 Score 895 Length 1220

Sequence View: Difference Format, Color behind non-matches

AArac2440	11	gccgtacccttctggtgcatcctcggcacttctgatcacgggacagccccctgtatgcccaccaccggttctcgatggacaacggcaccaacacccctgaccctgcaaacagcaatgcctgggtcgaagtccagggcc
AArac12996	11c.....c..t.g.....c..c.....g.....c..c.....g..cc.....c.g.....c...g.....c.....a.....t...
AArac2440	151	agcgcctgcagcacaacatccgcacgctgcagggcagctggcgggcaagtccaagctgtgcccgtgctcaagggcgaatgcctatggccaccggtatcggcctggtaatgccatcgatcatcgcccaaggcgtgcctg
AArac12996	151	g....a....a.....t..ct.....t...g.....c.....c.....g.....g.....g.....g.....g.....
AArac2440	291	cgtggcgggtggccagcaacgaggagcccgcgctggtccgcgccagtggcttcaccgggcaactggtgcccgtacgctggccagcctcagcgagctggaagatggcttcagctacgacatggaagagctggtgggcagcg
AArac12996	291a.....g....ag.....c.....t.....
AArac2440	431	cggaattgcccgcagggccgatgccatcgccggcgccatggcaagaccttgccgcatcacatggcgctcaactccagcggcatgagccgcaacgggtggagatggccacctggcggccgtggcgaagcgtgcag
AArac12996	431	.c.g.c.....ct.....aa.....c.....c.....t.....c.....a.a.....g.t.....
AArac2440	571	atcaccgaccagaagcacctcaagctggtcgcgctgatgaccacttcgcccgtggaagacaaggacgatgtacgcaagggcctggcggcattcaacgagcagaccgactggttgatcaagcacgcaggtcggaccgcag
AArac12996	571t.....c.....t.....t.....g.....a.....a.g.....a.....c.....c.....g.a...t..t....
AArac2440	711	caagtcaccctgcaagccgcaactcgttcgctacgctggaagtgccggaagcgccctggacatggtacgaacgggtggcgcgctgttcggcgacaccgtgcccggcgccaccgagtacaaacgtgcgatgcagtcca
AArac12996	711t.....c.....a.....g..t..c.....a.....a.....c.....t.c.....
AArac2440	851	aatcgcacgtggcggcggtgcacagctatccggccggcaacaccgtgggctatgaccgcaccttcaccctggcccgtgattcggcggctggccaacattacggctcgggtactccgatggctaccgccgggtattcaccacac
AArac12996	851	.g.....c.....a.....c.....c.....g.....c.....c.....g..t.....c..c.g.t.....g.....
AArac2440	991	aagggccatgtgctgatcaacggccaccgtgtgcccgtcgtgggcaaggtgtcgatgaacacgctgatggtcgatgtcaccgacttccctgatgtgaaggggggtaacgaagtggtgctgctcggcaagcagggccggggg
AArac12996	991a.....a.g.....ct.....t.....c.....c.....c.....a.....a.....a.....
AArac2440	1131	cgaaatcaccaggccgagatggaagaaatcaacggcgcttgctcgcggatgttacaccgtagggggcaattccaacccgaagatctcgtcgactga
AArac12996	1131	g..g.....a.....c.....cc.c.....g.....t.....

VI Rational protein design of AArac2440

Up- and down-primers were designed using the *QuikChange*[®] *Primer Design* program and synthesized by Eurofins MWG GmbH (Ebersberg) as shown in the synthesis report below. The gene encoding AArac2440 was amplified by standard PCR (Tables I and II) in an Eppendorf thermocycler and cloned into the expression vector pBC SK+, which was then used as a template plasmid for the *QuikChange*[®] PCR. A negative control without primers was carried along. The template DNA was digested twice with the restriction enzyme DpnI (New England BioLabs) for 2 h at 37 °C, and the PCR-product was purified with the QIAquick PCR Purification Kit according to the manufacturer's instructions (QIAGEN, 2002). The absolute DNA concentrations were determined by absorption measurement using the NanoDrop method.

Variant 1 (Met349Ala): 40.3 ng/μL

Variant 2 (Met349Gly): 39.6 ng/μL

Negative control: 5.5 ng/μL

Gel-electrophoresis (1 % agarose, 140 V, 30 min) of the digested and purified PCR-products confirmed the presence of the mutation carrying construct pBC SK+*rac* (4630 base pairs). Competent *E. coli* XL1-blue cells were transformed by electroporation (Bio-Rad Gene Pulser: 25 μF, 1.5 kV, 800 Ω, ca. 15 ms), incubated for 2 h at 37 °C in LB-medium (50 μg/mL chloramphenicol, Cm), transferred to LB-plates (50 μg_{Cm}/mL) and incubated at 37 °C. For protein expression competent *E. coli* BL21(DE3) cells, used for overexpression of proteins cloned under the T7 expression system, were transformed with the mutation carrying plasmids. One colony of each variant was grown in 5 LB-medium (50 μg_{Cm}/mL) and induced with 400 μM IPTG (2 h, 37 °C).

Oligonucleotide synthesis report of PCR primers.

eurofins mwg operon		Oligonukleotid Synthese Report											Seite 1/1		
Frau Kerstin Würges Forschungszentrum Jülich IBT 2		Auftragsnummer: 1953980		Kundennummer: 10167		Kd-Auftragsnummer: Nr. 41816648 Pos. 4		Auftragsdatum: 18/06/2009		Labor Nr.: 4311		Anzahl Oligos: 4/4		Eurofins MWG Operon Anzingersraße 7a D- 85560 Ebersberg	
Nr.	Oligoname	Sequenz (5' -> 3')	OD	μg	nmol	Konzentration [pmol/μl]	Vol. für 100pmol/μl	Tm [°C]	MW [g/mol]	GC-Gehalt	Synthese Maßstab	Reinigung	Modifikation	Barcode IDO	QC Report
1	Met349GAla_up	CGTGGGCAAGGTGTCGG CGAACACGCTGATGGTC (34)	14.3	407	38,5	-	385	> 75	10564	64,7 %	0.01 μmol	HPSF	-	010669445	-
2	Met349GAla_down	GACCATCAGCGTGTTCG CCGACACCTTGCCACG (34)	14.7	438	42,5	-	425	> 75	10324	64,7 %	0.01 μmol	HPSF	-	010669446	-
3	Met349Gly_up	CGTGGGCAAGGTGTCGG GGAACACGCTGATGGTC (34)	13.3	376	35,4	-	354	> 75	10604	64,7 %	0.01 μmol	HPSF	-	010669447	-
4	Met349Gly_down	GACCATCAGCGTGTTCG CCGACACCTTGCCACG (34)	12.4	373	36,3	-	363	> 75	10284	64,7 %	0.01 μmol	HPSF	-	010669448	-

Table I: Pipetting table for QuikChange[®] PCR

	volume [μL]	concentration
H ₂ O	19,7	
10x buffer for KOD Hot Start Polymerase	4	1x
dNTPs (2 mM each)	2	0,2 mM
Up-primer (2,5 μ M)	4	0,25 μ M
Down-primer (2,5 μ M)	4	0,25 μ M
MgSO ₄ (25 mM)	1,6	1 mM
Betain (5 mM)	1,2	0.15 mM
KOD Hot Start Polymerase	1	0,025 U/ μ L
Template plasmid: pBC SK <i>rac</i> (46,2 ng/ μ L)	2,5	2,9 ng/ μ L

Table II: Thermocycler program for QuikChange[®] PCR

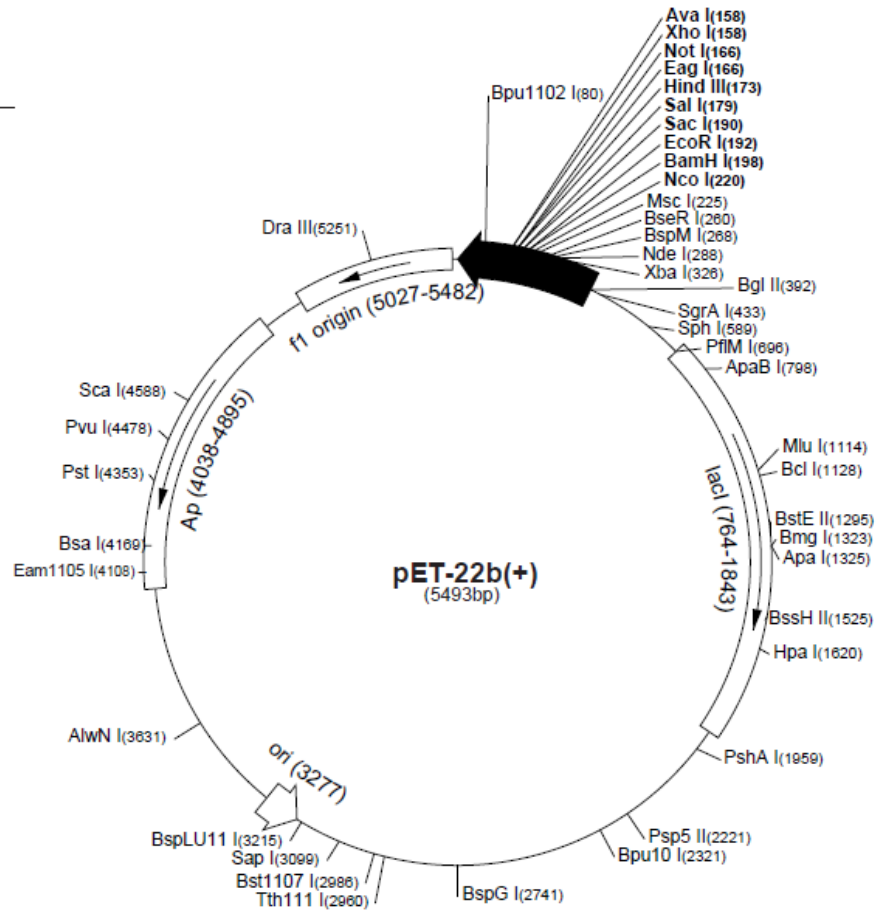
cycle no.	hot start	denaturing	annealing	elongation	final elongation
1	94 °C				
2		3 min / 94 °C			
3-28		1 min / 94 °C	1 min / 65 °C	5 min / 72 °C	
29				10 min / 72 °C	
Hold					4 °C

VII Plasmids

pET-22b(+)

High copy plasmid for overexpression of AArac2440 and AArac12996. Genes were cloned into pET-22b(+) after digestion with NdeI / XhoI.

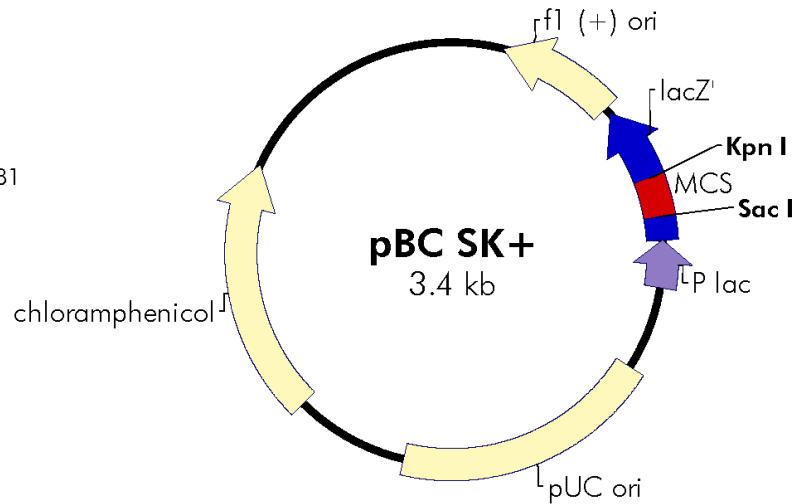
pET-22b(+) sequence landmarks	
T7 promoter	361-377
T7 transcription start	360
<i>peIB</i> coding sequence	224-289
Multiple cloning sites (<i>Nco</i> I - <i>Xho</i> I)	158-225
His•Tag coding sequence	140-157
T7 terminator	26-72
<i>lacI</i> coding sequence	764-1843
pBR322 origin	3277
<i>bla</i> coding sequence	4038-4895
f1 origin	5027-5482



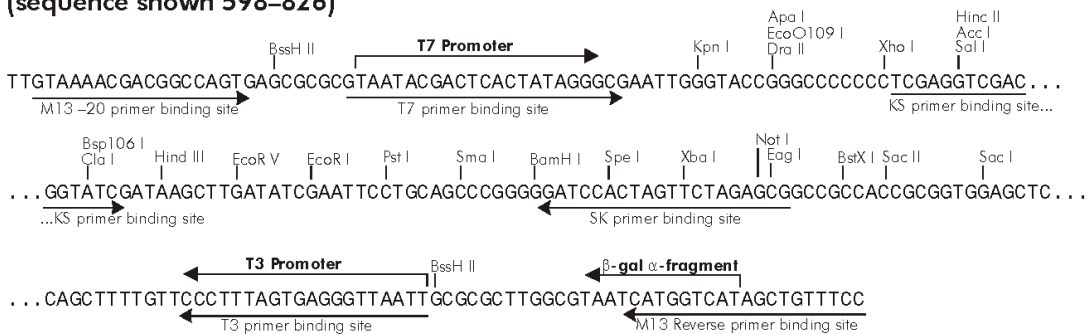
pBC SK+

Template plasmid for rational protein design of AArac2440. Gene was cloned into pBC SK+ after digestion with EcoRV / HindIII.

f1 (+) origin 135–441
 β -galactosidase α -fragment 460–816
multiple cloning site 653–760
lac promoter 817–938
pUC origin 1158–1825
chloramphenicol resistance ORF 2125–2781



pBC SK (+/-) Multiple Cloning Site Region (sequence shown 598–826)



AFFIRMATION

Die vorliegende Dissertation habe ich vollständig und ohne unerlaubte Hilfe angefertigt. Die Dissertation wurde in der vorgelegten oder in ähnlicher Form noch bei keiner anderen Institution eingereicht. Ich habe bisher keine erfolglosen Promotionsversuche unternommen.

Köln, März 2011